Acta Universitatis Agriculturae Sueciae

Doctoral Thesis No. 2022:8
Faculty of Natural Resources and Agricultural Sciences

Relations between soil organic carbon, soil structure and physical processes in an agricultural topsoil

The role of soil mineral constituents

Jumpei Fukumasu

Relations between soil organic carbon, soil structure and physical processes in an agricultural topsoil

The role of soil mineral constituents

Jumpei Fukumasu
Faculty of Natural Resources and Agricultural Sciences
Department of Soil and Environment
Uppsala

SWEDISH UNIVERSITY
OF AGRICULTURAL
SCIENCES

DOCTORAL THESIS
Uppsala 2022

Acta Universitatis Agriculturae Sueciae
2022:8

Cover: The Bjertorp field in late August 2021
(photo: J. Fukumasu)

ISSN 1652-6880
ISBN (print version) 978-91-7760-891-2
ISBN (electronic version) 978-91-7760-892-9

Uppsala
Print: SLU Grafisk Service, Uppsala 2022

Relations between soil organic carbon, soil structure and physical processes in an agricultural topsoil. The role of soil mineral constituents

Abstract

A better understanding of the interactions between soil organic carbon (SOC) and mineral constituents (e.g. clay and reactive oxide phases) and their consequences for soil structure and physical processes is important for assessing the potential for, and benefits of, carbon sequestration in arable soils. This thesis investigated the factors determining topsoil SOC content at the field scale for an arable field with large variations in soil properties. Relationships between SOC, soil pore size distributions, macropore network characteristics, water flow and solute transport were also examined using intact soil samples from the field.

The spatial variation in SOC content at the Bjertorp field was mainly explained by the oxalate-extractable aluminum (Alox) content followed by carbon input from crops that was estimated from crop yield. In contrast, clay and oxalate-extractable iron (Feox) seemed not to play a major role in SOC stabilization/accumulation, possibly due to the occurrence of stagnant water in soils with larger clay contents. It was concluded that reactive Al phases may be important for physico-chemical stabilization of SOC for arable topsoils in humid continental climates.

Multiple linear regression analysis revealed that an increase of SOC was associated with relatively large increases of porosities in the 0.2–5 µm and 480–720 µm diameter classes, which can contribute to enhancing both water supply to crops and water flow rates. The degree of preferential solute transport under steady state near-saturated conditions was reduced with larger volumes of small macropores (240–480 µm diameter) and mesopores (30–100 µm diameter), whereas it was not correlated with measures of macropore connectivity. The statistical analysis indicated that SOC had only limited effects on the degree of preferential transport, being overshadowed by the large variation in clay content across the field.

Keywords: Soil organic carbon, pore structure, macropore flow, preferential transport, arable soil, crop productivity, mineral constituents, X-ray tomography

Author's address: Jumpei Fukumasu, Swedish University of Agricultural Sciences, Department of Soil and Environment, P.O. Box 7014, 750 07 Uppsala, Sweden

表層農地土壌における土壌有機態炭素、土壌構造および物理プロセスの関係．土壌鉱物成分の役割

研究概要

土壌有機態炭素と土壌鉱物（粘土粒子や活性酸化物相）の相互作用と、それが結果として土壌構造や物理プロセスに及ぼす影響を理解することは、農地土壌における炭素隔離の可能性とその効果を評価する上で重要である。本研究では、土壌特性の空間変動性が大きい圃場において、表層土壌の有機態炭素量を規定する要因を調べた。加えて、不撹乱土壌を用いて有機態炭素量と土壌間隙構造サイズ分布、マクロ間隙特性および水・溶質移動の関係について調べた。

ビアトープ圃場において、有機態炭素の空間変動性はおもにシュウ酸抽出アルミニウム量（Alox）と作物収量から推定した炭素流入量によって説明された。一方で、粘土量およびシュウ酸抽出鉄量（Feox）が炭素貯留に及ぼす影響は限定的であることが示唆された。これは粘土量の増加に伴って起こりうる排水不良が原因として考えられる。また、湿潤大陸性気候の表層土壌において、活性アルミニウム相が有機態炭素の物理・化学的安定化に重要である可能性が示唆された。

重回帰分析より、有機態炭素量の増加は主に直径 0.2–5 µm と 480–720 µm サイズの間隙構造の増加と関連していることが明らかとなり、炭素貯留の促進は植物が利用可能な水分量と土壌基質の透水性の増加に貢献できることが示唆された。不飽和定常流下におけるプレファレンシャルフローの発生度合いは、小マクロ間隙（240–480 µm）とメソ間隙（30–100 µm）の増加に伴って低下することが明らかとなった。一方で、マクロ間隙構造の接続性がプレファレンシャルフローに及ぼす影響は限定的であった。また相関分析から、対象圃場において、有機態炭素量がプレファレンシャルフローの発生に及ぼす影響は限定的であり、圃場全体における粘土量の大きなばらつきの影響を受けていることが示唆された。

キーワード: (有機態炭素、間隙構造、マクロ間隙流、プレファレンシャルフロー、農地土壌、作物生産性、鉱物成分、X 線トモグラフィ)

著者住所: 福桝純平 スウェーデン農業科学大学 土壌と環境学部 750 07 スウェーデン ウプサラ

Dedication

To my parents.

Contents

List of publications

This thesis is based on the work contained in the following papers, referred to by Roman numerals in the text:

I. Fukumasu, J., Poeplau, C., Coucheney, E., Jarvis, N., Klöffel, T., Koestel, J., Kätterer, T., Nimblad Svensson, D., Wetterlind, J., Larsbo, M. (2021). Oxalate-extractable aluminum alongside carbon inputs may be a major determinant for organic carbon content in agricultural topsoils in humid continental climate. Geoderma 402, 115345.

II. Fukumasu, J., Jarvis, N., Koestel, J., Kätterer, T., Larsbo, M. Relations between soil organic carbon content and the pore size distribution for an arable topsoil with large variations in soil properties. (Accepted for publication in European Journal of Soil Science).

III. Fukumasu, J., Jarvis, N., Koestel, J., Larsbo, M. Links between soil pore structure, water flow and solute transport in an arable topsoil: Does soil organic carbon matter? (manuscript)

The contribution of Jumpei Fukumasu to the papers included in this thesis was as follows:

I. Planned the experiments together with the co-authors. Performed field work, laboratory work and data analysis together with the co-authors. Prepared the manuscript with assistance from the co-authors.

II. Planned the experiments together with the co-authors. Performed field work, laboratory work and data analysis together with the co-authors. Prepared the manuscript with assistance from the co-authors.

III. Planned the experiments together with the co-authors. Performed field work, laboratory work and data analysis together with the co-authors. Prepared the manuscript with assistance from the co-authors.

Abbreviations

Alox	Oxalate-extractable aluminum
C:N	Carbon to nitrogen ratio
DSR	Dispersion by SOM removal
Feox	Oxalate-extractable iron
POM	Particulate organic matter
POM-C	SOC in POM fraction
MD	Mechanical dispersion
MRY	Mean relative yield
Sand-C	SOC in Sand-sized fraction (>63 μm)
Sand-OM	SOM in Sand-sized fraction (>63 μm)
SC	Silt- and clay-sized fraction (<63 μm)
SC-C	SOC in SC fraction (<63 μm)
SC-OM	SOM in SC fraction (<63 μm)
SOC	Soil organic carbon
SOM	Soil organic matter
rSOC	Oxidation-resistant SOC in SC fraction
rSOM	Oxidation-resistant SOM in SC fraction

1. Introduction

Soil is the largest reservoir of carbon in the terrestrial environment. It contains more carbon than plant biomass and the atmosphere combined. However, intensive agriculture, with soil tillage, and land use changes from natural ecosystems (e.g. grassland and forest) to cultivated land, have led to significant losses of soil organic carbon (SOC) in arable soils worldwide (Sanderman et al., 2013; Li et al., 2018). If this depletion of SOC was reversed through the sequestration of organic carbon in arable soils, it would be beneficial in mitigating global warming and climate change (Lal, 2004). In addition, SOC strongly influences soil physical, chemical and biological quality, which are important for crop production and ecosystem services (Lal, 2014). Crop productivity also influences SOC content through its carbon supply through crop residues and root growth. For example, Wiesmeier et al. (2015) attributed the trends of decreasing SOC stocks in agricultural fields across Europe to the stagnation of crop yield, as it would potentially decrease carbon inputs from crops into the soil (Bolinder et al., 2007). Proper land management is, therefore, required to enhance SOC sequestration and to realize the beneficial effects of SOC for the soil environment and for sustainable crop production (Chenu et al., 2019).

For arable soils, a large proportion of SOC (ca. 90%) is usually associated with silt- and clay-sized (SC) particle fractions (Gregorich et al., 2006; Matus, 2021). SOC stabilization is then thought to be governed by the content of clay-sized particles because they determine the specific surface area of soils that is available for chemical adsorption of SOC. Clay-sized particles are also key constituents of the soil aggregate structure that is thought to provide physical protection of SOC (Horn et al., 1994; Totsche et al., 2018). Therefore, clay content has been used for modelling organic-carbon dynamics in soils (Rasmussen et al., 2018; Wiesmeier et al., 2019). However, recent studies have shown that depending on soil pH and climate, reactive aluminum and iron phases can be more important for SOC stabilization than clay content (Rasmussen et al., 2018). Identification of key variables that better explain the spatial variation in SOC contents in arable soils is important for a better understanding of SOC stabilization mechanisms and their consequences for soil quality including soil structure.

Soil structure is defined as the three-dimensional arrangement of pores and solid phases. It reflects the physical status of the soil and, hence, influences water dynamics, biogeochemical cycling and crop production (Rabot et al., 2018). Soil structure has traditionally been studied from two contrasting perspectives, namely the soil aggregate perspective, where aggregate stability has been a central property, and from the pore perspective, where pore network properties have been central (Rabot et al., 2018). The effects of SOC and organic amendments on aggregate stability have been extensively studied (Bronick and Lal, 2005). On the other hand, the relationship between SOC and soil pore architecture (e.g. the pore size distribution) has been much less studied and is still a controversial topic (e.g. Rawls et al., 2003; Minasny and McBratney, 2018; Lal, 2020). Pore size distributions are often quantified from measurements of soil water retention. Additionally, the advent of X-ray tomography has enabled quantification not only of pore size distributions, but also other characteristics of pore networks (Lucas et al., 2019). However, there is a limitation of resolution of pore sizes that can be quantified by X-ray tomography (e.g. ca. 300 µm resolution for a column with 12.5 cm diameter and 20 cm height). Combining X-ray tomography and soil water retention measurements would therefore enable quantification of a wide range of pore size classes and may potentially be useful to identify pore sizes and characteristics that are strongly associated with SOC.

Soil pore structure determines water flow and solute transport in soils. In particular, a better understanding of how SOC influences water flow in macropores and preferential solute transport in arable soils is important, because these processes enhance the leaching of agrochemicals below the root zone and consequently decrease water quality in ditches and streams surrounding arable fields (Jarvis, 2007; Sandin et al., 2018). In this respect, exploring relationships between SOC content, X-ray derived macropore characteristics and preferential transport would be useful to identify key variables that govern water flow and solute transport (Jarvis et al. 2016). This would enable an appreciation of the potential benefits and limitations of SOC sequestration in arable soils for the regulation of water and solute dynamics.

2. Aim and objectives

The overall aim of this thesis was to investigate the interactions between SOC and soil mineral constituents and their consequences for the relationships between SOC, soil structure, water flow and solute transport in arable topsoils. The specific objectives of this thesis were:

- To examine factors determining spatial variations in SOC content for arable topsoils in humid continental climate and to examine interactions between SOC and soil mineral constituents at the field scale (Paper I)
- To examine relationships between SOC and pore size distributions quantified by X-ray tomography and soil water retention measurements for an arable topsoil with large variations in soil properties (Paper II)
- To examine relationships between soil pore structure and preferential solute transport for arable topsoil and assess the potential role of SOC in these flow processes (Paper III)

This thesis focuses on the topsoil of a large (47 ha) arable field at Bjertorp in south-west Sweden that has large spatial variations in SOC and clay content. This approach minimizes the influence of confounding factors that may mask the effects of SOC and clay on soil structure and flow processes, as the climate is the same and the field has also been under similar management for most of the last 60 years.

3. Background

3.1 Soil organic carbon dynamics in arable soil

The global store of soil carbon down to 1 m depth is 1505 Pg. This is more than the carbon stored in the atmosphere (867 Pg) and in vegetation (620 Pg) combined (Lal, 2018). However, an estimated 116 Pg C has been released into the atmosphere from the top 2 m of soil during the last 12,000 years due to intensive agriculture (Sanderman et al., 2017). This loss of SOC from arable land has also caused soil degradation and reduced crop productivity. This is because SOC plays a vital role in maintaining soil fertility in arable soils (Lal, 2004). Therefore, agricultural land management that enhances SOC sequestration can be a win-win solution for achieving sustainable crop production and regulating the future climate. Accordingly, an initiative called "4per1000" was launched by the French Ministry of Agriculture in 2015. The goal is to increase the SOC content in arable soils by 0.4% of the initial SOC stock annually in the uppermost 0.4 m (Chenu et al. 2019).

To achieve agricultural land management that enhances SOC sequestration, it is pivotal to identify factors that determine spatial variations in SOC in arable soils and to understand the processes causing these variations. SOC content is determined by the balance between input and output of organic carbon. The input into the soil in agricultural systems is driven by organic amendments (e.g. manure) and the carbon supply from crops. The crop-derived carbon supply can be further separated into above- and belowground sources, and it has been reported that the carbon input from belowground biomass (i.e. roots and their exudates) is more efficiently stabilized compared to carbon originating from aboveground biomass (Kätterer et al., 2011, Figure 1). Since direct measurements of total crop biomass are tedious and expensive, grain yield has often been used as a proxy for carbon input from crops (Bolinder et al., 2007) and it has been used to explain, for example, the difference in SOC content between tilled and no-tilled soils (Ogle et al., 2012). A part of the carbon in plant residues is incorporated into microbial biomass through microbial metabolism and anabolism and when microbes die, their biomass becomes part of SOM. Miltner et al. (2012) suggested that a large fraction of SOM originated from microbial biomass. The output of SOC, i.e. microbial decomposition of SOM, is considered to be regulated by three factors, namely biochemical quality and chemical and physical protection (Figure 1). Biochemical quality refers to the biochemical composition of organic matter supplied by plants. For example, lignin is more slowly decomposed by microbes compared to labile organic carbon such as glucose and amino acids (Six et al., 2002). Chemical protection refers to the chemical association between soil minerals and SOC. For example, SOC can be adsorbed to mineral surfaces, which potentially reduces the availability of SOC to microbes (Schmidt et al., 2011). Physical protection means that SOC can be entrapped within the soil aggregate structure, which regulates microbial and enzymatic accessibility to SOC (Sollins et al., 1996; Lützow et al., 2006). These chemical and physical stabilization mechanisms are suggested to be more important compared with biochemical quality, since even easily decomposable SOM such as amino acids can be stored in soil for more than 100 years (Schmidt et al., 2011; Dungait et al., 2012; Lehmann and Kleber, 2015). Hence, in this thesis, I will focus on the mechanisms of physical and chemical stabilization of SOC.

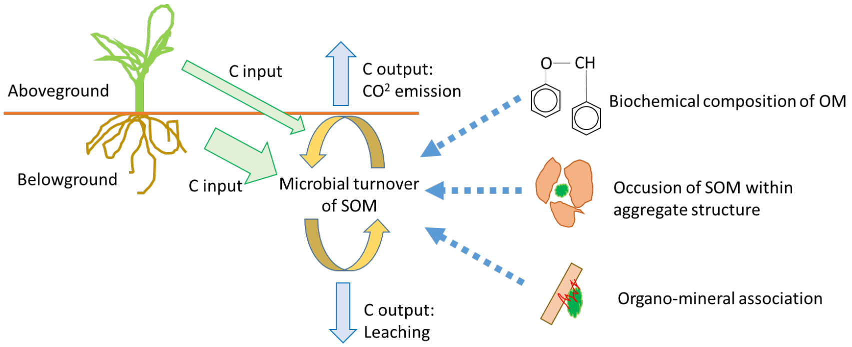

Figure 1. Schematic figure depicting SOM dynamics as affected by C input and three stabilization drivers.

3.2 Interaction between SOC and mineral constituents

3.2.1 The role of minerals in SOC stabilization

The chemical and physical stabilization of SOC is known to be driven by clay-sized particles (<2 μm diameter). This is because clay-sized particles have a large specific surface area, which can adsorb SOC and hence protect it chemically from microbial degradation (Sollins et al., 1996). Clay-sized particles are also a key component in the formation of an aggregated structure, which provides physical protection of SOC from microbial decomposition. Keiluweit et al. (2018) reported that the abundance of anoxic sites within soil aggregates for upland soils was positively correlated with clay content. These anoxic sites reduced the rate of microbial decomposition of SOM. Based on these well-known effects of clay-sized particles on microbial decomposition processes, clay content, and sometimes also silt content, have been used as input to models of SOC dynamics (Zimmermann et al., 2007; Rasmussen et al., 2018) and for estimating SOC saturation points, namely the maximum SOC content that can be stored in silt- and clay-sized fractions (Six et al., 2002).

The importance of clay content for SOC stabilization is supported empirically by the positive correlations between clay and SOC contents that have been reported at regional (e.g. Li et al., 2020) and national scales (e.g. Poeplau et al., 2020). On the other hand, several studies have reported no correlation between clay and SOC contents (e.g. Thomsen et al., 2009; Beare et al., 2014; Augustin and Cihacek, 2016; Van De Vreken et al., 2016; McNally et al., 2017; Mayer et al., 2019). These studies indicate that there may also be other factors determining SOC stabilization, rather than clay content alone. Thus, based on an analysis of a continental scale dataset for over 5,500 soil profiles, Rasmussen et al. (2018) reported that for soils with a pH less than 6.5, the SOC content was more strongly correlated with oxalate-extractable aluminum (Alox) and iron (Feox) than with clay content. Alox and Feox are proxies for reactive mineral constituents in soil. The importance of such reactive mineral phases for SOC stabilization is well established for acidic forest soils (e.g. Mikutta et al., 2006) and Andisols (e.g. Matus et al., 2006, Percival et al., 2000). However, some recent studies from sub-Saharan Africa also reported strong correlations between SOC and the content of Alox and Feox (Ouédraogo et al., 2020; Traoré et al., 2020; von Fromm et al., 2021). Nevertheless, the relationships between SOC and the reactive mineral phases have not been explored for arable soils in humid continental climates (Beck et al., 2018), such as in Sweden.

Reactive mineral phases can be important for both physical and chemical protection of SOC. The reactive mineral phases can be associated with SOC by organo-mineral complexation and/or co-precipitation, which can reduce microbial and enzymatic accessibility to SOC (Kleber et al., 2015). Organo-metal associations were also suggested, as a binding agent, to enhance the clay-sized aggregation in which SOC can be physically protected (Asano et al., 2018).

3.2.2 SOM fractionation

To examine how and where SOC is stored in soils, SOM fractionation is often conducted. It enables separation of SOM into fractions with different SOC stability. There are many different fractionation methods and the choice of method depends on the research questions and soil types (Poeplau et al., 2018). However, it is now recognized that the separation of a particulate organic matter (POM) fraction from mineral-associated organic matter is particularly important, because these two fractions have distinct differences in their stability and function (Lavallee et al., 2020). SOC in the POM fraction is considered to be labile and hence to be a good indicator for short-term changes of SOC due to, for example, land use change. In contrast, SOC in the mineral-associated organic matter fraction is considered to be more resistant to microbial decomposition and, thereby, to show larger long-term stability, which is important for SOC sequestration (Six et al., 2002). These two fractions can be quantified by wet-sieving and density fractionation (Poeplau et al., 2018), separating the sand-sized fraction (e.g. >63 μm), which mainly consists of plant-derived SOM, from the silt- and clay-sized fraction (e.g. <63 μm), which mainly consists of SOM derived from microbial biomass. In addition, chemical fractionation through oxidation of SOM using peroxide and sodium hypochlorite can be used to isolate stable SOC from the bulk soil. For example, using ^{14}C analysis, Mikutta et al. (2006) reported that the C age for SOC in the oxidation-resistant SOM fraction was older than that in the bulk soil.

Poeplau et al. (2018) compared different SOC fractionation methods comprising particle, aggregate, density and chemical separations and demonstrated that there was no method that could completely separate fresh organic carbon from old. However, they concluded that combining physical and chemical fractionation methods can satisfactorily separate fresh from old SOC fractions, thereby isolating SOC pools with different stability.

3.3 Soil structure in arable soils

3.3.1 Methods to quantify soil pore structure

The quantification of soil pore structure is useful to help understand soil C sequestration, since it influences physical processes such as aeration, water flow and solute transport that influence microbial activity (Vogel et al., 2021). The pore size distribution exerts an important control on these processes (Rabot et al., 2018). Pore size distributions have traditionally been estimated from measurements of either soil water retention or mercury porosimetry. However, pore size distributions estimated by soil water retention does not contain information on the spatial distribution of pores and their connectivity within a given soil sample. Recent developments in X-ray tomography have allowed for direct quantification of soil pore structure, including not only pore size distributions but also pore network characteristics (e.g. pore connectivity) and biopores (e.g. created by soil fauna and root development) (Rabot et al., 2018; Lucas et al., 2019).

3.3.2 Soil pore structure and SOC

Soil pore structure influences SOC stability (Strong et al., 2004; Ruamps et al., 2011; Dugaint et al., 2012; Kravchenko and Guber, 2017). For example, Kravchenko et al. (2015) showed that a larger abundance of connected pores >13 μm in diameter was associated with a faster rate of decomposition of intra-aggregate POM. Lützow et al. (2006) suggested that micropores smaller than 0.2 μm in diameter regulate microbial accessibility to SOC. In turn, SOC also influences soil pore structure, although much less is known about this. There are many studies reporting negative correlations between SOC and bulk density at various scales (i.e. plot, field, regional and global, Nemes et al., 2005; Kätterer et al., 2006; Yang et al., 2014; Meurer et al., 2020b), which indicate that a larger SOC content leads to a larger total porosity. This can be attributed to soil aggregation enhanced by SOC (Meurer et al., 2020b) and the decrease of the mean particle density with larger SOC content (Rüehlmann et al., 2006). However, the effects of the reduction in particle density with larger SOC content is expected to be small in arable soils (e.g. Li et al., 2007) because the typical SOC content for arable soils is small (e.g. <3%, Oldfield et al., 2019). Therefore, there is clearly a link between SOC and the development of soil pore structure. However, the role of SOC in the formation of pores of different sizes is not clear. For example, positive effects of SOC on plant available water content, corresponding to the porosity in the 0.2–10 μm diameter class, possibly through enhanced soil aggregation have been recognized (Hudson, 1994). However, Minasny and McBratney (2018) reported in their global meta-analysis that the effects of SOC on plant available water was limited to a volumetric increase of 1.4–1.9 mm H_2O per 100 mm soil depth with a 1% mass increase of SOC content, suggesting that a change in SOC content would not have a significant impact on plant available water content. Instead, the authors suggested that the effects of SOC on pore size distribution is significant for pores larger than 10 μm. Relations between soil macroporosity and SOC contents have been investigated in several studies, with relationships reported to be either positive (Larsbo et al., 2016; Xu et al., 2018) or statistically insignificant (Paradelo et al., 2016b; Jarvis et al., 2017), which shows that generalizations are difficult.

Soil pore size distribution is also strongly influenced by soil texture (Rawls et al., 2003; Lal, 2020). It is, therefore, important to separate the roles of soil texture from SOC in pore structure formation. Additionally, reactive mineral phases (Al and Fe) are known to be key stabilizers for soil aggregate structure through their variable charges and large specific surface area (Six et al., 2004). However, only a few studies have investigated the relationships between reactive mineral phases and pore structure (e.g. Shoji et al., 1996; Regelink et al., 2015).

3.4 Water flow and solute transport in arable soils

3.4.1 Flow processes regulated by soil structure

The prediction of saturated hydraulic conductivity and water flow in macropores is difficult compared to the prediction of soil matrix flow, because the development of macropore networks is more influenced by factors such as land use, biological activity and climate rather than basic soil properties such as texture and SOC (Jarvis et al., 2013). The direct quantification of macropore characteristics by X-ray tomography can potentially increse our understanding of water flow in macropores. For example, Koestel et al. (2018) reported a positive correlation between the critical pore diameter (i.e. the smallest pore diameter of the largest macropore connecting the top and the bottom) and saturated hydraulic conductivity in a national scale dataset for Norway. They showed that percolation theory was useful for the prediction of the saturated hydraulic conductivity. Some other studies have reported significant correlations between (near-) saturated hydraulic conductivity and pore connection probability (Sandin et al., 2017) or bioporosity (Zhang et al., 2019). On the other hand, the activation of water flow in macopores and preferential solute transport may be more dependent on the abundance of smaller macropores and mesopores (Jarvis et al., 2012; Larsbo et al., 2014; Nimmo et al., 2021), rather than the properties of the entire macropore network. However, only a limited number of studies (e.g. Larsbo et al., 2014, 2016; Paradelo et al., 2016b) has investigated relationships between the degree of preferential transport, X-ray derived pore characteristics and mesoporosity for the same soil samples.

3.4.2 Potential role of SOC for flow processes in soils

Considering the potential associations between SOC and soil pore structure, SOC should be expected to have significant effects on water flow and solute transport. However, the relationships between SOC and hydraulic conductivity are not clear: Studies from both field scale and global scale have showed negative correlations between SOC and saturated hydraulic conductivity (Nemes et al., 2005; Wang et al., 2009; Jarvis et al., 2013). This negative correlation may be attributed to the fact that a larger SOC content may be related to a larger degree of water repellency of soils (Nemes et al., 2005). On the other hand, Araya and Ghezzehei (2019) reported positive correlations between SOC and saturated hydraulic conductivity for their continental-scale dataset grouped by soil texture.

Studies that have investigated the effects of SOC on the degree of preferential transport indicated that a large variation in SOC contents is important to detect any effects. For example, Vendelboe et al. (2013) and Soares et al. (2015) reported no correlations between SOC and the degree of preferential transport for soils with SOC contents in the ranges 1.2–1.7% and 1.7–2.2%, respectively. On the other hand, Larsbo et al. (2016) and Paradelo et al. (2016b) reported that larger SOC contents reduced the risk of preferential transport among soils with large variations in SOC content (4–15% and 1.8–

8.4%, respectively). Larsbo et al. (2016) further indicated that the larger SOC content was associated with larger abundance of small macropores (200–600 µm in diameter) that can prevent the activation of preferential transport. In the perspective of Swedish arable soils, 75% of the soils have SOC content smaller than 3.5% (Eriksson et al., 2010). It is, therefore, required to evaluate if larger SOC content can reduce the risk of preferential transport and protect water resources in agricultural fields, for soils covering the typical range of SOC content in arable soils.

4. Material and Methods

4.1 Field description

The field (46.9 ha) is located in Bjertorp, Västergötland, in South-west Sweden (58°14'00"N 13°08'00"E) – one of the most productive agricultural regions in Sweden (Lindahl et al., 2008). The field is located about 500 m from a long-term experimental field managed by the SLU. The field has been cultivated for at least 60 years under similar soil management across the field except that (1) precision fertilization of nitrogen, phosphorus and potassium has been carried out for some years and (2) different types of crops have been grown in different parts of the field for some years. Soil profile classification was conducted at three locations within the field based on the World Reference Base (WRB, 2015) system, and the three soil profiles were classified as Stagnic Eutric Cambisol, Eutric Stagnosol and Haplic Phaeozem respectively (Figure 2). Mean precipitation and temperature, which were taken from the nearby meteorological station at Hällum (Swedish Meteorological and Hydrological Institute), were 624 mm and 7.3 °C respectively. A previous soil sampling campaign conducted in 2000 showed that there were large variations in clay (ca. 9–45%) and SOC (ca. 0.6–2.7%) contents across the field (Lindahl et al., 2008). A digital elevation model of the field was imported from Lantmäteriet (https://www.lantmateriet.se/sv/) to extract elevation data across the field.

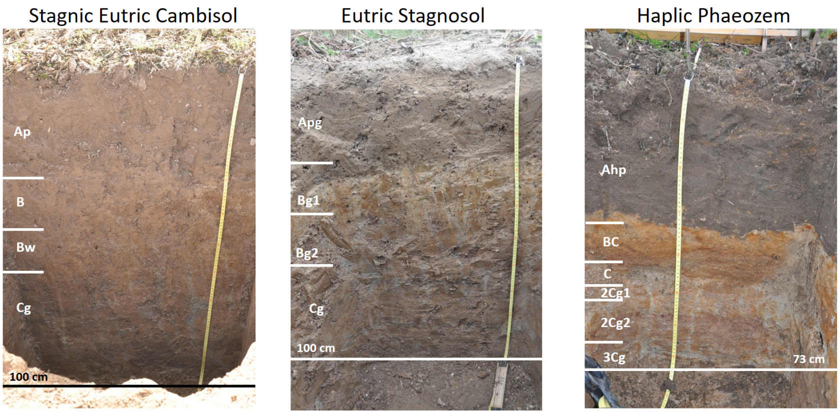

Figure 2. Photos of soil profiles at three different locations.

4.2 Soil sampling

In late August 2017, after the harvest of oilseed rape but before tillage, soil samples were taken at 35 locations, which were determined using stratified sampling to cover the variations in SOC and clay contents measured in 2000 (Figure 3 and 4). At each location, intact topsoil samples in polyvinyl chloride (PVC) cylinders (20 cm height, 12.5 cm diameter) and steel cylinders (10 cm height, 6.8 cm diameter, at a depth of ca. 3–13 cm) were taken using a tractor-mounted hydraulic press and a drop hammer, respectively. Additionally, loose topsoil from the same depth (ca. 3–13 cm) was also collected. The samples in the PVC columns were used for X-ray tomography scanning of soil structure, solute transport experiments and measurements of near-saturated hydraulic conductivity. After these experiments, soils collected from within the columns at ca. 3–13 cm depth were air-dried at 38 °C, crushed and sieved to <2 mm. These soil samples were used for soil texture analysis, SOM fractionation and the oxalate extraction experiment and are referred to as bulk soils from now on. The soil samples in steel cylinders were used for measurements of soil water retention and bulk density. The loose soil samples were also air-dried at 38 °C, crushed, sieved to <2 mm and then used for measurements of soil pH and soil water retention at wilting point.

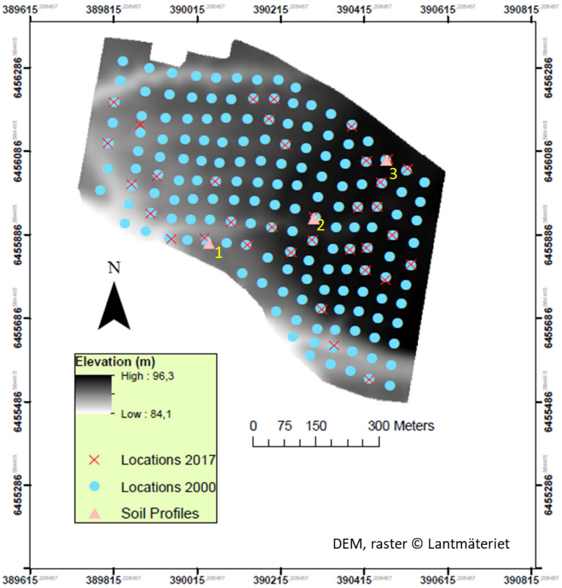

Figure 3. A field map of a digital elevation model (DEM) and soil sampling locations in 2000 and 2017. The coordinate system used here is SWEREF99 TM (unit: m). The DEM of raster data was downloaded from Lantmäteriet. The map was created using ArcGIS 10.7.1 (ESRI).

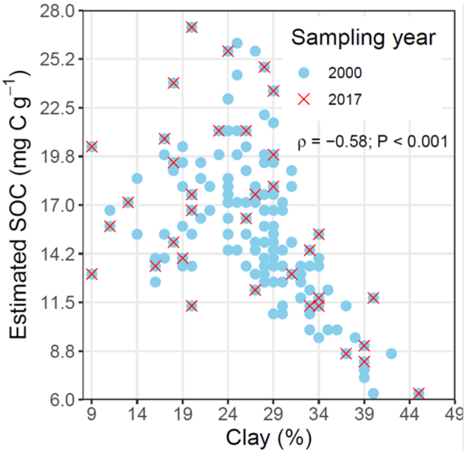

Figure 4. The relationship between SOC and clay contents in the Bjertorp field as reported in Lindahl et al. (2008). The blue circles show soil sampling locations in 2000 while the red crosses show soil sampling locations in 2017 selected using stratified sampling.

4.3 Basic soil properties

Soil texture was measured using wet-sieving and the pipette method. Soil organic matter was first removed by 10 mL peroxide (35%) and then the samples were dispersed by adding 25 mL of chemical dispersant (7 g L^{-1} sodium carbonate, Na_2CO_3 + 33 g L^{-1} sodium metaphosphate, $(NaPO_3)_n$). As proxies for reactive aluminum and iron phases, the oxalate-extraction of aluminum and iron was conducted using 100 mL of oxalate extraction solution (0.2 mol/L oxalate: mixture of 4.8 L ammonium oxalate solution and 3.6 L oxalic acid solution, pH adjusted to 3.0) in the dark. Extracted aluminum and iron concentrations were then measured by inductively coupled plasma optical emission spectrometry (ICP-OES).

4.4 SOM fractionation

SOM fractionation was conducted according to the method proposed by Zimmermann et al. (2007) and modified by Poeplau et al. (2013). Briefly, a mixture of 30 g of bulk soil and 150 mL deionized water was dispersed by an ultrasonic probe with 22 J mL^{-1} energy having a constant power of 20 W. The dispersed samples were then wet-sieved using a 63 μm mesh and ca. 2 L of deionized water, which enabled separation of the sand-sized particle and aggregates and POM fraction (>63 μm) from the silt- and clay-sized (SC) fraction (<63 μm). After wet-sieving, these fractions were dried at 36–38 °C. The POM and sand-sized particle and aggregates fractions were then separated into a POM fraction and a sand-sized particles and aggregates fraction by density fractionation using a sodium polytungstate solution with 1.8 g cm^{-3} density. To isolate oxidation-resistant SOM, 1 g of soil from the SC fraction was treated with 50 mL of 7% NaOCl (adjusted to pH 8 by HCl addition) three times. This fractionation method gave five distinct SOM fractions: POM, SOM associated with sand and aggregates (sand-OM), SOM associated with silt and clay (SC-OM), oxidation-resistant SOM in the SC fraction (rSOM) and non-oxidation resistant in the SC fraction (SC-OM – rSOM). The SOC in each fraction was then defined as POM-C, Sand-C, SC-C, rSOC and SC-C – rSOC. Carbon and nitrogen contents in bulk soil and in these fractions were measured by dry-combustion on a TruMac CN (LECO Corp.). The inorganic carbon content was very small (<0.024 mg g^{-1} bulk soil, which corresponds to <0.2% of the total C). It was therefore assumed that SOC was equivalent to the total C content. SOC content in fractions are reported on a basis of mg C g^{-1} bulk soil except for the results of silt-sized aggregate analysis where SC-C content is reported on a basis of mg C g^{-1} SC fraction.

4.5 Silt-sized soil aggregates

The SC fraction (particle size <63 µm) was used to quantify the presence of silt-sized aggregates. For this purpose, two treatments were prepared: mechanical dispersion (MD) and dispersion by SOM removal (DSR). For the MD treatment, 0.08 g of the SC fraction was placed in a beaker with 40 mL deionized water and mechanically dispersed with a magnetic stirrer overnight (350 rpm). For the DSR treatment, SOM in the SC fraction (ca. 0.08 g) was removed by peroxide addition and boiling for at least 6 hours. Then, 1 mL of chemical dispersant (7 g L^{-1} sodium carbonate, Na_2CO_3 + 33 g L^{-1} sodium metaphosphate, $(NaPO_3)_n$) was added to the samples. Finally, the samples were filled with deionized water up to ca. 40 mL of total volume. The samples were then mechanically dispersed overnight as for the MD treatment. The particle and aggregate size distributions were measured using a laser particle size analyzer (Partica LA-950 V2, Horiba). Here it was assumed that the result for the MD treatment represented the particle- and aggregate-size distribution whereas the result for the DSR treatment represented the particle size distribution. The difference in the size distributions between DSR and MD (defined as DSR – MD) treatments was also calculated. If DSR – MD <0, this was interpreted as the amount of silt-sized aggregates consisting of clay-sized particles, while if DSR – MD >0, it was interpreted as the amount of clay-sized particles released upon destruction of silt-sized aggregates. These size distributions were divided into seven size classes (i.e. <0.5 µm, 0.5–1 µm, 1–2 µm, 2–6 µm, 6–20 µm, 20–60 µm and 60–100 µm).

4.6 Literature search on the relation of SOC to basic soil properties

I searched the literature database for studies that reported SOC, soil texture, soil pH, Alox and Feox for arable topsoils in humid continental climates (Beck et al., 2018). Four studies were found: one from Sweden (Blombäck et al., 2021), one from Norway (Grønsten and Børresen, 2009), one from

Denmark (Paradelo et al., 2016a) and one from Canada (Beauchemin et al., 2003). The results from Bjertorp and from these studies, except Paradelo et al. (2016a) for which the raw data were not available, were combined to investigate the extent to which the results for the Bjertorp field could be generalized to similar sites. From now on, I refer to this data as "the combined dataset".

4.7 Analysis of crop yield data using GIS

Grain yield data across the field measured by a combine harvester were available from 1997, 1999–2004, 2007, 2010–2013, 2015 and 2016. The yield data in 2003, 2004 and 2011 were excluded, because data were missing for large parts of the field area (>30%) (see the details of calculation of the missing areas in Page S7, Paper I). As different crops (winter wheat, oats and oilseed rape) were grown in different years, relative yields were calculated by normalizing the measured yields by the mean yield for a given year (Keller et al., 2012). Interpolation of the relative yield data across the field was performed using the Inverse Distance Weighting (IDW) method in ArcGIS 10.7.1 (ESRI, http://www.esri.com). The relative yield data at locations where soil properties were measured in 2000 and 2017 were extracted and the mean of relative yields (MRY) for the considered years were calculated at each soil sampling location (Keller et al., 2012). The MRY was used as a proxy for C input from crops (Bolinder et al., 2007).

4.8 Soil water retention

Soil water retention at pressure potentials (ψ) of -30 and -100 cm were measured using a sand box and at -300 and -600 cm using a suction plate. Soil water retention at -15,000 cm was measured using a pressure plate extractor with disturbed bulk samples (i.e. sieved to <2 mm). The pressure potentials were converted to equivalent pore diameters using the Young-Laplace equation: d (in cm) = -3000/ψ (in cm). Soil porosities in the pore diameter classes of <0.2, 0.2–5, 5–10, 10–30, 30–100 and >100 µm were then estimated by calculating differences in volumetric water content between pressure potentials. Total porosity was also estimated from bulk density with an assumed particle density of 2.65 g cm^{-3}. In this thesis, the porosities in the <10 µm diameter classes and 10–100 µm diameter classes were defined as microporosity and mesoporosity respectively (Luxmoore, 1981).

4.9 X-ray tomography

Scanning of the soil samples in the PVC cylinders was performed using the GE Phoenix X-ray scanner (v|tome|x 240) available at the Department of Soil and Environment, SLU, which is equipped with a tungsten target, a 240-kV X-ray tube and a GE 16’’ flat panel detector. The samples with a clay content >30% were scanned at a voltage of 170 kV, a current of 740 µA and exposure time of 1000 µs, whereas the samples with clay content <30% were scanned at 180 kV, 630 µA and 333 µs. In total, 2000 radiographs were collected and a three-dimensional image was created using the GE image reconstruction software Datos|x. A cylindrical region of interest (ROI) of the samples (8.4 cm diameter and 10 cm height at 3–13 cm depth) was defined. The length of each image voxel was approximately 120 µm in all directions and the minimum pore diameter that can be quantified was 240 µm. In this thesis, X-ray derived porosities are defined as macroporosity.

4.10 Image analysis

Image analysis was carried out using the open-source software ImageJ and the plugins included in FIJI (Schindelin et al., 2012). First, noise in the images was reduced by applying a three-dimensional median filter with a radius of one. Using the plugin SoilJ (Koestel, 2018), illumination differences between images and within images in the vertical direction were then corrected using the grey values in the wall of the PVC cylinders and the air inside the columns as references. All the images were segmented into pore and solid phases using a single gray value threshold. The total visible porosity, pore size distribution and macropore characteristics were then calculated using SoilJ. The macropore characteristics analyzed here are critical pore diameter, the percolating fraction, surface fractal dimension, connection probability, average pore thickness and specific surface area of macropores. The critical pore diameter is the diameter of the largest sphere that could pass through the pore network from top to bottom in a given ROI. The percolating fraction is the fraction of the pore network that is connected between the top and the bottom of a given ROI. The surface fractal dimension indicates the abundance of smaller macropores and the homogeneity and roughness of macropores. The connection probability is the probability that two randomly selected pore voxels belong to the same pore cluster. Additionally, total visible bioporosity and its size distribution were quantified using a method based on that described by Lucas et al. (2019). More details are available in Paper II. To facilitate this analysis, the image resolution was reduced by a factor of two to a voxel edge length of 240 µm, which corresponds to a minimum detectable pore diameter of 480 µm. Total visible porosity and bioporosity were divided into the following pore diameter classes: 240–480, 480–720, 720–1220, 1220–1920, 1920–3120 and >3120 µm.

4.11 Solute transport experiments

Solute transport experiments for the soil samples in the PVC cylinders were performed under steady-state water flow using an irrigation chamber at the Department of Soil and Environment, SLU. Details on the method are presented in Larsbo et al. (2014, 2016). Briefly, the bottom of the PVC cylinders were covered with polyamide cloth with a 50 µm mesh size to prevent soil loss during the irrigation experiment. Artificial rainwater was used to irrigate the soil samples at an intensity of 2 mm h^{-1}. Effluent concentrations were measured at 5-minute resolution using Cond 3310 electrical conductivity meters (WTW GmbH, Weilheim, Germany). When steady-state flow was achieved and the effluent concentration was stable, a pulse of 2 mL potassium bromide (250 mg Br mL^{-1} distilled water) was applied to the soil surface. This application was restricted to the central part (diameter ca. 10 cm) of the soil surface to limit effects of any artificial pores present close to the PVC walls on solute transport. From the measurements of effluent concentrations, a breakthrough curve was obtained for each sample. After the irrigation at 2 mm h^{-1} intensity, the intensity was increased to 5 mm h^{-1} and a second pulse of potassium bromide was applied.

To determine the degree of preferential transport, the normalized 5% arrival time was derived from the breakthrough curves. This is an indicator for early arrival of the applied solute (Knudby and Carrera, 2005; Koestel et al., 2011). Details of the calculation of the 5% arrival time are given in Larsbo et al. (2014). A large value of the normalized 5% arrival time indicates a low degree of preferential transport.

4.12 Near-saturated hydraulic conductivity

After the solute transport experiment, near-saturated hydraulic conductivity was measured at pressure potentials of -1.3 and -6 cm for the samples in the PVC cylinders under steady-state conditions using a tension disc infiltrometer. The soil surface was carefully smoothed, and a layer of about 0.5 cm of fine sand was applied on top to ensure good contact between the soil and the infiltrometer.

The diameter of the largest water-filled pores during the irrigation experiments at both intensities were estimated by assuming a linear relationship between log-transformed pressure potentials and near-saturated hydraulic conductivities (Jarvis et al., 2013; Larsbo et al., 2014). Pressure potentials were then converted to effective pore diameters using the Young-Laplace equation as in section 4.6. The degree of saturation in macropores during the solute transport experiments was estimated from the diameters of largest water-filled pores and macropore size distributions derived from the X-ray tomography.

4.13 Statistical analysis

Spearman rank correlation coefficients were calculated to investigate the relationships between basic soil properties, field characteristics (i.e. topography and yield), soil structure metrics, soil hydraulic properties and solute transport characteristics. This is because some of the variables were not normally distributed. Also, ordinary, multiple and step-wise linear regression analyses were carried out to examine the extent to which predictor variables could explain the variations in dependent variables. For Paper II, the results of multiple linear regression analysis were further analyzed to derive the relative contributions of SOC and clay to the total variances of the dependent variables (i.e. soil porosities) using the function “lmg” available in the R package “relaimpo”. Details of the statistical analyses are available in the respective papers. $P < 0.05$ was used as significance level. All the statistical analyses were performed using R (R core team, 2019).

5. Results

5.1 Explanatory variables for the spatial variation in soil organic carbon: Field scale results and regional data comparison (Paper I)

The measurements of soil texture and SOC contents from 2017 (Table 1) were very similar to the ones from 2000 (i.e. clay: 9–45%, SOC: 0.6–2.7%). There was a larger variation in Feox content compared to Alox content (Table 1). The variation in mean relative yield (MRY) across the field ranged from 82% to 108% (Table 1). The elevation at the soil sampling locations varied between 87.4 m and 95.4 m.

Table 1. Basic soil properties, MRY and elevation.

	Mean	S.D.	Max.	Min.
Clay (%)	27.2	9.1	42.2	8.4
Silt (%)	47.0	12.0	61.3	19.5
Sand (%)	25.8	20.4	72.0	4.7
Soil pH	6.02	0.25	6.57	5.63
Alox (g kg^{-1})	1.61	0.25	2.13	1.08
Feox (g kg^{-1})	5.64	1.91	8.81	2.53
Elevation (m)	92.6	2.7	95.4	87.4
MRY	1.00	0.07	1.08	0.82
SOC (g kg^{-1})	17.0	4.5	27.2	11.2

There were strong correlations between soil texture, Feox and elevation (Figure 5). The MRY was positively correlated with elevation and negatively with clay (Figure 5). The SOC content was most strongly and positively correlated with Alox content compared to the other soil properties and elevation. SOC was also positively correlated with MRY and elevation and negatively with clay and soil pH.

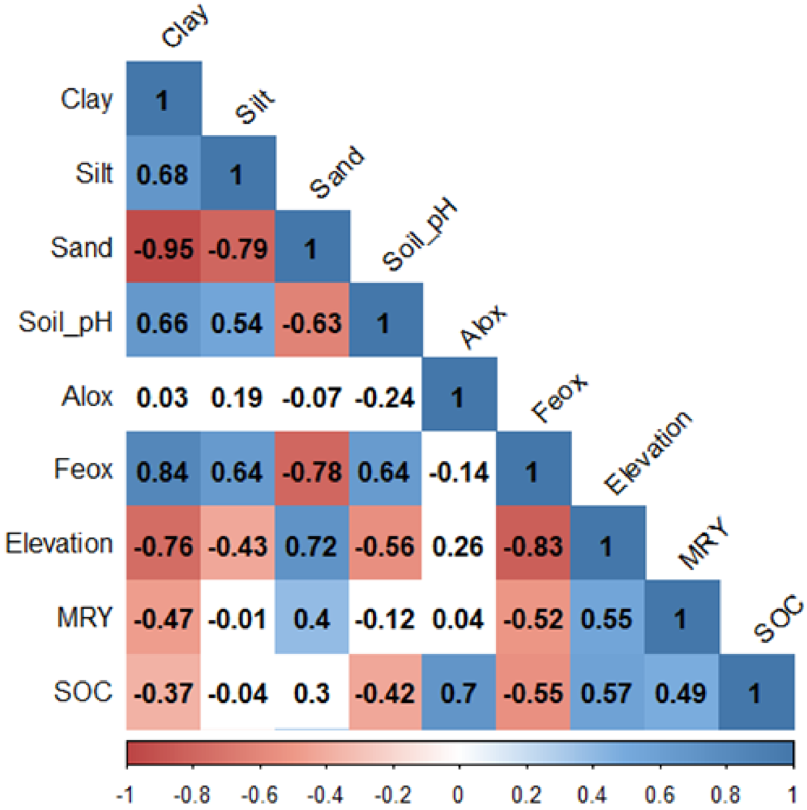

	Clay	Silt	Sand	Soil_pH	Alox	Feox	Elevation	MRY	SOC
Clay	1								
Silt	0.68	1							
Sand	-0.95	-0.79	1						
Soil_pH	0.66	0.54	-0.63	1					
Alox	0.03	0.19	-0.07	-0.24	1				
Feox	0.84	0.64	-0.78	0.64	-0.14	1			
Elevation	-0.76	-0.43	0.72	-0.56	0.26	-0.83	1		
MRY	-0.47	-0.01	0.4	-0.12	0.04	-0.52	0.55	1	
SOC	-0.37	-0.04	0.3	-0.42	0.7	-0.55	0.57	0.49	1

Figure 5. Spearman rank correlation coefficients for relationships between basic soil properties, MRY and elevation. Significant correlations ($P < 0.05$) were highlighted either in red (negative) or in blue (positive).

From step-wise regression analysis, Alox, Feox, silt and MRY were selected as explanatory variables and this best-fit model explained 77% of the variation in SOC (Table 2). The multiple linear models using Alox with either Feox or MRY also explained 70% of the variation in SOC. Finally, Alox content alone explained 48% of the SOC variation.

A similar correlation analysis performed on the literature data sets showed that SOC was positively correlated with Alox, whereas it was not correlated with clay, soil pH and Feox, except that SOC was positively correlated with clay for samples with clay content >15% in Blombäck et al. (2021) (Table 5 in Paper I). The combined dataset also showed a positive correlation between Alox and SOC, while there were no correlations between SOC and the other soil properties (Figure 6).

Table 2. The results of regression analysis. The units of variables are reported in Table 1.

	Regression model	Adj. R^2
1	SOC = 10.1 Alox – 1.4 Feox+ 0.1 Silt + 12.8 MRY – 9.3	77.1 %
2	SOC = 11.8 Alox – 1.1 Feox + 5.0	69.6 %
3	SOC = 12.5 Alox + 30 MRY – 33.2	69.6 %
4	SOC = 12.8 Alox – 3.6	48.4 %

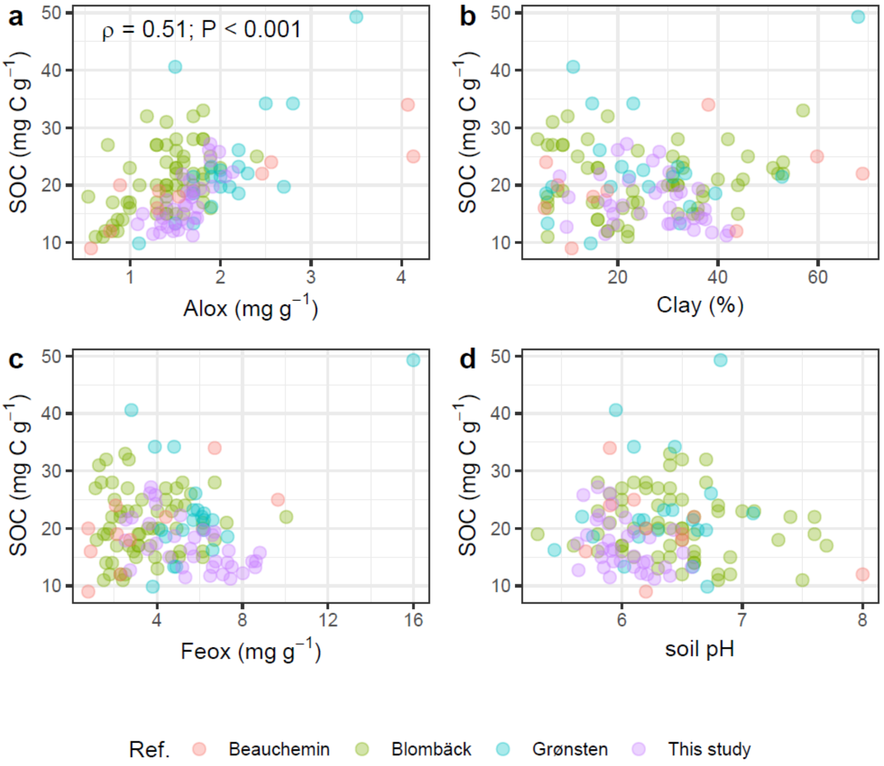

Figure 6. The relationships between SOC (or total C) and basic soil properties for the combined dataset (this study + literature data).

5.2 SOM fractionation and silt-sized aggregates (Papers I and II)

Mechanical soil dispersion and wet-sieving completely destroyed aggregates >63 µm (i.e. the sand content measured by the texture analysis and the sand-sized mass fraction fell on the 1:1 line, see Figure S3 in Paper I). Therefore, the Sand-OM fraction was regarded as being associated with sand-sized particles alone and not with aggregates. A statistical summary of the results of SOM fractionation is shown in Table 3 in Paper I. A large proportion of SOC was contained in the silt- and clay-sized (SC) fraction (ca. 80%) and SC-C and rSOC contents contributed to 67.5% and 14.2% of total SOC content (Table 3 in Paper I). The proportions of POM-C and Sand-C to total SOC were 5.0% and 5.6%, respectively (Table 3 in Paper I). The C:N ratios of the

Sand-OM and POM fractions (20.7 and 19.8) were much higher than in the bulk SOM (11.6) and SC-OM fraction (11.3). The C:N ratio for the rSOM in the SC fraction was the largest among the SOM fractions; however, this result may not be reliable because nitrogen contents in this fraction were close to the detection limit.

The Sand-C content was negatively correlated with soil pH, clay and Feox (Figure 7). POM-C content was positively correlated with SOC content and negatively with soil pH (Figure 7). SC-C and rSOC were positively correlated with Alox, SOC, MRY and elevation (Figure 7).

	Clay	Silt	Sand	SOC	Soil_pH	Alox	Feox	Elevation	MRY
SC-C	-0.34	0	0.24	0.98	-0.35	0.64	-0.53	0.58	0.55
Sand-C	-0.6	-0.43	0.58	0.17	-0.53	0.05	-0.35	0.17	0.13
POM-C	-0.15	-0.17	0.21	0.43	-0.34	0.28	-0.25	0.23	-0.09
rSOC	-0.45	-0.1	0.35	0.89	-0.47	0.72	-0.6	0.7	0.47

Figure 7. Spearman rank correlation coefficients for relations between SOC fractions, basic soil properties, MRY and elevation). The unit for the SOC content in each fraction is mg C g^{-1} bulk soil. Significant correlations ($P < 0.05$) were highlighted either in red (negative) or in blue (positive).

The C:N ratios of bulk SOM and Sand-OM, SC-OM and rSOM in the SC fractions were negatively correlated with clay, soil pH and Feox, while they were positively correlated with the sand content (Table 3). The C:N ratios in the bulk SOM and SC-OM fractions were also positively correlated with Alox and with the total SOC content in bulk soil and SC-C content (Table 3).

Table 3. Spearman rank correlation coefficients for the relationships between soil properties and C:N ratios of bulk SOM and SOM fractions. Values in bold indicates significant correlations ($P < 0.05$).

	Clay	Sand	Soil pH	Alox	Feox	SOC
Bulk SOM	**-0.81**	**0.78**	**-0.74**	**0.41**	**-0.81**	**0.66**[1]
POM	-0.28	0.27	-0.25	-0.28	-0.01	-0.14[2]
Sand-OM	**-0.58**	**0.63**	**-0.41**	-0.01	**-0.47**	-0.06[3]
SC-OM	**-0.75**	**0.70**	**-0.69**	**0.47**	**-0.82**	**0.69**[4]
rSOM in SC	**-0.80**	**0.74**	**-0.57**	0.21	**-0.70**	**0.65**[5]

SOC content in bulk soil (total SOC)[1] or each SOM fraction (POM-C[2], sand-C[3], SC-C[4] or rSOC[5]). The unit is mg C g^{-1} bulk soil.

Figure 8a shows an example of how the removal of SOM changed particle and aggregate size distributions in the MD treatment relative to the particle size distribution in the DSR treatment. Figure 8b shows that the removal of SOM increased the volume of particles in the diameter classes <0.5, 0.5–1 and 1–2 µm, whereas it decreased volumes in the 2–6 and 6–20 µm diameter classes. Also, there was a positive correlation between SC-C content and the difference DSR – MD in the < 2 µm diameter range (Figure 8c).

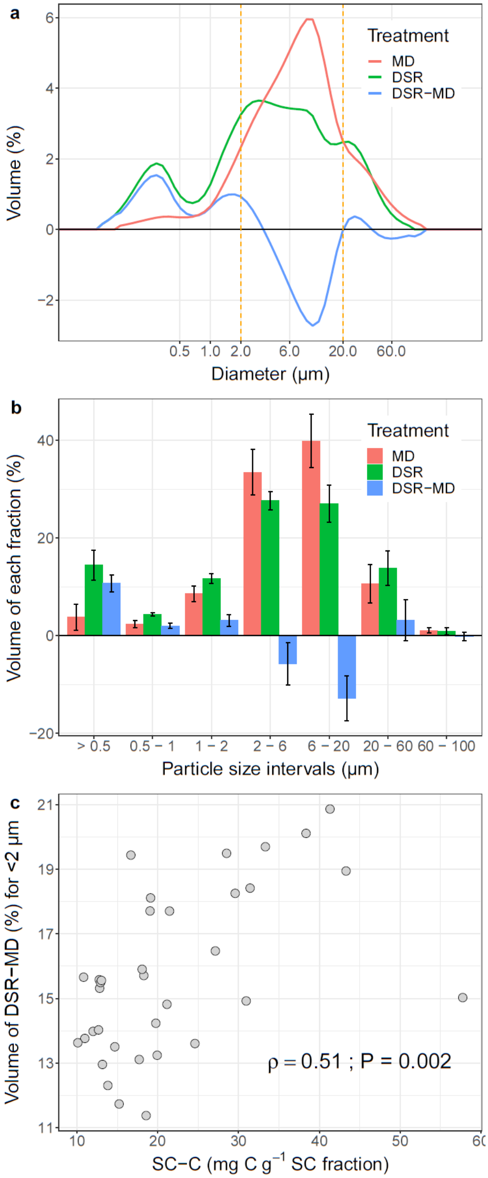

Figure 8. (a) An example of particle and aggregate size distributions of volumes in MD and DSR and their differences (DSR – MD), (b) mean and standard deviation of volumes of particles and aggregates in the fractions of <0.5, 0.5–1, 1–2, 2–6, 6–20, 20–60 and 60–100 µm diameter classes for the MD and DSR treatments and their difference and (c) the relationship between SOC content in the SC fraction and volume of clay-sized particles (<2 µm) that was released upon SOM removal (i.e. DSR – MD).

5.3 Relations between SOC and the pore size distribution as affected by variations in soil properties (Paper II)

In this section and in Paper II, the POM-C and Sand-C contents were combined and denoted POM-C. Both components were considered to represent labile SOC, with their high and similar C:N ratios (see section 5.2).

Correlations between soil properties and macroporosity and bioporosity derived by X-ray tomography and the porosities derived by soil water retention are reported in Figures 3, 4 and 5 in Paper II. With respect to the macropore size distributions, the porosities in the 720–3120 µm diameter classes were positively correlated with the clay content but not with SOC, while the porosities in the 240–720 µm diameter classes were positively correlated with SOC (Figure 3, Paper II). The biopore size distribution was also mostly correlated with soil texture but not with SOC content (Figure 4, Paper II). The porosities estimated from soil water retention were also more strongly correlated with the clay content than the SOC content, except for total porosity and porosities in the 0.2–5 and >100 µm classes (Figure 5, Paper II). The porosities larger than 0.2 µm diameter were positively correlated with SOC content.

The soil porosities in all diameter classes were generally not correlated with Alox. Also, due to strong correlations of POM-C, Feox and the C:N ratio of SOM with clay content (Figure 2 in Paper II), their importance for the pore size distribution are unclear. Finally, volumetric water contents at the applied pressure potential were strongly correlated with clay content, but not with SOC content except at -30 cm (Figure S4 in Paper II).

Multiple linear regression analysis using SOC and clay content as explanatory variables was performed to (1) quantify the responses of soil porosity in different diameter classes to increases in SOC and clay contents, and (2) examine the extent to which SOC and clay can explain the variations in these pore size classes as presently observed. Since in this thesis, the focus is on the relationship between SOC and pore size distribution, this analysis was performed for pore classes that were significantly correlated with SOC based on Spearman correlation coefficients. There were larger increases of the porosities in the 0.2–5 and 480–720 µm diameter classes with a 1% mass increase of SOC compared to the other pore diameter classes (Figure 9a). The multiple linear regression coefficients for SOC for the porosities in 10–30 and 30–100 µm diameter classes were not significantly different from zero (Figure 9a), because these porosities were more strongly correlated with clay content (Figure S5 and S6, Paper II). There was a much larger increase in porosity in the <0.2 µm diameter class with an increase of clay content compared to the porosities in the other pore diameter classes (Figure 9b). The analysis of the relative importance of SOC and clay in explaining the total variances in soil porosities indicated that the total porosity and the porosities in the 0.2–5 and 480–720 µm diameter classes were more strongly associated with SOC content compared to clay content (Figure 9c).

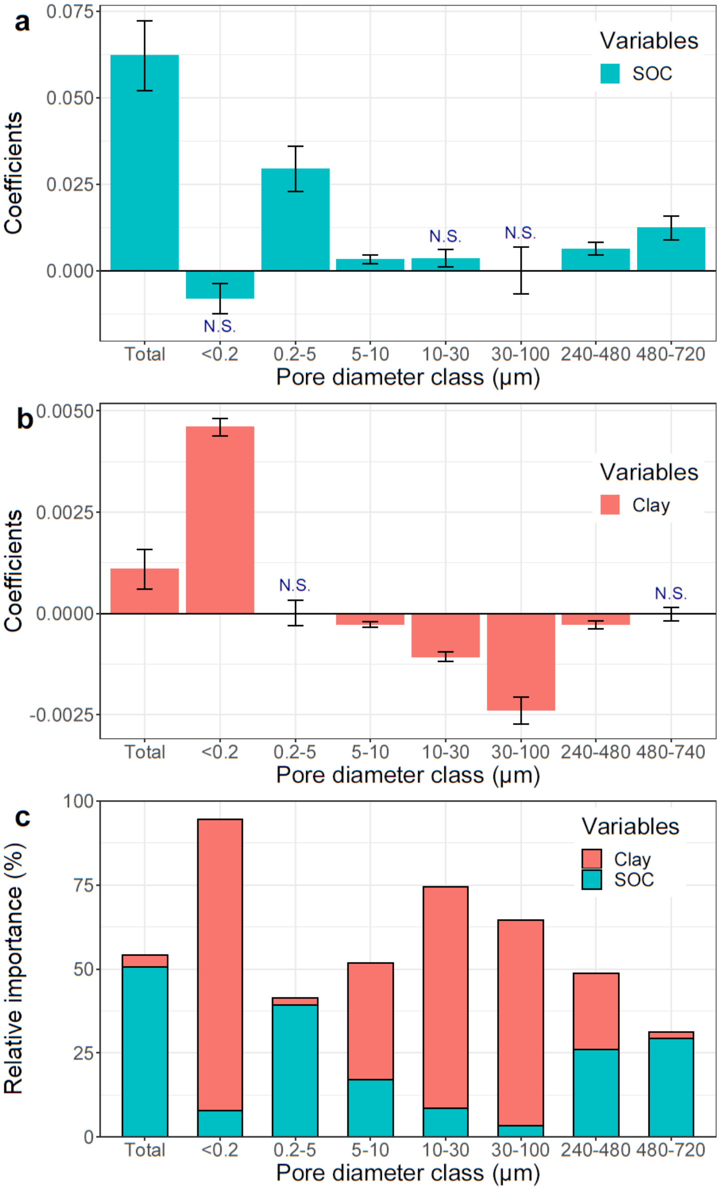

Figure 9. The results of multiple linear regression analysis with SOC (%) and Clay (%) as explanatory variables for the selected soil porosities. (a) Coefficients for SOC for each regression model, (b) coefficients for Clay for each regression model and (c) relative importance of SOC and Clay to total variance of each porosity explained by the models. Total porosity and the porosities <100 µm diameter classes were calculated from bulk density and soil water retention whereas the porosities in 240 – 720 µm diameter classes were derived from X-ray tomography.

5.4 Soil pore characteristics, water flow and solute transport (Paper III)

A correlation analysis of relationships between X-ray derived pore size distribution and macropore characteristics showed that specific macropore surface area and fractal dimension were strongly correlated with the abundance of smaller macropores (<720 µm in diameter) than larger macropores, whereas the opposite was true for connection probability, critical pore diameter and percolating fraction (Figure 10). It should be noted that 34 out of 35 samples were percolating (i.e. the pore network was connected from top to bottom of the ROI).

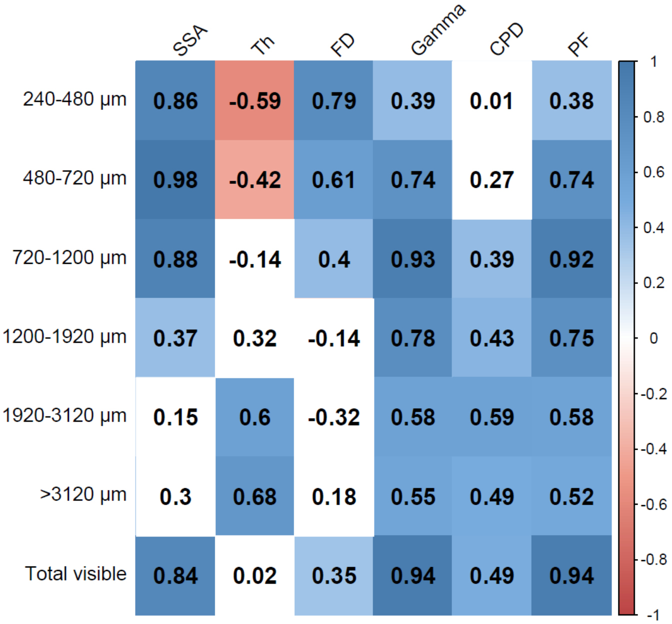

	SSA	Th	FD	Gamma	CPD	PF
240-480 µm	0.86	-0.59	0.79	0.39	0.01	0.38
480-720 µm	0.98	-0.42	0.61	0.74	0.27	0.74
720-1200 µm	0.88	-0.14	0.4	0.93	0.39	0.92
1200-1920 µm	0.37	0.32	-0.14	0.78	0.43	0.75
1920-3120 µm	0.15	0.6	-0.32	0.58	0.59	0.58
>3120 µm	0.3	0.68	0.18	0.55	0.49	0.52
Total visible	0.84	0.02	0.35	0.94	0.49	0.94

Figure 10. Correlation matrix of X-ray derived pore size distributions and macropore network characteristics. Significant correlations ($P < 0.05$) were highlighted either in red (negative) or in blue (positive). SSA: specific surface area of macropores, Th: average macropore thickness, FD: surface fractal dimension, Gamma: connection probability, CPD: critical pore diameter, PF: percolating fraction.

The normalized 5% arrival times were positively correlated with the near-saturated hydraulic conductivities at both pressure potentials, while they were negatively correlated with the estimates of the diameters of the largest water-filled pores and the degree of saturation in macropores (Figure 11).

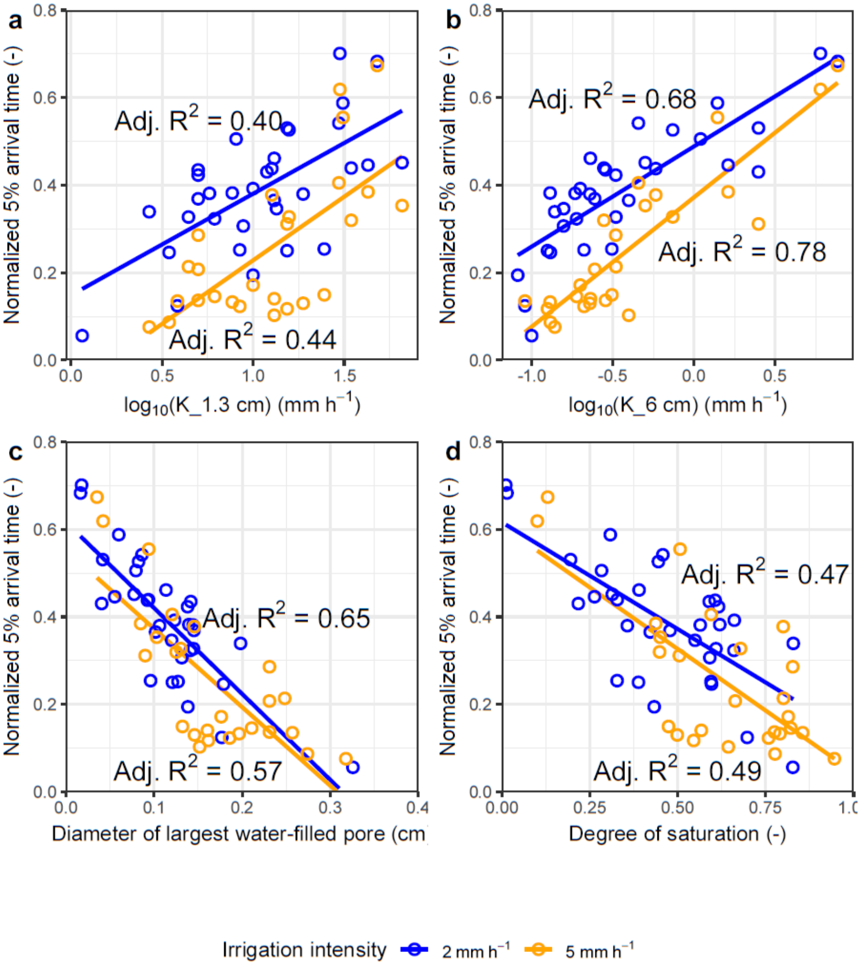

Figure 11. The relationships between (a) log-transformed near-saturated hydraulic conductivity at -1.3 cm and normalized 5% arrival time, (b) log-transformed near-saturated hydraulic conductivity at -6 cm and normalized 5% arrival time, (c) the diameters of largest water-filled pores during the irrigation experiments and normalized 5% arrival time and (d) the degree of saturation in macropores during the irrigation experiments and normalized 5% arrival time. The linear regression lines with adjusted R^2 values are displayed when the relationship was significant ($P < 0.05$).

With respect to macropore characteristics, normalized 5% arrival times were most strongly correlated with the surface fractal dimension, which explained 53% and 65% of the variation in the arrival times at the two irrigation rates (Figure 12). In contrast, arrival times were not correlated with any of the analyzed connectivity measures (i.e. connection probability, critical pore diameter and percolating fraction, Figure 5 in Paper III).

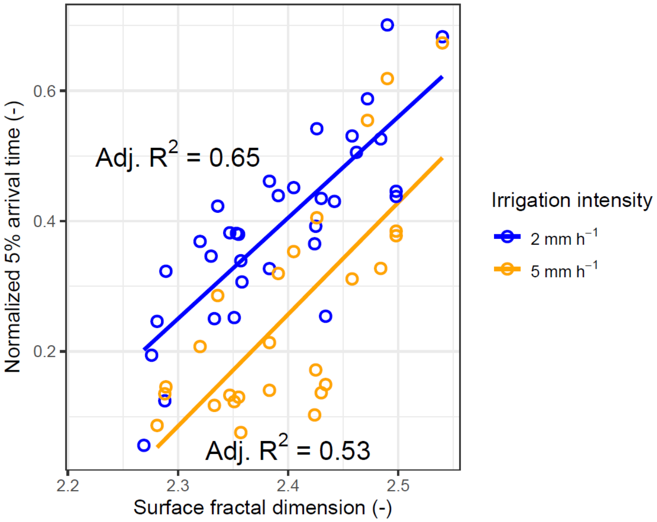

Figure 12. The relationship between surface fractal dimension and normalized 5% arrival time. The linear regression lines with adjusted R^2 values are displayed when the relationship was significant ($P < 0.05$).

Near-saturated hydraulic conductivities and normalized 5% arrival times were also positively correlated with the macroporosity in the 240–480 µm diameter class (Figure S2 in Paper III). The arrival time at an irrigation intensity of 2 mm h^{-1} was also positively correlated with the porosity in the 480–720 µm diameter class, whereas the arrival time at 5 mm h^{-1} intensity was negatively correlated with the porosities in the 1200–3120 µm diameter classes (Figure S2 in Paper III). The arrival times were positively correlated with bioporosity in the 240–480 µm diameter class, while they were negatively correlated with the bioporosities in the 720–1920 µm diameter classes except that the arrival time under 5 mm h^{-1} intensity was not correlated with the bioporosity in the 720–1200 µm diameter class (Figure S3 in Paper III).

The linear regression analyses indicated that the macroporosity in the 240–480 µm diameter class and the bioporosity in the 1200–1920 µm diameter class explained 40% and 39% of the variation in the arrival times at 2 mm h^{-1} and 5 mm h^{-1}, respectively (Figure 13a and 13d), whereas the porosities in the 480–720 µm diameter and in the 1200–1920 µm diameter classes only explained 15% of the variations in the arrival times at 2 mm h^{-1} and 5 mm h^{-1}, respectively (Figure 13b and 13c).

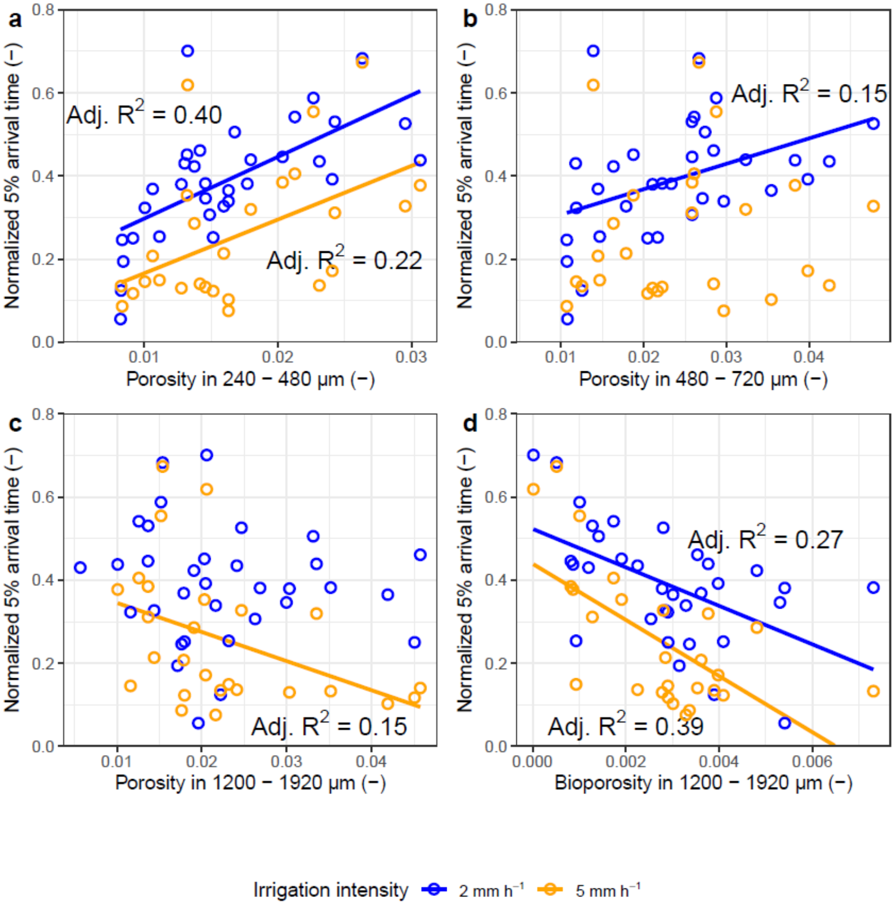

Figure 13. Relationships between normalized 5% arrival time and (a) the porosity in the 240–480 µm diameter class, (b) the porosity in the 480–720 µm diameter class, (c) the porosity in the 1200–1920 µm diameter class and (d) the bioporosity in the 1200–1920 µm diameter class. The linear regression lines with adjusted R^2 values are displayed when the relationship was significant ($P < 0.05$).

For the soil water retention data, 5% arrival times were positively correlated with the porosities in the 5–100 µm classes (Figure S4 in Paper III). In particular, the arrival times were strongly correlated with the porosity in the 30–100 µm diameter class, which explained 67–70% of the variation (Figure 14).

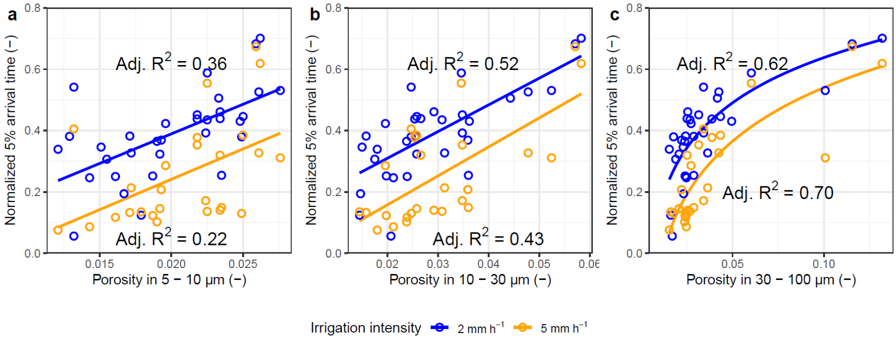

Figure 14. The relationship between normalized 5% arrival times and porosities in (a) the 5–10 µm diameter class, (b) the 10–30 µm diameter class and (c) the 30–100 µm diameter class. The regression lines with adjusted R^2 values are displayed when the relationship was significant ($P < 0.05$).

5.5 Soil properties and solute transport (Paper III)

Normalized 5% arrival times and near-saturated hydraulic conductivities were negatively correlated with clay content and positively with sand content, while the diameters of the largest water-filled pore and the degree of saturation in macropores were positively correlated with clay contents ($P < 0.05$, Figure 15). Arrival times, hydraulic conductivities and the diameters of the largest water-filled pores were not correlated with SOC content except for the conductivity at -6 cm (Figure 15).

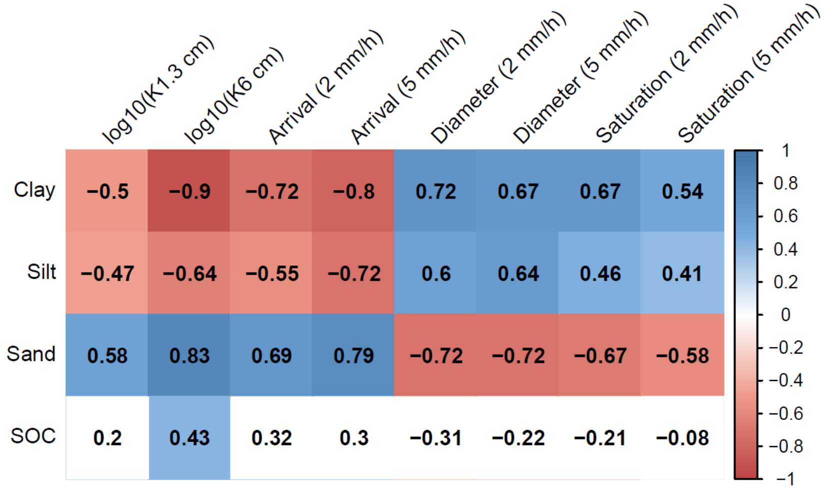

	log10(K1.3 cm)	log10(K6 cm)	Arrival (2 mm/h)	Arrival (5 mm/h)	Diameter (2 mm/h)	Diameter (5 mm/h)	Saturation (2 mm/h)	Saturation (5 mm/h)
Clay	−0.5	−0.9	−0.72	−0.8	0.72	0.67	0.67	0.54
Silt	−0.47	−0.64	−0.55	−0.72	0.6	0.64	0.46	0.41
Sand	0.58	0.83	0.69	0.79	−0.72	−0.72	−0.67	−0.58
SOC	0.2	0.43	0.32	0.3	−0.31	−0.22	−0.21	−0.08

Figure 15. Spearman rank correlation coefficients for relations between basic soil properties, normalized 5% arrival times (Arrival), log-transformed near-saturated hydraulic conductivities (K1.3 cm and K6 cm), diameters of the largest water-filled pore (Diameter) and the degree of saturation in macropores (Saturation). Significant correlations ($P < 0.05$) were highlighted either in red (negative) or in blue (positive).

6. Discussion

6.1 Alox as a key predictor for SOC

In the Bjertorp field, SOC content was most strongly correlated with Alox compared with the other measured soil properties, MRY and elevation. Since 80% of SOC was retained in the SC fraction for the Bjertorp soils, and most Alox was also expected to be present in the SC fraction (Curtin et al., 2016), it is hypothesized that the association between Alox and SOC is a key driver for the physico-chemical stabilization of SOC in these soils. The positive correlation between rSOC and Alox also indicated that Alox may be important for the formation of the stable SOC fraction. These results are consistent with previous studies (Mikutta et al., 2006; Wiaux et al., 2014). Siregar et al. (2005) and Mikutta and Kaiser (2011) also reported that NaOCl treatment did not change Alox and Feox contents. Moreover, about 67% of total SOC was present as the non-oxidation resistant SOC (SC-C – rSOC) in the SC fraction. The fractionation method used in this study does not allow a distinct separation between physically and chemically protected SOM, because chemically adsorbed SOC could be desorbed at the pH (= 8) which was used for the NaOCl treatment (Mikutta et al., 2005). However, the relatively large proportion of the non-oxidation resistant SOC content indicates that a large proportion of SOC was physically protected within silt-sized aggregates as reported in Virto et al. (2008). The analysis of particle- and aggregate-size distributions in the SC fraction showed that the removal of SOM by peroxide destroyed silt-sized aggregates (2–20 μm in diameter) and, consequently, released clay-sized particles. This result was in line with previous studies reporting the importance of SOC for aggregation where SOC acts as a binding agent for clay-sized particles (Dexter et al., 2008; Jensen et al., 2019). This result may also indicate that these silt-sized aggregates are a key driver for the physical protection of SOC in the Bjertorp field. This interpretation is supported by a positive correlation between the SC-C content and the C:N ratio of the SC-OM fraction, which indicates that a larger SC-C content is associated with fresh, less microbially-processed SC-OM possibly due to the physical protection of fine POM within the silt-sized aggregates (Shang and Tiessen, 1998; Steffens et al., 2017). As a binding agent, Alox may also play a key role in aggregation and associated physical protection (Shang and Tiessen, 1998; Asano et al., 2018). The strong correlation between SC-C and Alox found at Bjertorp suggests that Alox may have been important for the physical protection also in this study.

The field-scale result was consistent with the results from the four studies found through the literature search and with the combined dataset, which showed positive correlations between Alox and SOC for arable topsoils in humid continental climates. However, it should be noted that the coefficients of determination from linear simple regression analyses ranged from 23.1 to 74.5% in the respective studies, which indicated that other factors such as carbon input from crop production, land management and unexamined soil properties (e.g. exchangeable calcium) may also have been important (Moni et al., 2010; Ogle et al., 2012, Rasmussen et al., 2018).

6.2 Soil properties, topography and crop productivity across the field

Negative correlations were found between Feox and SOC, SC-C and rSOC in the Bjertorp field. These results suggest that the Feox may not be a key driver for SOC stabilization in the Bjertorp soil, which is in contrast to the commonly reported role of reactive Fe phases in SOC dynamics (Bailey et al., 2019; Rasmussen et al., 2018). Plausible reasons for these findings in the Bjertorp field are that (1) soil pH at Bjertorp may be too high for reactive Fe phases to effectively protect SOC (Wagai and Mayer, 2007; Bailey et al., 2019) and (2) redox cycling occurred in the field, which reduced the reactive Fe phases and decreased their capacity to protect SOC (i.e. adsorbed SOC is desorbed; Hall et al., 2018). The first explanation is supported by a positive correlation between Feox and soil pH, which means that larger Feox contents were associated with smaller adsorption capacity per mass of Feox. The soil pH in the Bjertorp field (mean = 6.0) is also relatively high compared to acidic soils for which the importance of Feox for SOC stabilization is well established (Kaiser and Guggenberger, 2000). Regarding the second possibility, redox cycles in the field were not measured in the present study, but signs of redox cycling (oxidized and reduced soil colors, Figure 2) were noted in the soil survey and profile descriptions. The positive correlation between clay and Feox and the negative correlation between Feox and elevation imply that the larger clay content in the low-lying areas could induce partially anaerobic conditions within soil aggregates (Keiluweit et al, 2018), which in turn would reduce the reactive Fe phases and prevent Feox from being effective for SOC stabilization (Hall et al., 2018; Inagaki et al., 2020). This hypothesis was also supported by the results presented in Papers II and III, which indicated that larger clay contents may lead to waterlogging and anaerobic condition due to larger water holding capacity and smaller near-saturated hydraulic conductivities.

SOC content was negatively but weakly correlated with clay content in the Bjertorp field, which suggested that clay content itself was not a key driver for SOC stabilization. These results are in line with the results from the combined dataset presented in Figure 6 as well as the studies cited in section 3.2.1. Clay (and fine silt) content has been used for modelling SOC dynamics and for estimating the degree of SOC saturation; however, based on the results in this thesis, I suggest that measuring Alox and Feox content as proxies for reactive mineral phases, in addition to clay content, should be useful for these purposes for arable topsoils in humid continental climate.

Finally, the multiple linear regression analysis indicated that carbon input from crop production, which was estimated from mean relative yield accounting for 11 years of yield records, explained ca. 20% of the spatial variation in SOC content in the Bjertorp field. Positive relationships between SOC and yield have been reported in several studies at different scales (e.g. Kravchenko and Bullock, 2000, Oldfield et al., 2019). It should be noted that this positive correlation can also be caused by the positive effects of SOC on crop growth (Oldfield et al., 2020) and there should actually be interactive feedbacks between SOC content and crop production (Henryson et al., 2018). The MRY was also negatively correlated with clay content and positively correlated with elevation, which indicated that the lower lying areas may not be as suitable for crop production as the higher lying areas in the Bjertorp field possibly due to waterlogging, which may cause lower C inputs for soils with larger clay contents. This relationship may also explain why SOC was negatively correlated with clay and Feox contents and positively with elevation, since these variables were highly correlated with one another.

6.3 Pore size distribution quantified by X-ray tomography and soil water retention

6.3.1 SOC and pore size distribution

The relatively strong association between SOC and the abundance of smaller macropores (<720 µm in diameter) found in this study was also noted by Larsbo et al. (2016), Xu et al. (2018), Singh et al., (2020) and Wang et al. (2021). A plausible mechanism behind this correlation is that the aggregation of clay-sized particles enhanced by SOC as a binding agent (as discussed in section 6.1) may have contributed to the stabilization of these small macropores. It should be noted that this positive correlation can also be caused by fine roots which can create small macropores (Bodner et al., 2014; Meurer et al., 2020a; Lucas et al., 2021) and, at the same time, be an important source of carbon (Kätterer et al., 2011). However, bioporosities were not correlated with SOC except for the bioporosity in the 480–720 µm class, which constituted a minor fraction of the total X-ray visible porosity (<0.1% of total visible porosity) and hence may have little influence on soil processes (e.g. biogeochemical cycling and water dynamics).

The porosity in diameter classes larger than 0.2 µm estimated from soil water retention data were positively correlated with SOC content. In particular, a relatively strong positive correlation between SOC and the porosity in the 0.2–5 µm dimeter class was observed. This relationship may be explained by the finding that SOC was the key binding agent for the silt-sized aggregation as shown in Figure 8, which may also enhance the formation of pores in the 0.2–5 µm class between or within the silt-sized aggregates. Again, it should be noted that there is a two-way interaction between SOC and soil pore structure (Meurer et al., 2020b), which means that pores in this diameter class can also physically protect SOC from microbial decomposition (Dugaint et al., 2012; Kravchenko and Guber, 2017). Pore diameters of 0.2 to 5 µm are too small for microbes to colonize and SOC may therefore not be accessible to them (Kravchenko et al., 2020).

The results from the Bjertorp field are in line with the analysis of the data reported in Jensen et al. (2020) and Kirchmann et al. (1999), who showed that the porosities in the 0.2–30 µm and 1–5 µm diameter classes were positively and most strongly correlated with SOC content (Table S2 and S3 in Paper II). Also, a very recent study by Fu et al. (2021) reported a strong positive correlation between SOC and porosity in the 0.2–7.5 µm diameter class compared with other pore size classes. Interestingly, the causes for variations in SOC content vary between these studies and the Bjertorp field. As discussed above, the variation in SOC in this thesis was most likely caused by variations in Alox content and the C input from crop production, whereas the variation in Jensen et al. (2020) was caused by land use changes (bare fallow, grassland and crop land). In Kirchmann et al. (1999), the variation was caused by different organic and inorganic amendments, while the variation in SOC in Fu et al. (2021) was likely caused by different land use and management (pasture and cropland with and without irrigation). On the other hand, Zhou et al. (2020) reported no correlation between SOC and the porosity in the 0.2–10 µm diameter class for Vertisols under arable land use as water contents at both field capacity and wilting point were positively correlated with SOC content. This discrepancy between the studies may indicate that the relationships between SOC and pore size distribution are dependent on soil type, particularly clay mineralogy, which can determine water adsorption capacity in micropores (Libohova et al., 2018; Lehmann et al., 2021).

6.3.2 Texture effects

Porosities in some of the macropore diameter classes were positively correlated with clay content. This can be explained by the fact that a larger clay content enhances the formation of soil cracks on drying (Horn et al., 1994; Paradelo et al., 2016b; Colombi et al., 2021). The positive correlations between clay content and bioporosity may be associated with a larger macrofaunal activity (e.g. earthworm) in loamy soils compared to sandy soils (Capowiez et al., 1998; Baker et al., 1998; Lindahl, et al., 2009).

Soil water retention and pore-size distribution estimated from soil water retention measurements were generally more strongly correlated with clay content than with SOC content. The results of multiple linear regression analyses also indicated that more SOC would be required to achieve a given soil porosity for samples with larger clay content compared with soils of smaller clay content. This is in line with previous findings that soils with larger clay content will require larger SOC content to achieve a similar degree of aggregate stability, soil structural quality and clay dispersibility (Feller and Beare, 1997; Soinne et al., 2016; Johannes et al., 2017; Jones et al., 2020; Prout et al., 2021).

Also, I found that the importance of Feox, POM-C and the C:N ratio of SOM and POM (as indicators of SOM quality) for the pore size distribution was less clear. This is because they were correlated with the clay content, and their possible influence on pore sizes cannot be discerned. Nevertheless, in the Bjertorp soils, pore size distribution could be well explained by clay and SOC content rather than other soil properties.

6.4 Preferential solute transport and soil pore structure

Based on correlation analysis, macroporosity in the 240–720 µm diameter, mesoporosity and surface fractal dimension were identified as key explanatory variables for the variations in the strength of preferential transport. These results indicate that a larger abundance of small macropores (<720 µm) and mesopores and their homogeneous distribution in soil may decrease the risk of macropore flow and preferential transport, by reducing the diameter of the largest water-filled pore and the degree of saturation in macropores. This is in line with the findings of Larsbo et al. (2014, 2016). It should be noted that the degree of preferential transport was more strongly correlated with the soil water retention derived mesoporosity than the X-ray derived macroporosity. This may be because small macropores (240–480 µm) themselves were not connected with one another and their connectivity may have been regulated by mesopores. It was confirmed, by analyzing the connectivity of small macropores (i.e. excluding macropores >480 µm diameter) illustrated in Figure 10 in Paper III, that the connection probability was smaller than 0.01 for 34 out of 35 soil samples and that none of the samples were percolating. The mesopores may also enhance diffusion of solutes into micropores (<5 µm diameter) due to their large surface area in relation to volume compared to macropores. This will further reduce the degree of preferential transport (Jarvis, 2007).

On the other hand, measures of macropore connectivity were not correlated with the degree of preferential transport. This is probably because only a small part of the macropore networks were active for water flow during the solute transport experiments as also reported by Mori et al. (1999), Luo et al. (2008) and Sammartino et al. (2015).

6.5 The potential role of SOC in water dynamics in an arable field as affected by clay content

An increase of SOC was associated with relatively large increases of the porosities in the 0.2–5 µm and the 240–480 µm diameter classes. As discussed above, the causality of the observed correlations between SOC content and soil pore size distribution is complicated. However, the results indicate that SOC sequestration would potentially be beneficial for increasing plant available water content in the Bjertorp soils. The positive relationship between smaller macropores (240–720 µm diameter class) and SOC content also indicates that the increased SOC content may be associated with an increase of the hydraulic conductivity of this pore diameter class. However, correlation analysis showed a limited effect of SOC content on hydraulic conductivity at -6 cm and, hence, on the prevention of preferential transport, possibly because the near-saturated hydraulic conductivities and the mesoporosities in the 30–100 µm diameter class were much more strongly correlated with clay content than SOC content. In other words, if there would have been no or small variations in clay content in the studied soils, positive effects of SOC on near-saturated hydraulic conductivity and the degree of preferential transport may have been detected. Thus, for sites where clay content was relatively constant among samples, Larsbo et al. (2016) and Paradelo et al. (2016b) reported that larger SOC content reduced the risk of preferential transport. It should, however, be noted that the variations in the SOC content in these studies (4–15% and 1.8–8.4% SOC, respectively) were much larger than in the Bjertorp field (1.1–2.7% SOC).

7. Conclusions and future perspectives

In this thesis, relationships between SOC, soil structure, water flow and solute transport were investigated for an arable field with a topsoil that has large variations in soil properties, including texture and reactive mineral phases. The conclusions are summarized in Figure 16. In the Bjertorp field, the reactive Al phases, estimated from Alox content, were found to be a key driver for physico-chemical stabilization of SOC in the silt- and clay-sized fraction, based on the results from SOM fractionation and analysis of silt-sized aggregate distributions. These results for one field were supported by data from the literature collected at sites with similar climates. This indicates the potential importance of Alox for SOC stabilization in arable topsoils in humid continental climates. On the other hand, clay and Feox were neither key predictors for SOC in the Bjertorp field, nor for the SOC data collected from the literature.

The relationships found between SOC and the soil pore size distribution indicated that increased SOC sequestration in arable topsoils may lead to an increase in plant available water and water infiltration in smaller macropores. The activation of preferential transport was regulated by the abundance of small macropores and mesopores (5–100 and 240–720 µm), but not by the large diameter macroporores and their connectivity. Larger SOC contents may therefore potentially reduce the risk of preferential transport; however, correlation analysis indicated limited effects of SOC on the degree of preferential transport at Bjertorp probably due to the large variations in clay content.

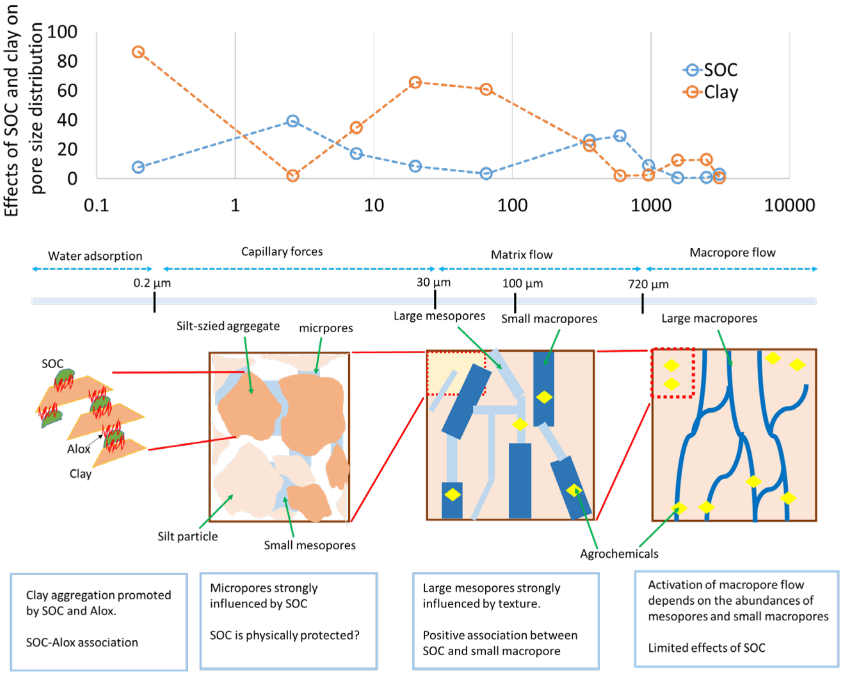

Clay aggregation promoted by SOC and Alox.

SOC-Alox association

Micropores strongly influenced by SOC

SOC is physically protected?

Large mesopores strongly influenced by texture.

Positive association between SOC and small macropore

Activation of macropore flow depends on the abundances of mesopores and small macropores

Limited effects of SOC

Figure 16. Schematic illustration of the findings presented in the thesis. The graph at the top shows the relative importance of SOC and clay for explaining the total variance in soil porosities in various pore diameter classes (unit: µm).

The results presented in this thesis were mainly based on correlation and regression analyses for data obtained at the field scale. This type of analysis is very useful for describing possible interactions in a system and for developing hypotheses. However, causalities cannot be determined from correlations alone. I have tried to explain the observed correlations from available theory and, in some cases, by conducting additional experiments. Still, in many cases the causality remains an open question. For future studies I would suggest the following perspectives.

To better clarify the role of Alox for the stabilization of SOC for arable soils under humid continental climates, the relation between Alox and SOC turnover rate needs to be examined by conducting, for example, incubations experiments using soil samples with large variations in SOC and Alox. Quantification of organo-metal associations will also be helpful. This could be achieved by (1) measuring dissolved reactive mineral phases (Al and Fe) and dissolved organic carbon after extraction experiments (e.g. sodium-pyrophosphate, Wagai et al., 2020) and examining relationships between dissolved metals and organic carbon and (2) mapping the spatial variations in carbon, Fe and Al on the surface of soil clay- and silt-sized particles (e.g. with NanoSIMS, Inagaki et al., 2020). If these kinds of studies provide further evidence for the role of Alox for the protection of SOC, the Alox and SOC relationships should then be up-scaled to regional or national scale by conducting national soil inventory. For this purpose, carbon input and other soil properties should ideally also be considered.

The complex dynamic interactions between soil macropores, SOC, root growth and faunal activity has not been extensively studied (Meurer et al., 2020a). More work needs to be done to examine and clarify the causalities behind the observed correlations between SOC and smaller-diameter macropores. In particular, root growth can influence both macropore abundance and SOC content. Also, compared to the effects of mesoporosity on POM-C turnover rate (Kravchenko et al., 2015), the direct evidence of physical protection of SOC within micropores (e.g. 0.2–5 µm) is not fully understood. Combining different high resolution imaging techniques may allow us to determine the extent to which SOC is located within such small pores (e.g. Schlüter et al., 2019; Ost et al., 2021; Witzgall et al., 2021).

The results from Paper III indicated that smaller macropores and mesopores, instead of larger macropores and their connectivity, may play a key role in preventing the activation of water flow even for well-connected macropore networks. Direct imaging of water flow and solute transport through soil macropores (e.g. Koestel and Larsbo, 2014; Sammartino et al., 2015) may help to obtain useful parameters of macropore networks for modelling purposes, as attempted by Lissy et al. (2020). Finally, to evaluate the role of SOC in regulating preferential transport, solute transport experiments should be carried out on samples with a more typical range of SOC contents for arable soils (e.g. in Sweden, SOC <3.5%, Eriksson et al., 2010), but without large variations in soil texture.

References

Araya, S. N., & Ghezzehei, T. A. (2019). Using Machine Learning for Prediction of Saturated Hydraulic Conductivity and Its Sensitivity to Soil Structural Perturbations. *Water Resources Research,* 55(7), 5715-5737. https://doi.org/10.1029/2018WR024357

Asano, M., Wagai, R., Yamaguchi, N., Takeichi, Y., Maeda, M., Suga, H., & Takahashi, Y. (2018). In Search of a Binding Agent: Nano-Scale Evidence of Preferential Carbon Associations with Poorly-Crystalline Mineral Phases in Physically-Stable, Clay-Sized Aggregates. *Soil Systems*, 2(2), 32. https://doi.org/10.3390/soilsystems2020032

Augustin, C., & Cihacek, L. J. (2016). Relationships Between Soil Carbon and Soil Texture in the Northern Great Plains. *Soil Science*, 181(8), 386-392. doi:10.1097/ss.0000000000000173

Bailey, V. L., Pries, C. H. & Lajtha, K. (2019). What do we know about soil carbon destabilization? *Environmental Research Letters*, 14(8), 083004. https://doi.org/10.1088/1748-9326/ab2c11

Baker, G. H., Carter, P. J., Curry, J. P., Cultreri, O. & Beck, A. (1998). Clay content of soil and its influence on the abundance of Aporrectodea trapezoides Dugès (Lumbricidae). *Applied Soil Ecology*, 9(1), 333-337. https://doi.org/10.1016/S0929-1393(98)00085-7

Beare, M.H., McNeill, S.J., Curtin, D., Parfitt, R.L., Jones, H.S., Dodd, M.B. & Sharp, J. (2014). Estimating the organic carbon stabilisation capacity and saturation deficit of soils: a New Zealand case study. *Biogeochemistry*, 120(1), 71-87. https://doi.org/10.1007/s10533-014-9982-1

Beauchemin, S., Simard, R.R., Bolinder, M.A., Nolin, M.C. & Cluis, D. (2003). Prediction of phosphorus concentration in tile-drainage water from the Montreal Lowlands soils. *Canadian Journal of Soil Science*, 83(1), 73-87. https://doi.org/10.4141/S02-029

Beck, H.E., Zimmermann, N.E., McVicar, T.R., Vergopolan, N., Berg, A. & Wood, E.F. (2018). Present and future Köppen-Geiger climate classification maps at 1-km resolution. *Scientific Data*, 5(1), 180214. https://doi.org/10.1038/sdata.2018.214

Blombäck, K., Bolster, C. H., Lindsjö, A., Hesse, K., Linefur, H. & Parvage, M.M. (2021). Comparing measures for determination of phosphorus saturation as a method to estimate dissolved P in soil solution. *Geoderma*, 383, 114708. https://doi.org/10.1016/j.geoderma.2020.114708

Bodner, G., Leitner, D., & Kaul, H.-P. (2014). Coarse and fine root plants affect pore size distributions differently. *Plant and Soil*, 380(1), 133-151. https://doi.org/10.1007/s11104-014-2079-8

Bolinder, M. A., Janzen, H. H., Gregorich, E. G., Angers, D. A. & VandenBygaart, A. J. (2007). An approach for estimating net primary productivity and annual carbon inputs to soil for common agricultural crops in Canada. *Agriculture, Ecosystems & Environment*, 118(1), 29-42. https://doi.org/10.1016/j.agee.2006.05.013

Bronick, C.J. & Lal, R. (2005). Soil structure and management: a review. *Geoderma*, 124(1), 3-22. https://doi.org/10.1016/j.geoderma.2004.03.005

Capowiez, Y., Pierret, A., Daniel, O., Monestiez, P. & Kretzschmar, A. (1998). 3D skeleton reconstructions of natural earthworm burrow systems using CAT scan images of soil cores. *Biology and Fertility of Soils*, 27(1), 51-59. https://doi.org/10.1007/s003740050399

Chenu, C., Angers, D.A., Barré, P., Derrien, D., Arrouays, D. & Balesdent, J. (2019). Increasing organic stocks in agricultural soils: Knowledge gaps and potential innovations. *Soil and Tillage Research*, 188, 41-52 https://doi.org/10.1016/j.still.2018.04.011

Colombi, T., Kirchgessner, N., Iseskog, D., Alexandersson, S., Larsbo, M. & Keller, T. (2021). A time-lapse imaging platform for quantification of soil crack development due to simulated root water uptake. *Soil and Tillage Research*, 205, 104769. https://doi.org/10.1016/j.still.2020.104769

Curtin, D., Beare, M.H. & Qiu, W. (2016). Texture effects on carbon stabilisation and storage in New Zealand soils containing predominantly 2 : 1 clays. *Soil Research*, 54(1), 30-37. https://doi.org/10.1071/SR14292

Dexter, A.R., Richard, G., Arrouays, D., Czyż, E.A., Jolivet, C. & Duval, O. (2008). Complexed organic matter controls soil physical properties. *Geoderma*, 144(3), 620-627. https://doi.org/10.1016/j.geoderma.2008.01.022

Dungait, J.A.J., Hopkins, D.W., Gregory, A.S. & Whitmore, A.P. (2012). Soil organic matter turnover is governed by accessibility not recalcitrance. *Global Change Biology*, 18(6), 1781-1796. https://doi.org/10.1111/j.1365-2486.2012.02665.x

Eriksson, J., Matsson, L. Söderström, M. (2010). Tillståndet i svensk åkermark och gr¨oda, data från 2001–2007. (“Current status of Swedish arable soils and cereal crops. Swedish Environmental Protection Agency, Stockholm, Sweden (In Swedish).

Feller, C. & Beare, M. H. (1997). Physical control of soil organic matter dynamics in the tropics. *Geoderma*, 79(1), 69-116. https://doi.org/10.1016/S0016-7061(97)00039-6

Fu, Z., Hu, W., Beare, M., Thomas, S., Carrick, S., Dando, J., Langer, S., Müller, K., Baird, D. & Lilburne, L. (2021). Land use effects on soil hydraulic properties and the contribution of soil organic carbon. *Journal of Hydrology*, 602, 126741. https://doi.org/10.1016/j.jhydrol.2021.126741

Grønsten, H.A. & Børresen, T. (2009). Comparison of two methods for assessment of aggregate stability of agricultural soils in southeast Norway. *Acta Agriculturae Scandinavica, Section B — Soil & Plant Science*, 59(6), 567-575. https://doi.org/10.1080/09064710802495356

Gregorich, E.G., Beare, M.H., McKim, U.F. & Skjemstad, J.O. (2006). Chemical and Biological Characteristics of Physically Uncomplexed Organic Matter. *Soil Science Society of America Journal*, 70(3), 975-985. https://doi.org/10.2136/sssaj2005.0116

Hall, S.J., Berhe, A.A. & Thompson, A. (2018). Order from disorder: do soil organic matter composition and turnover co-vary with iron phase crystallinity? *Biogeochemistry*, 140(1), 93-110. https://doi.org/10.1007/s10533-018-0476-4

Henryson, K., Sundberg, C., Kätterer, T., & Hansson, P.-A. (2018). Accounting for long-term soil fertility effects when assessing the climate impact of crop cultivation. *Agricultural Systems*, 164, 185-192. https://doi.org/10.1016/j.agsy.2018.03.001

Horn, R., Taubner, H., Wuttke, M. & Baumgartl, T. (1994). Soil physical properties related to soil structure. *Soil and Tillage Research*, 30(2), 187-216. http://doi.org/10.1016/0167-1987(94)90005-1

Hudson, B. D. (1994). Soil organic matter and available water capacity. *Journal of Soil and Water Conservation*, 49(2), 189-194. Retrieved from http://www.jswconline.org/content/49/2/189.abstract

Inagaki, T.M., Possinger, A.R., Grant, K.E., Schweizer, S.A., Mueller, C.W., Derry, L.A., Lehmann, J. & Kögel-Knabner, I. (2020). Subsoil organo-mineral associations under contrasting climate conditions. *Geochimica et Cosmochimica Acta*, 270, 244-263. https://doi.org/10.1016/j.gca.2019.11.030

Jarvis, N., Forkman, J., Koestel, J., Kätterer, T., Larsbo, M. & Taylor, A. (2017). Long-term effects of grass-clover leys on the structure of a silt loam soil in a cold climate. *Agriculture, Ecosystems & Environment*, 247, 319-328. https://doi.org/10.1016/j.agee.2017.06.042

Jarvis, N., Koestel, J. & Larsbo, M. (2016). Understanding Preferential Flow in the Vadose Zone: Recent Advances and Future Prospects. *Vadose Zone Journal*, 15(12), https://doi.org/10.2136/vzj2016.09.0075

Jarvis, N., Koestel, J., Messing, I., Moeys, J. & Lindahl, A. (2013). Influence of soil, land use and climatic factors on the hydraulic conductivity of soil. *Hydrology and Earth System Sciences,* 17(12), 5185-5195. https://doi.org/10.5194/hess-17-5185-2013, 2013.

Jarvis, N.J. (2007). A review of non-equilibrium water flow and solute transport in soil macropores: principles, controlling factors and consequences for water quality. *European Journal of Soil Science*, 58(3), 523-546. https://doi.org/10.1111/j.1365-2389.2007.00915.x

Jarvis, N.J., Moeys, J., Koestel, J. & Hollis, J.M. (2012). Chapter 3 - Preferential Flow in a Pedological Perspective. In H. Lin (Ed.), *Hydropedology* (pp. 75-120). Boston: Academic Press. https://doi.org/10.1016/B978-0-12-386941-8.00003-4

Jensen, J.L., Schjønning, P., Watts, C.W., Christensen, B.T. & Munkholm, L.J. (2020). Short-term changes in soil pore size distribution: Impact of land use. *Soil and Tillage Research*, 199, 104597. https://doi.org/10.1016/j.still.2020.104597

Jensen, J.L., Schjønning, P., Watts, C.W., Christensen, B.T., Peltre, C. & Munkholm, L.J. (2019). Relating soil C and organic matter fractions to soil structural stability. *Geoderma*, 337, 834-843. https://doi.org/10.1016/j.geoderma.2018.10.034

Johannes, A., Matter, A., Schulin, R., Weisskopf, P., Baveye, P.C. & Boivin, P. (2017). Optimal organic carbon values for soil structure quality of arable soils. Does clay content matter? *Geoderma*, 302, 14-21. http://doi.org/10.1016/j.geoderma.2017.04.021

Jones, E. J., Filippi, P., Wittig, R., Fajardo, M., Pino, V. & McBratney, A.B. (2021). Mapping soil slaking index and assessing the impact of management in a mixed agricultural landscape. *SOIL*, 7(1), 33-46. https://doi.org/10.5194/soil-7-33-2021

Kaiser, K. & Guggenberger, G. (2000). The role of DOM sorption to mineral surfaces in the preservation of organic matter in soils. *Organic Geochemistry*, 31(7), 711-725. doi:https://doi.org/10.1016/S0146-6380(00)00046-2

Kätterer, T., Andrén, O. & Jansson, P.E. (2006). Pedotransfer functions for estimating plant available water and bulk density in Swedish agricultural soils. *Acta Agriculturae Scandinavica, Section B — Soil & Plant Science*, 56(4), 263-276. https://doi.org/10.1080/09064710500310170

Kätterer, T., Bolinder, M.A., Andrén, O., Kirchmann, H. & Menichetti, L. (2011). Roots contribute more to refractory soil organic matter than above-ground crop residues, as revealed by a long-term field experiment. *Agriculture, Ecosystems & Environment*, 141(1), 184-192. doi:https://doi.org/10.1016/j.agee.2011.02.029

Keiluweit, M., Gee, K., Denney, A. & Fendorf, S. (2018). Anoxic microsites in upland soils dominantly controlled by clay content. *Soil Biology and Biochemistry*, 118, 42-50. https://doi.org/10.1016/j.soilbio.2017.12.002

Keller, T., Sutter, J. A., Nissen, K., & Rydberg, T. (2012). Using field measurement of saturated soil hydraulic conductivity to detect low-yielding zones in three

Swedish fields. *Soil and Tillage Research*, 124, 68-77. https://doi.org/10.1016/j.still.2012.05.002

Kirchmann, H. & Gerzabek, M.H. (1999). Relationship between soil organic matter and micropores in a long-term experiment at Ultuna, Sweden. *Journal of Plant Nutrition and Soil Science*, 162(5), 493-498. https://doi.org/10.1002/(SICI)1522-2624(199910)162:5<493::AID-JPLN493>3.0.CO;2-S

Kleber, M., Eusterhues, K., Keiluweit, M., Mikutta, C., Mikutta, R. & Nico, P.S. (2015). Chapter One - Mineral–Organic Associations: Formation, Properties, and Relevance in Soil Environments. In D. L. Sparks (Ed.), *Advances in Agronomy* (Vol. 130, pp. 1-140): Academic Press. https://doi.org/10.1016/bs.agron.2014.10.005

Knudby, C. & Carrera, J. (2005). On the relationship between indicators of geostatistical, flow and transport connectivity. *Advances in Water Resources*, 28(4), 405-421. http://doi.org/10.1016/j.advwatres.2004.09.001

Koestel, J. (2018). SoilJ: An ImageJ Plugin for the Semiautomatic Processing of Three-Dimensional X-ray Images of Soils. *Vadose Zone Journal*, 17(1), 170062. https://doi.org/10.2136/vzj2017.03.0062

Koestel, J., Dathe, A., Skaggs, T.H., Klakegg, O., Ahmad, M.A., Babko, M., Giménez, D., Farkas, C., Nemes, A. & Jarvis, N. (2018). Estimating the Permeability of Naturally Structured Soil From Percolation Theory and Pore Space Characteristics Imaged by X-Ray. *Water Resources Research*, 54(11), 9255-9263. https://doi.org/10.1029/2018WR023609

Koestel, J. & Larsbo, M. (2014). Imaging and quantification of preferential solute transport in soil macropores. *Water Resources Research*, 50(5), 4357-4378. https://doi.org/10.1002/2014WR015351

Koestel, J.K., Moeys, J. & Jarvis, N.J. (2011). Evaluation of Nonparametric Shape Measures for Solute Breakthrough Curves. *Vadose Zone Journal*, 10(4), 1261-1275. https://doi.org/10.2136/vzj2011.0010

Kravchenko, A.N. & Bullock, D.G. (2000). Correlation of Corn and Soybean Grain Yield with Topography and Soil Properties. *Agronomy Journal*, 92(1), 75-83. https://doi.org/10.2134/agronj2000.92175x

Kravchenko, A.N. & Guber, A.K. (2017). Soil pores and their contributions to soil carbon processes. *Geoderma*, 287, 31-39. https://doi.org/10.1016/j.geoderma.2016.06.027

Kravchenko, A.N., Guber, A.K., Razavi, B.S., Koestel, J., Quigley, M.Y., Robertson, G.P. & Kuzyakov, Y. (2020). Reply to: “Variables in the effect of land use on soil extrapore enzymatic activity and carbon stabilization” by Glenn (2020). *Nature Communications*, 11(1), 6427. https://doi.org/10.1038/s41467-020-19901-8

Kravchenko, A.N., Negassa, W.C., Guber, A.K. & Rivers, M.L. (2015). Protection of soil carbon within macro-aggregates depends on intra-aggregate pore characteristics. *Scientific Reports* 5, 16261. https://doi.org/10.1038/srep16261

Lal, R. (2004). Soil Carbon Sequestration Impacts on Global Climate Change and Food Security. *Science*, 304(5677), 1623-1627. doi:10.1126/science.1097396

Lal, R. (2014). Societal value of soil carbon. *Journal of Soil and Water Conservation*, 69(6), 186A-192A. https://doi.org/10.2489/jswc.69.6.186A

Lal, R. (2018). Digging deeper: A holistic perspective of factors affecting soil organic carbon sequestration in agroecosystems. *Global Change Biology*, 24(8), 3285-3301. https://doi.org/10.1111/gcb.14054

Lal, R. (2020). Soil organic matter and water retention. *Agronomy Journal*, 112(5), 3265-3277. https://doi.org/10.1002/agj2.20282

Larsbo, M., Koestel, J. & Jarvis, N. (2014). Relations between macropore network characteristics and the degree of preferential solute transport. *Hydrology and Earth System Sciences*, 18(12), 5255-5269. https://doi.org/10.5194/hess-18-5255-2014

Larsbo, M., Koestel, J., Kätterer, T. & Jarvis, N. (2016). Preferential Transport in Macropores is Reduced by Soil Organic Carbon. *Vadose Zone Journal*, 15(9). https://doi.org/10.2136/vzj2016.03.0021

Lavallee, J. M., Soong, J.L. & Cotrufo, M. F. (2020). Conceptualizing soil organic matter into particulate and mineral-associated forms to address global change in the 21st century. *Global Change Biology*, 26(1), 261-273. https://doi.org/10.1111/gcb.14859

Lehmann, J. & Kleber, M. (2015). The contentious nature of soil organic matter. *Nature*, 528(7580), 60-68. https://doi.org/10.1038/nature16069

Lehmann, P., Leshchinsky, B., Gupta, S., Mirus, B.B., Bickel, S., Lu, N. & Or, D. (2021). Clays Are Not Created Equal: How Clay Mineral Type Affects Soil Parameterization. *Geophysical Research Letters*, 48(20), e2021GL095311. https://doi.org/10.1029/2021GL095311

Li, J., Nie, M. & Pendall, E. (2020). Soil physico-chemical properties are more important than microbial diversity and enzyme activity in controlling carbon and nitrogen stocks near Sydney, Australia. *Geoderma*, 366, 114201. https://doi.org/10.1016/j.geoderma.2020.114201

Li, W., Ciais, P., Guenet, B., Peng, S., Chang, J., Chaplot, V., Khudyaev, S., Peregon, A., Piao, S., Wang, Y. & Yue, C. (2018). Temporal response of soil organic carbon after grassland-related land-use change. *Global Change Biology*, 24(10), 4731-4746. https://doi.org/10.1111/gcb.14328

Li, X.-G., Li, F.-M., Zed, R., Zhan, Z.-Y. & Bhupinderpal, S. (2007). Soil physical properties and their relations to organic carbon pools as affected by land use in an alpine pastureland. *Geoderma*, 139(1), 98-105.

https://doi.org/10.1016/j.geoderma.2007.01.006

Libohova, Z., Seybold, C., Wysocki, D., Wills, S., Schoeneberger, P., Williams, C., Lindbo, D., Stott, D. & Owens, P.R. (2018). Reevaluating the effects of soil organic matter and other properties on available water-holding capacity using the National Cooperative Soil Survey Characterization Database. *Journal of Soil and Water Conservation*, 73(4), 411-421. https://doi.org/10.2489/jswc.73.4.411

Lindahl, A.M.L., Dubus, I.G. & Jarvis, N.J. (2009). Site Classification to Predict the Abundance of the Deep-Burrowing Earthworm Lumbricus terrestris L. *Vadose Zone Journal*, 8(4), 911-915. https://doi.org/10.2136/vzj2008.0140

Lindahl, A.M.L., Söderström, M. & Jarvis, N. (2008). Influence of input uncertainty on prediction of within-field pesticide leaching risks. *Journal of Contaminant Hydrology,* 98(3), 106-114. https://doi.org/10.1016/j.jconhyd.2008.03.006

Lissy, A. S., Sammartino, S. & Ruy, S. (2020). Can structure data obtained from CT images substitute for parameters of a preferential flow model? *Geoderma*, 380, 114643. https://doi.org/10.1016/j.geoderma.2020.114643

Lucas, M., Schlüter, S., Vogel, H.-J. & Vetterlein, D. (2019). Soil structure formation along an agricultural chronosequence. *Geoderma*, 350, 61-72. https://doi.org/10.1016/j.geoderma.2019.04.041

Lucas, M., Vetterlein, D., Vogel, H.-J. & Schlüter, S. (2021). Revealing pore connectivity across scales and resolutions with X-ray CT. *European Journal of Soil Science*, 72(2), 546-560. https://doi.org/10.1111/ejss.12961

Luo, L., Lin, H. & Halleck, P. (2008). Quantifying Soil Structure and Preferential Flow in Intact Soil Using X-ray Computed Tomography. *Soil Science Society of America Journal,* 72(4), 1058-1069. https://doi.org/10.2136/sssaj2007.0179

Lützow, M.v., Kögel-Knabner, I., Ekschmitt, K., Matzner, E., Guggenberger, G., Marschner, B. & Flessa, H. (2006). Stabilization of organic matter in temperate soils: mechanisms and their relevance under different soil conditions – a review. *European Journal of Soil Science*, 57(4), 426-445. https://doi.org/10.1111/j.1365-2389.2006.00809.x

Luxmoore, R. J. (1981). Micro-, Meso-, and Macroporosity of Soil. Soil Science Society of America Journal, 45(3), 671-672. https://doi.org/10.2136/sssaj1981.03615995004500030051x

Matus, F., Amigo, X. & Kristiansen, S.M. (2006). Aluminium stabilization controls organic carbon levels in Chilean volcanic soils. *Geoderma*, 132(1), 158-168. https://doi.org/10.1016/j.geoderma.2005.05.005

Matus, F. J. (2021). Fine silt and clay content is the main factor defining maximal C and N accumulations in soils: a meta-analysis. *Scientific Reports*, 11(1), 6438. https://doi.org/10.1038/s41598-021-84821-6

Mayer, S., Kühnel, A., Burmeister, J., Kögel-Knabner, I. & Wiesmeier, M. (2019). Controlling factors of organic carbon stocks in agricultural topsoils and subsoils of Bavaria. *Soil and Tillage Research*, 192, 22-32. https://doi.org/10.1016/j.still.2019.04.021

McNally, S. R., Beare, M. H., Curtin, D., Meenken, E. D., Kelliher, F. M., Calvelo Pereira, R., Shen, Q. & Baldock, J. (2017). Soil carbon sequestration potential of permanent pasture and continuous cropping soils in New Zealand. *Global Change Biology*, 23(11), 4544-4555. https://doi.org/10.1111/gcb.13720

Meurer, K., Barron, J., Chenu, C., Coucheney, E., Fielding, M., Hallett, P., Herrmann, A.M., Keller, T., Koestel, J., Larsbo, M., Lewan, E., Or, D., Parsons, D., Parvin, N., Tay-lor, A., Vereecken, H. & Jarvis, N. (2020a). A framework for modelling soil structure dynamics induced by biological activity. *Global Change Biology*, 26(10), 5382-5403. https://doi.org/10.1111/gcb.15289

Meurer, K.H E., Chenu, C., Coucheney, E., Herrmann, A. M., Keller, T., Kätterer, T., Nimblad Svensson, D. & Jarvis, N. (2020b). Modelling dynamic interactions between soil structure and the storage and turnover of soil organic matter. *Biogeosciences*, 17(20), 5025-5042. https://doi.org/10.5194/bg-17-5025-2020

Mikutta, R. & Kaiser, K. (2011). Organic matter bound to mineral surfaces: Resistance to chemical and biological oxidation. *Soil Biology and Biochemistry*, 43(8), 1738-1741. https://doi.org/10.1016/j.soilbio.2011.04.012

Mikutta, R., Kleber, M., Kaiser, K. & Jahn, R. (2005). Review. *Soil Science Society of America Journal*, 69(1), 120-135. https://doi.org/10.2136/sssaj2005.0120

Mikutta, R., Kleber, M., Torn, M. S. & Jahn, R. (2006). Stabilization of Soil Organic Matter: Association with Minerals or Chemical Recalcitrance? *Biogeochemistry*, 77(1), 25-56. https://doi.org/10.1007/s10533-005-0712-6

Miltner, A., Bombach, P., Schmidt-Brücken, B. & Kästner, M. (2012). SOM genesis: microbial biomass as a significant source. *Biogeochemistry*, 111(1), 41-55. https://doi.org/10.1007/s10533-011-9658-z

Minasny, B. & McBratney, A. B. (2018). Limited effect of organic matter on soil available water capacity. *European Journal of Soil Science*, 69(1), 39-47. ney, A.B. (2018), Limited effect of organic matter on soil available water capacity. *European Journal of Soil Science*, 69: 39-47. https://doi.org/10.1111/ejss.12475

Moni, C., Chabbi, A., Nunan, N., Rumpel, C. & Chenu, C. (2010). Spatial dependance of organic carbon–metal relationships: A multi-scale statistical analysis, from horizon to field. *Geoderma*, 158(3), 120-127. https://doi.org/10.1016/j.geoderma.2010.04.014

Mori, Y., Maruyama, T. & Mitsuno, T. (1999). Soft X-ray Radiography of Drainage Patterns of Structured Soils. *Soil Science Society of America Journal*, 63(4), 733-740. https://doi.org/10.2136/sssaj1999.634733x

Nemes, A., Rawls, W.J. & Pachepsky, Y.A. (2005). Influence of Organic Matter on the Estimation of Saturated Hydraulic Conductivity. *Soil Science Society of America Journal*, 69(4), 1330-1337. https://doi.org/10.2136/sssaj2004.0055

Nimmo, J. R. (2021). The processes of preferential flow in the unsaturated zone. *Soil Science Society of America Journal*, 85(1), 1-27. https://doi.org/10.1002/saj2.20143

Ogle, S.M., Swan, A. & Paustian, K. (2012). No-till management impacts on crop productivity, carbon input and soil carbon sequestration. *Agriculture, Ecosystems & Environment*, 149, 37-49. https://doi.org/10.1016/j.agee.2011.12.010

Oldfield, E.E., Bradford, M.A. & Wood, S.A. (2019). Global meta-analysis of the relationship between soil organic matter and crop yields. *SOIL*, 5(1), 15-32. https://doi.org/10.5194/soil-5-15-2019

Oldfield, E.E., Wood, S.A. & Bradford, M.A. (2020). Direct evidence using a controlled greenhouse study for threshold effects of soil organic matter on crop growth. *Ecological Applications*, 30(4), e02073. https://doi.org/10.1002/eap.2073

Ost, A. D., Wu, T., Höschen, C., Mueller, C.W., Wirtz, T. & Audinot, J.-N. (2021). 4D Surface Reconstructions to Study Microscale Structures and Functions in Soil Biogeochemistry. *Environmental Science & Technology*, 55(13), 9384-9393. https://doi.org/10.1021/acs.est.1c02971

Ouédraogo, R.A., Chartin, C., Kambiré, F.C., van Wesemael, B., Delvaux, B., Milogo, H. & Bielders, C.L. (2020). Short and long-term impact of urban gardening on soil organic carbon fractions in Lixisols (Burkina Faso). *Geoderma*, 362, 114110. https://doi.org/10.1016/j.geoderma.2019.114110

Paradelo, M., Hermansen, C., Knadel, M., Moldrup, P., Greve, M.H. & de Jonge, L. W. (2016a). Field-Scale Predictions of Soil Contaminant Sorption Using Visible–Near Infrared Spectroscopy. *Journal of Near Infrared Spectroscopy*, 24(3), 281-291. https://doi.org/10.1255/jnirs.1228

Paradelo, M., Katuwal, S., Moldrup, P., Norgaard, T., Herath, L. & de Jonge, L.W. (2016b). X-ray CT-Derived Soil Characteristics Explain Varying Air, Water, and Solute Transport Properties across a Loamy Field. *Vadose Zone Journal*, 15(4). https://doi.org/10.2136/vzj2015.07.0104

Percival, H.J., Parfitt, R.L. & Scott, N.A. (2000). Factors Controlling Soil Carbon Levels in New Zealand Grasslands Is Clay Content Important? *Soil Science Society of America Journal*, 64(5), 1623-1630. https://doi.org/10.2136/sssaj2000.6451623x

Poeplau, C., Don, A., Dondini, M., Leifeld, J., Nemo, R., Schumacher, J., Senapati, N. & Wiesmeier, M. (2013). Reproducibility of a soil organic carbon fractionation method to derive RothC carbon pools. *European Journal of Soil Science*, 64(6), 735-746. https://doi.org/10.1111/ejss.12088

Poeplau, C., Don, A., Six, J., Kaiser, M., Benbi, D., Chenu, C., Cotrufo, M.F., Derrien, D., Gioacchini, P., Grand, S., Gregorich, E., Griepentrog, M., Gunina, A., Haddix, M., Kuzyakov, Y., Kühnel, A., Macdonald, L.M., Soong, J., Trigalet, S., Vermeire, M.-L., Rovira, P., van Wesemael, B., Wiesmeier, M., Yeasmin, S., Yevdokimov, I. & Nieder, R. (2018). Isolating organic carbon fractions with varying turnover rates in temperate agricultural soils – A comprehensive method comparison. *Soil Biology and Biochemistry*, 125, 10-26. https://doi.org/10.1016/j.soilbio.2018.06.025

Poeplau, C., Jacobs, A., Don, A., Vos, C., Schneider, F., Wittnebel, M., Tiemeyer, B., Heidkamp, A., Prietz, R. & Flessa, H. (2020). Stocks of organic carbon in German agricultural soils—Key results of the first comprehensive inventory. *Journal of Plant Nutrition and Soil Science*, 183(6), 665-681. https://doi.org/10.1002/jpln.202000113

Prout, J. M., Shepherd, K.D., McGrath, S.P., Kirk, G.J.D. & Haefele, S.M. (2021) What is a good level of soil organic matter? An index based on organic carbon to clay ratio. *European Journal of Soil Science*, 72, 2493-2503. https://doi.org/10.1111/ejss.13012

R Core Team (2019). R: A language and environment for statistical computing. R Foundation for Statistical Computing, Vienna, Austria. URL https://www.R-project.org/. [2020-05-04].

Rabot, E., Wiesmeier, M., Schlüter, S. & Vogel, H.J. (2018). Soil structure as an indicator of soil functions: A review. *Geoderma*, 314, 122-137. https://doi.org/10.1016/j.geoderma.2017.11.009

Rasmussen, C., Heckman, K., Wieder, W.R., Keiluweit, M., Lawrence, C.R., Berhe, A.A., Blankinship, J.C., Crow, S.E., Druhan, J.L., Hicks Pries, C.E., Marin-Spiotta, E., Plante, A.F., Schädel, C., Schimel, J.P., Sierra, C.A., Thompson, A. & Wagai, R. (2018). Beyond clay: towards an improved set of variables for predicting soil organic matter content. *Biogeochemistry*, 137(3), 297-306. https://doi.org/10.1007/s10533-018-0424-3

Rawls, W.J., Pachepsky, Y.A., Ritchie, J.C., Sobecki, T.M. & Bloodworth, H. (2003). Effect of soil organic carbon on soil water retention. *Geoderma*, 116(1), 61-76. https://doi.org/10.1016/S0016-7061(03)00094-6

Regelink, I.C., Stoof, C.R., Rousseva, S., Weng, L., Lair, G.J., Kram, P., Nikolaidis, N.P., Kercheva, M., Banwart, S. & Comans, R.N.J. (2015). Linkages between aggregate formation, porosity and soil chemical properties. *Geoderma*, 247(Supplement C), 24-37. https://doi.org/10.1016/j.geoderma.2015.01.022

Ruamps, L.S., Nunan, N., & Chenu, C. (2011). Microbial biogeography at the soil pore scale. *Soil Biology and Biochemistry*, 43(2), 280-286. https://doi.org/10.1016/j.soilbio.2010.10.010

Rühlmann, J., Körschens, M. & Graefe, J. (2006). A new approach to calculate the particle density of soils considering properties of the soil organic matter and the mineral matrix. *Geoderma*, 130(3), 272-283. https://doi.org/10.1016/j.geoderma.2005.01.024

Sammartino, S., Lissy, A.-S., Bogner, C., Van Den Bogaert, R., Capowiez, Y., Ruy, S. & Cornu, S. (2015). Identifying the Functional Macropore Network Related to Preferential Flow in Structured Soils. *Vadose Zone Journal*, 14(10). https://doi.org/10.2136/vzj2015.05.0070

Sanderman, J., Hengl, T. & Fiske, G.J. (2017). Soil carbon debt of 12,000 years of human land use. *Proceedings of the National Academy of Sciences*, 114(36), 9575-9580. https://doi.org/10.1073/pnas.1706103114

Sandin, M., Koestel, J., Jarvis, N. & Larsbo, M. (2017). Post-tillage evolution of structural pore space and saturated and near-saturated hydraulic conductivity in a clay loam soil. *Soil and Tillage Research*, 165, 161-168. https://doi.org/10.1016/j.still.2016.08.004

Sandin, M., Piikki, K., Jarvis, N., Larsbo, M., Bishop, K. & Kreuger, J. (2018). Spatial and temporal patterns of pesticide concentrations in streamflow, drainage and runoff in a small Swedish agricultural catchment. *Science of The Total Environment,* 610-611, 623-634. https://doi.org/10.1016/j.scitotenv.2017.08.068

Schindelin, J., Arganda-Carreras, I., Frise, E., Kaynig, V., Longair, M., Pietzsch, T., Preibisch, S., Rueden, C., Saalfeld, S., Schmid, B, Tinevez, J.-Y., White, D.J., Hartenstein, V., Eliceiri, K., Tomancak, P. & Cardona, A. (2012). Fiji: an open-source platform for biological-image analysis. *Nature Methods*, 9(7), 676-682. https://doi.org/10.1038/nmeth.2019

Schlüter, S., Eickhorst, T. & Mueller, C.W. (2019). Correlative Imaging Reveals Holistic View of Soil *Microenvironments. Environmental Science & Technology*, 53(2), 829-837. https://doi.org/10.1021/acs.est.8b05245

Schmidt, M.W.I., Torn, M.S., Abiven, S., Dittmar, T., Guggenberger, G., Janssens, I.A., Kleber, M., Kögel-Knabner, I., Lehmann, J., Manning, D.A.C., Nannipieri, P., Rasse, D.P., Weiner, S & Trumbore, S.E. (2011). Persistence of soil organic matter as an ecosystem property. *Nature*, 478, 49. https://doi.org/10.1038/nature10386

Shang, C. & Tiessen, H. (1998). Organic Matter Stabilization in Two Semiarid Tropical Soils: Size, Density, and Magnetic Separations. *Soil Science Society of America Journal*, 62(5), 1247-1257. https://doi.org/10.2136/sssaj1998.03615995006200050015x

Shoji, S., Nanzyo, M., Dahlgren, R. A. & Quantin, P. (1996). EVALUATION AND PROPOSED REVISIONS OF CRITERIA FOR ANDOSOLS IN THE

WORLD REFERENCE BASE FOR SOIL RESOURCES. *Soil Science*, 161(9), 604-615.

Singh, J., Singh, N. & Kumar, S. (2020). X-ray computed tomography–measured soil pore parameters as influenced by crop rotations and cover crops. *Soil Science Society of America Journal*, 84(4), 1267-1279. https://doi.org/10.1002/saj2.20105

Siregar, A., Kleber, M., Mikutta, R. & Jahn, R. (2005). Sodium hypochlorite oxidation reduces soil organic matter concentrations without affecting inorganic soil constituents. *European Journal of Soil Science*, 56(4), 481-490. https://doi.org/10.1111/j.1365-2389.2004.00680.x

Six, J., Bossuyt, H., Degryze, S. & Denef, K. (2004). A history of research on the link between (micro)aggregates, soil biota, and soil organic matter dynamics. *Soil and Tillage Research*, 79(1), 7-31. https://doi.org/10.1016/j.still.2004.03.008

Six, J., Conant, R.T., Paul, E.A. & Paustian, K. (2002). Stabilization mechanisms of soil organic matter: Implications for C-saturation of soils. *Plant and Soil*, 241(2), 155-176. https://doi.org/10.1023/A:1016125726789

Soares, A., Moldrup, P., Vendelboe, A.L., Katuwal, S., Norgaard, T., Delerue-Matos, C., Markus, T. & de Jonge, L. W. (2015). Effects of Soil Compaction and Organic Carbon Content on Preferential Flow in Loamy Field Soils. *Soil Science*, 180(1), 10-20. https://doi.org/10.1097/SS.0000000000000105

Soinne, H., Hyväluoma, J., Ketoja, E. & Turtola, E. (2016). Relative importance of organic carbon, land use and moisture conditions for the aggregate stability of post-glacial clay soils. *Soil and Tillage Research*, 158(Supplement C), 1-9. https://doi.org/10.1016/j.still.2015.10.014

Sollins, P., Homann, P. & Caldwell, B.A. (1996). Stabilization and destabilization of soil organic matter: mechanisms and controls. *Geoderma*, 74(1), 65-105. https://doi.org/10.1016/S0016-7061(96)00036-5

Steffens, M., Rogge, D.M., Mueller, C.W., Höschen, C., Lugmeier, J., Kölbl, A. & Kögel-Knabner, I. (2017). Identification of Distinct Functional Microstructural Domains Controlling C Storage in Soil. *Environmental Science & Technology*, 51(21), 12182-12189. https://doi.org/10.1021/acs.est.7b03715

Strong, D.T., Wever, H.D., Merckx, R. & Recous, S. (2004). Spatial location of carbon decomposition in the soil pore system. *European Journal of Soil Science*, 55(4), 739-750. https://doi.org/10.1111/j.1365-2389.2004.00639.x

Thomsen, I.K., Bruun, S., Jensen, L.S. & Christensen, B.T. (2009). Assessing soil carbon lability by near infrared spectroscopy and NaOCl oxidation. *Soil Biology and Biochemistry*, 41(10), 2170-2177. https://doi.org/10.1016/j.soilbio.2009.08.002

Totsche, K.U., Amelung, W., Gerzabek, M.H., Guggenberger, G., Klumpp, E., Knief, C., Lehndorff, E., Mikutta, R., Peth, S., Prechtel, A., Ray, N. &

Kögel-Knabner, I. (2018). Microaggregates in soils. *Journal of Plant Nutrition and Soil Science,* 181(1), 104-136. https://doi.org/10.1002/jpln.201600451

Traoré, S., Thiombiano, L., Bationo, B.A., Kögel-Knabner, I. & Wiesmeier, M. (2020). Organic carbon fractional distribution and saturation in tropical soils of West African savannas with contrasting mineral composition. *CATENA*, 190, 104550. https://doi.org/10.1016/j.catena.2020.104550

Van De Vreken, P., Gobin, A., Baken, S., Van Holm, L., Verhasselt, A., Smolders, E. & Merckx, R. (2016). Crop residue management and oxalate-extractable iron and aluminium explain long-term soil organic carbon sequestration and dynamics. *European Journal of Soil Science*, 67(3), 332-340. https://doi.org/10.1111/ejss.12343

Vendelboe, A.L., Schjønning, P., de Jonge, L.W. & Moldrup, P. (2013). Long-Term Effect of Different Carbon Management Strategies on Water Flow and Related Processes for Three Loamy Soils. *Soil Science*, 178(8), 379-388. https://doi.org/10.1097/SS.0000000000000011

Virto, I., Barré, P. & Chenu, C. (2008). Microaggregation and organic matter storage at the silt-size scale. *Geoderma*, 146(1), 326-335. https://doi.org/10.1016/j.geoderma.2008.05.021

Vogel, H.-J., Balseiro-Romero, M., Kravchenko, A., Otten, W., Pot, V., Schlüter, S., Weller, U. & Baveye, P.C. (2021). A holistic perspective on soil architecture is needed as a key to soil functions. *European Journal of Soil Science*, 1-14. https://doi.org/10.1111/ejss.13152

von Fromm, S.F., Hoyt, A.M., Acquah, G.E., Aynekulu, E., Berhe, A.A., Haefele, S.M., McGrath, S.P., Shepherd, K.D., Sila, A.M., Six, J., Towett, E.K., Trumbore, S.E., Vågen, T.G., Weullow, E., Winowiecki, L.A. & Doetterl, S. (2021). Continental-scale controls on soil organic carbon across sub-Saharan Africa. *SOI*L, 305-332. https://doi.org/10.5194/soil-7-305-2021

Wagai, R., Kajiura, M. & Asano, M. (2020). Iron and aluminum association with microbially processed organic matter via meso-density aggregate formation across soils: organo-metallic glue hypothesis. *SOIL*, 6(2), 597-627. https://doi.org/10.5194/soil-6-597-2020

Wagai, R. & Mayer, L.M. (2007). Sorptive stabilization of organic matter in soils by hydrous iron oxides. *Geochimica et Cosmochimica Acta*, 71(1), 25-35. https://doi.org/10.1016/j.gca.2006.08.047

Wang, M., Xu, S., Yang, J., Xu, L., Yu, Q., Xie, X., Shi, X. & Zhao, Y. (2021). The effect of organic and conventional management practices on soil macropore structure in greenhouse vegetable production. *European Journal of Soil Science*, 72(5), 2133-2149. https://doi.org/10.1111/ejss.13106

Wang, T., Wedin, D. & Zlotnik, V.A. (2009). Field evidence of a negative correlation between saturated hydraulic conductivity and soil carbon in a sandy soil. *Water Resources Research*, 45(7), W07503.

https://doi.org/10.1029/2008WR006865

Wiaux, F., Cornelis, J.T., Cao, W., Vanclooster, M. & Van Oost, K. (2014). Combined effect of geomorphic and pedogenic processes on the distribution of soil organic carbon quality along an eroding hillslope on loess soil. *Geoderma*, 216, 36-47. https://doi.org/10.1016/j.geoderma.2013.10.013

Wiesmeier, M., Hübner, R. & Kögel-Knabner, I. (2015). Stagnating crop yields: An overlooked risk for the carbon balance of agricultural soils? *Science of The Total Environment,* 536, 1045-1051. https://doi.org/10.1016/j.scitotenv.2015.07.064

Wiesmeier, M., Urbanski, L., Hobley, E., Lang, B., von Lützow, M., Marin-Spiotta, E., van Wesemael, B., Rabot, E., Ließ, M., Garcia-Franco, N., Wollschläger, U., Vogel, H.-J. & Kögel-Knabner, I. (2019). Soil organic carbon storage as a key function of soils - A review of drivers and indicators at various scales. *Geoderma*, 333, 149-162. https://doi.org/10.1016/j.geoderma.2018.07.026

Witzgall, K., Vidal, A., Schubert, D. ., Höschen, C., Schweizer, S.A., Buegger, F., Pouteau, V., Chenu, C. & Mueller, C.W. (2021). Particulate organic matter as a functional soil component for persistent soil organic carbon. *Nature Communications*, 12(1), 4115. https://doi.org/10.1038/s41467-021-24192-8

Xu, L.Y., Wang, M.Y., Shi, X.Z., Yu, Q. B., Shi, Y. J., Xu, S. X. & Sun, W.X. (2018). Effect of long-term organic fertilization on the soil pore characteristics of greenhouse vegetable fields converted from rice-wheat rotation fields. *Science of The Total Environment*, 631-632, 1243-1250. https://doi.org/10.1016/j.scitotenv.2018.03.070

Yang, F., Zhang, G.-L., Yang, J.-L., Li, D.-C., Zhao, Y.-G., Liu, F., Yang, R.-M. & Yang, F. (2014). Organic matter controls of soil water retention in an alpine grassland and its significance for hydrological processes. *Journal of Hydrology*, 519, 3086-3093. https://doi.org/10.1016/j.jhydrol.2014.10.054

Zhang, Z., Liu, K., Zhou, H., Lin, H., Li, D. & Peng, X. (2019). Linking saturated hydraulic conductivity and air permeability to the characteristics of biopores derived from X-ray computed tomography. *Journal of Hydrology*, 571, 1-10. https://doi.org/10.1016/j.jhydrol.2019.01.041

Zhou, H., Chen, C., Wang, D., Arthur, E., Zhang, Z., Guo, Z., Peng, X. & Mooney, S.J. (2020). Effect of long-term organic amendments on the full-range soil water retention characteristics of a Vertisol. *Soil and Tillage Research*, 202, 104663. https://doi.org/10.1016/j.still.2020.104663

Zimmermann, M., Leifeld, J., Schmidt, M.W.I., Smith, P. & Fuhrer, J. (2007). Measured soil organic matter fractions can be related to pools in the RothC model. *European Journal of Soil Science*, 58(3), 658-667. https://doi.org/10.1111/j.1365-2389.2006.00855.x

Popular science summary

Soil is a porous medium and has, like a sponge, a large variety of pore sizes. Depending on their size, soil pores have different functions. For example, water available to plants is mainly stored in small mesopores (0.2–10 µm diameter), whereas macropores (>300 µm diameter) are important for water infiltration and oxygen supply to plant roots. In agricultural systems, understanding of water dynamics in relation to soil structure (i.e. the spatial arrangement of solids and pores) is important, because water carries with agrochemicals, such as chemical fertilizers and pesticides. If these agrochemicals are leached out of the crop root zone to, for example, groundwater and ditches around agricultural fields, they can be harmful to aquatic organisms and make groundwater unsuitable for human consumption. The leaching of these chemicals is often promoted through water flow in macropores where solutes can be quickly transported through the soil profile and reach groundwater or drainage systems. We therefore need to know what a good soil pore structure is, both for crop production and for water quality management.

The storage of carbon in soils is larger than the storage in plant biomass and in the atmosphere combined. Most carbon in soil is present as organic carbon. Large amounts of soil organic carbon (SOC) has been depleted from arable soils and released into the atmosphere as carbon dioxide due to historical intensive agriculture. It is therefore important to know how to increase SOC content in arable soils, which can then help regulate our future climate. It is also important to evaluate how SOC is associated with soil pore structure and consequently water flow and solute transport. SOC often interacts with soil mineral constituents (clay-sized particle <2 µm and reactive mineral phases therein), which can determine how SOC is stored in soils and hence have implications for carbon sequestration.

In this thesis, I examined how SOC was stored (e.g in which particle size fractions it was stored and how much of the carbon that was resisitant to oxidation) and how it interacted with soil mineral constituents for arable topsoils. I then investigated relationships between SOC and soil pore structure, water flow and solute transport. This thesis is mostly based on results from one field with large variations in clay and SOC contents located in Bjertorp in Västergötland; by doing so, the effects of other factors such as climate and land management were minimized.

A large proportion of SOC (80%) was present in the silt- and clay-sized fraction (<63 µm), which indicated that most SOC was physico-chemically protected against microbial decomposition. This stabilization seemed to be governed by reactive aluminum. On the other hand, clay content and reactive iron, which are both known to be important for SOC stabilization, did not seem important for SOC stabilization in the Bjertorp field. In addition to these mineral constituents, there was a large variation in crop productivity across the field, which possibly caused a spatial variation in carbon input from crop roots. This variation partly explained the spatial variation in SOC content.

Soil pore size distributions were quantified using X-ray tomography and soil water retention measurements. I found that soil texture (clay content) had a stronger impact than SOC content on pore structure. However, I also found a relatively large increase of soil pore abundance in the 0.2–5 (mesopore) and 480–720 µm (macropore) diameter ranges with an increase in SOC content. This suggested that SOC sequestration in arable topsoils is potentially beneficial for the water supply to plants and for soil infiltration capacity.

Laboratory experiments were conducted to evaluate the risk of fast solute transport in soil macropores and its relationship with soil pore structure and soil properties. I found that the risk for fast transport was smaller with larger abundance of mesopores and small macropores (30–480 µm diameter ranges), whereas the abundances of large macropores (>720 µm diameter range) and their networks (i.e. how macropores were connected through the soil) had limited effects on the risk of preferential transport. I could not find any positive effects of SOC content on the risk of fast transport. This was possibly due to the much stronger effects of clay content. To assess the effects of SOC on preferential transport, further studies will be needed using soils with a smaller variation in clay content.

Populärvetenskaplig sammanfattning

Jorden är ett poröst medium och har, precis som en tvättsvamp, många olika porstorlekar. Beroende på storleken har jordens porer olika funktion. Till exempel lagras vatten som är tillgängligt för växter i små mesoporer (0,2-10 µm i diameter), medan makroporer (>300 µm i diameter) är viktiga för vatteninfiltration och syretillförsel till växternas rötter. Det är viktigt att förstå vattendynamiken i förhållande till markens struktur (dvs. det rumsliga arrangemanget av fasta partiklar och porer), eftersom vatten för med sig kemikalier som används inom jordbruket (t.ex. konstgödsel och bekämpningsmedel). Om dessa kemikalier lakas ut från grödans rotzon till, till exempel, grundvatten och dikesvatten runt jordbruksfält, kan de vara skadliga för vattenlevande organismer och göra grundvattnet olämpligt för mänsklig konsumtion. Läckaget av dessa ämnen blir ofta större när de transporteras genom makroporer där vattnets flödeshastighet kan vara hög och matjorden därför snabbt passeras. Vi måste därför veta hur en bra porstruktur i marken ser ut, både för växtproduktion och för att minimera risken för läckage.

Mängden kol som finns lagrad i marken är nästan dubbelt så stor som mängden kol i vegetationen och atmosfären tillsammans. Den största delen av detta kolförråd är i formen av organiskt kol. Historiskt sett så har jordbruk lett till en minskning av mängden kol i marken vilket har bidragit till ökade koldioxidhalter i atmosfären. En förändring av markanvändning och sättet att bruka jorden för att öka inlagringen av organiskt kol kan därför bidra till att minska vår påverkan på framtida klimat. Det är viktigt att utvärdera hur förändringar i markens organiska kolhalt kommer att påverka markens porstruktur och därmed vattenflöden och transporten av lösta ämnen ämnen genom marken. Eftersom organiskt kol ofta interagerar med markens fasta material (lerpartiklar < 2 µm och reaktiva mineral), är markens beståndsdelar avgörande för hur organiskt kol lagras i marken.

I den här avhandlingen undersökte jag hur organiskt kol lagras (t.ex. i vilka partikelstorleksfraktioner som det lagras och hur stor del av kolet som är stabilt mot oxidation) och hur det interagerar med markens fasta beståndsdelar i åkerjordar. Därefter undersökte jag sambanden mellan halten organiskt kol och markens porstruktur, vattenflöde och transport av lösta ämnen. Den här avhandlingen är huvudsakligen baserad på resultat från ett fält i Bjertorp i Västergötland. Markens lerhalt och halt av organiskt kol varierade inom fältet medan klimatet och brukningsmetoderna var desamma.

En stor del av markens organiska kol (80%) fanns i silt- och ler-fraktionerna (<63 µm), vilket tyder på att det mesta av markens organiska kol var skyddat mot mikrobiell nedbrytning. Denna stabilisering verkade drivas av reaktivt aluminium. Å andra sidan tycktes lerhalt och reaktivt järn, som båda är kända för att vara viktiga för stabiliseringen av organiskt kol, inte ha någon betydelse i Bjertorpfältet. Förutom variationen i dessa mineralbeståndsdelar fanns det en stor variation i grödornas produktivitet inom fältet, vilket kan ha orsakat en rumslig variation i koltillförseln från grödornas rötter. Denna variation kunde i viss mån förklara den rumsliga variationen i markens halt av organiskt kol.

Jordens porstorleksfördelning kvantifierades med hjälp av röntgentomografi och mätningar av markens vattenhållande förmåga. Jag fann att markens lerhalt hade en större inverkan på porstrukturen än markens halt av organiskt kol. Jag fann dock också att det sker en relativt stor ökning av antalet porer i diameterintervallen 0,2-5 (mesoporer) och 480-720 µm (makroporer) när halten organiskt kol ökar. Detta tyder på att en ökning av markens halt av organiskt kol potentiellt är fördelaktigt för att öka vattentillgången för växter och markens infiltrationsförmåga.

Laboratorieexperiment genomfördes för att utvärdera risken för snabb transport av lösta ämnen i markens makroporer och dess samband med markens porstruktur och markegenskaper. Jag fann att risken för snabb transport var beroende av förekomsten av mesoporer och små makroporer (30-480 µm i diameter) snarare än förekomsten av stora makroporer (>720 µm i diameter) och deras nätverk (dvs. hur makroporerna är sammankopplade genom jorden). Jag hittade inte några positiva effekter av halten av organiskt kol på risken för snabb transport. Det kan ha berott på de mycket starkare effekterna av lerhalten. Det behövs därför ytterligare studier med jordar med mindre variation i lerhalt för att bedöma effekterna av markens halt av organiskt kol på risken för snabb transport.

Acknowledgements

First of all, I would like to acknowledge my main supervisor, Mats Larsbo, for giving me the opportunity to conduct this PhD project. Mats, thank you for your invaluable guidance. You have been always logical and calm even when I asked you questions that were clearly not logical, been available and supportive when I need your help and read my (unnecessarily complicated!) manuscripts patiently. Also, I have always enjoyed our scientific discussions and appreciated your valuable inputs. Moreover, you have given me the freedom to develop this project myself especially for Paper I, through which I have learned that doing science is sometimes difficult, but it is still very exciting and inspiring.

I am also grateful to my co-supervisors Nick Jarvis, John Koestel, Elsa Couheney and Thomas Kätterer. Nick, thank you for your encouragement, your amazing language editing service, your valuable inputs and critical comments to my work and for leading the BGF group thoughtfully. I have been very inspired by your works to model different kinds of processes in soil! John, thank you for your valuable inputs on soil physics and image analysis. You have also given me the opportunity to participate in some of your projects, from which I have learned new things. What is more, it is a lot of fun to work with you! Elsa, thank you for your valuable inputs on my work and paper and for being very kind and cheerful since I joined the BGF group! Thomas, thank you for your essential inputs on SOC research and your prompt replies to my emails at any time!

I would like to thank my key collaborators Christopher Poeplau, Johanna Wetterlind, David Nimblad Svensson and Tobias Klöffel. Christopher, thank you for organizing my visit to Thünen, teaching me how to conduct the SOM fractionation, answering my questions patiently and for your valuable input into paper I. Johanna, thank you for your valuable input on the analysis of crop yield data and your efforts to collect the needed information on the field. David, thank you for performing laser particle size analyzer experiments with great motivation and interest and for giving me advice when I was stuck with my work. Tobias, thank you for your amazing expertise on soil classification and your enormous energy to dig three pits at Bjertorp within a day.

To complete my PhD work, I have received the valuable support from my colleagues. Anna S., thank you for your assistance in the laboratory and for guiding me during my PhD program (e.g. telling me which PhD course I should take). Miyanda C., thank you for working on your current PhD project that partly deals with what I could not figure out. Reza H., thank you for many interesting conversations that we have had and for your help in my very first intensive sampling at Bjertorp. Rebecca T.B., thank you for teaching me how to use ArcGIS properly. Mattias L., thank you for being always supportive and considerate as my line manager. Claudia v.B., thank you for your advice on statistics. Lisbet L., thank you for letting me join the MoM-FUN meetings and giving me a lot of advice on how to handle the challenges of PhD work. Magnus S., thank you for carefully reading my kappa and your valuable inputs on soil chemistry and pedology. I am also grateful to all my colleagues in the administrative, laboratory and IT sections of this department for helping me do my project smoothly. In particular, I would like to thank Åsa B., Josefine A., Lisa G. and Sara W. for their prompt responses to my requests, Mattias G. for his help for soil sampling at Bjertorp, Jan F. for many valuable discussions on the oxalate extraction, Mina S. for her kind help in the laboratory, Elin L. and Ambjörn E. for measuring carbon and nitrogen contents, Cecilia B. for maintaining the laboratory, Farid J. for always greeting me in Japanese and Ana M. for measuring soil water retention and texture of my samples, which were crucial for this work. I also wish to thank the manager of the Bjertop field, Kjell C. for allowing me to take soil samples even three times and to use the yield data and Knud N. for archiving the yield data.

This PhD project was funded by FORMAS (grant no: 2016-01320), which is greatly appreciated. I would also like to thank the Heiwa Nakajima Foundation for offering me the study-abroad scholarship.

I wish to thank the current and former members of the BGF group, Nick J., Mats L., John K., Elsa C., Maria S., Anna S., Tobias B., Nargish P., Ana V., Miyanda C., Gunnel A., Lisbet L., David N.S. and Katharina M. for maintaining a positive work environment within the group. I also wish to thank all my colleagues in this Department and beyond with whom I have had many valuable scientific and general discussions. In particular: Anke H., Thomas Ke., Tino C., Gizachew G., Harald C., Jon Petter G. and Karolina J. I would also like to thank all the current and former PhD students in this department and their friends & family for enjoyable moments including ordinary fika & fun pub-evenings. Special thanks to David N.S., Emelie S., Tobias K., Elsa A.V., Louise D., Fahri H. and Resti R. for spending memorable times with me on various occasions.

I would like to thank my friends in Sweden, Japan and literally around the world for continuous encouragement, support and advice especially when I was stuck with my work. Special thanks to Jan Andersson, my landlord, for renting out the cozy house to me from my very first day here in Sweden. I would also like to acknowledge the kind guidance that I have received from my former BSc & MSc supervisors and mentors: Takeo Akae, Yasushi Mori, Ayako Namba, Liz Shaw and Rota Wagai.

Last but not least, I would like to thank my family in Japan, especially my parents Hiroaki Fukumasu and Satomi Fukumasu, my sisters Mari and Yumi and my grandparents, for their unconditional support and encouragement from Japan.

Jumpei Fukumasu
Uppsala, Sweden
January 2022

Geoderma 402 (2021) 115345

Contents lists available at ScienceDirect

Geoderma

journal homepage: www.elsevier.com/locate/geoderma

Oxalate-extractable aluminum alongside carbon inputs may be a major determinant for organic carbon content in agricultural topsoils in humid continental climate

Jumpei Fukumasu [a,*], Christopher Poeplau [b], Elsa Coucheney [a], Nick Jarvis [a], Tobias Klöffel [a], John Koestel [a,c], Thomas Kätterer [d], David Nimblad Svensson [a], Johanna Wetterlind [e], Mats Larsbo [a]

[a] Department of Soil and Environment, Swedish University of Agricultural Sciences (SLU), Box 7014, 750 07 Uppsala, Sweden
[b] Thünen Institute of Climate-Smart Agriculture, Bundesallee 65, 38116 Braunschweig, Germany
[c] Soil Quality and Soil Use, Agroscope, Reckenholzstrasse 191, Zürich CH-8046, Switzerland
[d] Department of Ecology, Swedish University of Agricultural Sciences (SLU), Box 7044, 750 07 Uppsala, Sweden
[e] Department of Soil and Environment, Swedish University of Agricultural Sciences (SLU), Box 234, 532 23 Skara, Sweden

ARTICLE INFO

Handling Editor: Ingrid Kögel-Knabner

Keywords:
Soil organic carbon
Oxalate-extractable aluminum
Clay
Arable soil
Fractionation
Carbon input

ABSTRACT

The relative importance of various soil mineral constituents (e.g. clay-sized particles, aluminum- and iron-bearing mineral reactive phases) in protecting soil organic carbon (SOC) from decomposition is not yet fully understood in arable soils formed from quaternary deposits in humid continental climates. In this study, we investigated the relationships between soil physico-chemical properties (i.e. contents of oxalate-extractable aluminum (Alox) and iron (Feox) and clay size particle < 2 μm), grain yield (as a proxy for carbon input) and total SOC as well as SOC in different soil fractions for samples taken from the topsoil of an arable field at Bjertorp in south-west Sweden. We found a positive correlation between Alox and total SOC content, where Alox explained ca. 48% of the spatial variation in SOC. We also found that ca. 80% of SOC was stored in silt- and clay-sized (SC) fractions, where Al-bearing reactive mineral phases (estimated by Alox) may be important for organic-mineral associations and clay aggregation. Our results were supported by data collated from the literature for arable topsoil in similar climates, which also showed positive correlations between SOC and Alox contents ($R^2 = 23.1 - 74.5\%$). Multiple linear regression showed that including spatially-variable crop yields as a proxy for carbon inputs improved the prediction of SOC variation across the Bjertorp field. Other unquantified soil properties such as exchangeable calcium may account for the remaining unexplained variation in topsoil SOC. We conclude that Al-bearing reactive mineral phases are more important than clay content and Fe-bearing reactive mineral phases for SOC stabilization in arable topsoil in humid continental climates.

1. Introduction

Enhancing carbon (C) sequestration in arable soils has received attention for its potential to mitigate global warming and climate change as well as improving soil fertility (Lal, 2004; Chenu et al., 2019). To understand C cycling in agricultural soils, it is important to know how soil properties regulate the stabilization of soil organic carbon (SOC) against microbial decomposition. Today, it is widely acknowledged that the physico-chemical properties of soil rather than intrinsic biochemical recalcitrance of organic matter inputs determine the stability of SOC (Schmidt et al., 2011; Dungait et al., 2012; Lehmann and Kleber, 2015). Clay content (particle size fraction < 2 μm) has often been considered a key soil property for SOC stabilization because clay is a major component in the formation of soil aggregates in which SOC can be occluded and thereby physically protected from microbial decomposition (Horn et al., 1994; Totsche et al., 2018). Clay particles also have a large specific surface area and therefore a large capacity to protect SOC chemically by adsorption (Sollins et al., 1996; Lützow et al., 2006). In addition, clay content has been reported to be positively correlated with the prevalence of anoxic sites, which limits aerobic microbial decomposition of

---

[*] Corresponding author.
E-mail address: jumpei.fukumasu@slu.se (J. Fukumasu).

https://doi.org/10.1016/j.geoderma.2021.115345
Received 22 March 2021; Received in revised form 10 June 2021; Accepted 6 July 2021

SOC (Keiluweit et al., 2018). As a result, clay content (and sometimes fine silt content) has been used to estimate SOC turnover in C cycling models and to calculate the degree of carbon saturation to estimate the carbon sequestration potential of soils (Hassink, 1997; Feng et al., 2013; Wiesmeier et al., 2015; Rasmussen et al., 2018).

Indeed, many studies have reported positive correlations between clay and SOC contents at various scales (e.g. Arrouays et al., 2006; Homann et al., 2007; Li et al., 2020; Poeplau et al., 2020; Prout et al., 2020). However, in many other arable and grassland soils, clay or silt and clay content was not correlated with SOC content (e.g. Thomsen et al., 2009; Beare et al., 2014; Augustin and Cihacek, 2016; Van De Vreken et al., 2016; McNally et al., 2017; Mayer et al., 2019), which indicates either that the clay fraction was not saturated with SOC and/or that clay content itself was not a major determinant of physico-chemical stabilization of soil organic matter (SOM) for these soils. Rasmussen et al. (2018) showed that SOC was more strongly correlated with short range order (SRO) phases and organo-metal complexes (i.e. the reactive mineral fraction estimated from chemically extractable aluminum (Al) and iron (Fe)) for acidic to neutral soils and with the content of exchangeable calcium ions for alkaline soils, than with clay content. Their study was based on an analysis of the U.S. Department of Agriculture's National Cooperative Soil Survey. Positive correlations between SOC and chemically extractable Al and Fe have also previously been documented for acidic forest soils (e.g. Mikutta et al., 2006) and volcanic soils (i.e. Andisols, Percival et al., 2000; Matus et al., 2006; Asano and Wagai, 2014; Beare et al., 2014). In addition, recent studies have highlighted the importance of the reactive mineral fraction in the stabilization of SOC for soils of sub-Saharan Africa (Ouédraogo et al., 2020; Traoré et al., 2020; von Fromm et al., 2020). Typical pH values for arable soils in Sweden are below 7 (ca. 90% of arable soils according to the national soil inventory of Sweden; Eriksson et al., 2010), which suggests that the Al- and Fe-bearing reactive mineral fraction should also be important for SOC stabilization in Swedish agricultural soils. However, to the best of our knowledge, the relationship between SOC content and the physico-chemical properties of soil has not been fully examined in Swedish and other regions' arable soils formed from quaternary deposits with similar climatic conditions (i.e. humid continental climate; Beck et al., 2018).

Al- and Fe-bearing reactive mineral phases are considered to associate with SOC through organo-metal complexation and/or co-precipitation and thereby regulate microbial and enzymatic accessibility to SOC (Kleber et al., 2015). Wagai and Mayer (2007) argued that there should be other mechanisms that influence the overall protection of SOC because the proportion of SOC that can be directly associated with Fe- and Al-bearing reactive mineral phases is often small compared to bulk SOC contents. Asano et al. (2018) suggested that organo-metal association can facilitate the formation of clay-sized micro-aggregates and thereby enhance the physical stabilization of SOC. Since SOC is mainly associated with the silt and clay fraction in arable topsoil (ca. 90%; Gregorich et al., 2006; Matus, 2021), aggregation in silt- and / or clay-sizes may be more important than macro-aggregation for SOC stabilization (Wiesmeier et al., 2014). The studies cited above indicate that Al- and Fe-bearing reactive mineral phases can play an important role in the protection of SOC by both physical and chemical mechanisms.

SOM fractionation should be a useful method to investigate the relationship between the reactive mineral fraction, clay content and SOC contents, as it isolates SOM fractions with different stability against microbial decomposition. In particular, it is important to separate particulate organic matter (POM) from mineral-associated organic matter as these two fractions have been shown to differ in SOC stability and, hence, respond differently to environmental changes such as changes in land use (Lavallee et al., 2020). SOC in the mineral-associated organic matter fraction is considered to be more stable than POM and therefore important for long-term SOC stabilization, whereas the POM fraction is a useful indicator of short-term changes in SOC (Lavallee et al., 2020). Poeplau et al., (2018) studied SOC stability in different SOM fractions, applying 20 different fractionation methods to soils from fields where C3 plants had been replaced by C4 plants. They reported that SOC in the mineral-associated organic matter fraction was more stable (i.e. had a higher enrichment of C3-derived SOC) than POM and SOM associated with sand-sized fractions. They also found that SOC that was resistant to oxidation (e.g. by NaOCl) was the most stable fraction (i.e. had the lowest enrichment in C4-derived SOC). The latter finding is consistent with results presented by Mikutta et al. (2006) based on ^{14}C analysis, who found that oxidation-resistant SOC was older than the bulk SOC.

Apart from stabilization mechanisms, the SOC content is also strongly driven by carbon input from crop production (e.g. Bolinder et al., 2007; Börjesson et al., 2018; Ogle et al., 2012). Moni et al. (2010) found no significant correlations between SOC and reactive mineral phases in the topsoil of a mixed area of grassland and arable fields, leading them to conclude that variations in C input may have masked such relationships.

The objective of this study was to examine the relationships between physico-chemical properties (i.e. clay content and oxalate-extractable Al and Fe as a proxy for the reactive mineral phases), total SOC and SOC in different soil fractions in a Swedish arable topsoil. For this purpose, we chose a conventionally tilled field with large variations in soil texture and SOC content. By sampling soils at the field scale, we minimized the effects of variations in other factors such as management and climate that also influence SOC dynamics. Our field-scale relationships between physico-chemical properties and SOC were set in a wider context by comparison with available literature data from agricultural fields with similar climate and types of soils formed from quaternary deposit.

2. Materials and methods

2.1. Field description and soil sampling

The selected field (46.9 ha) is located at Bjertorp (58°14′00.0″N 13°08′00.0″E) in Västergötland in south-west Sweden (Lindahl et al., 2008). Mean annual precipitation and temperature are 624 mm and 7.3 °C, respectively (average for the period 2006 to 2019 taken from the nearby metrological station at Hällum, Swedish Meteorological and Hydrological Institute). The field has been used for conventional crop production for at least 60 years with winter wheat, barley, oats and oilseed rape as the dominant crops. Similar soil and crop management has been applied across the whole field with two exceptions: 1) different crops have occasionally been grown in different parts of the field, and 2) nitrogen, phosphorus and potassium fertilization has, since the late 1990s, varied across the field. Nitrogen fertilization has been optimized using a tractor mounted sensor (Yara N sensor, on average 167 kg ha^{-1} year^{-1}) while phosphorus and potassium fertilization rates were based on measurements of ammonium lactate extractable phosphorus and potassium contents (on average 25 kg ha^{-1} year^{-1} and 10 kg ha^{-1} year^{-1} respectively). The field has been mouldboard ploughed regularly down to 20 – 25 cm depth except during years when winter rape seed was grown, when the tillage depth was reduced. No farmyard manure has been applied since the 1960s. In September 2020, we carried out soil profile descriptions at three different locations following the FAO guidelines (FAO, 2006). According to the IUSS Working Group WRB (2015) classification system, these soil profiles were classified as Stagnic Eutric Cambisol, Eutric Stagnosol and Haplic Phaeozem respectively (Fig. 1). Further details of these soil profiles are available in Table S1. The parent material in this region is Quaternary silty clay, which was deposited during the Weichselian deglaciation (Stevens and Bayard, 1994; Simonsson et al., 2014). Eriksson (2016) reported soil mineralogy data from a field located approximately 500 m from our field; the proportion of quartz, plagioclase, K-feldspar, amphibole, iron oxides and clay minerals in bulk soil (<2 mm) were 33, 18, 16, 2.6, 2.7 and 15%, respectively. In the clay fraction (<2 μm), the proportions of kaolinite, mica and expandable minerals (e.g. smectite, vermiculite, hydroxy-interlayered minerals and mixed layer illite–smectite minerals) were

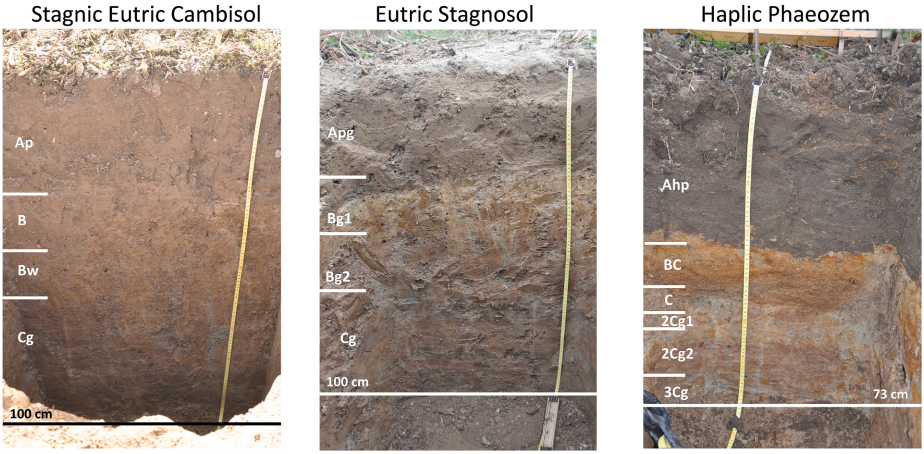

Fig. 1. Photos of soil profiles for three locations within the field. Elevation for Stagnic Eutric Cambisol, Eutric Stagnosol and Haplic Phaeozem are 90.6, 95.1 and 95.7 m respectively. These locations are shown in Fig. S1.

4, 27 and 69%, respectively. This field shows large variations in SOM and clay contents (Lindahl et al., 2008). SOM and clay contents were originally measured in topsoil samples (0 – 20 cm depth) in 2000. A weak negative correlation between clay content and bulk SOC (estimated from SOM) content was found (Fig. 2, original data from Lindahl et al., 2008). The elevation varies across the field from 87 to 95 m above sea level. Some significant statistical relationships were found between soil properties and elevation. These are reported in the supplementary material (Fig. S1). We do not know the origin of the spatial variation in soil texture at Bjertorp. However, the negative correlation between clay content and elevation (Fig. S1) suggests that it might be a result of sedimentation processes during the formation of the soil in the post-glacial period (Greve et al., 2012).

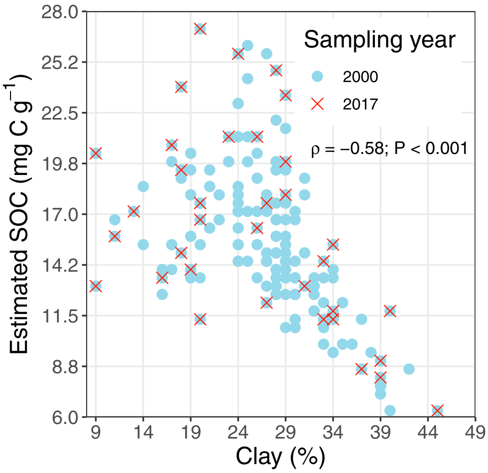

Fig. 2. A relationship between bulk soil organic carbon (SOC; estimated from soil organic matter) and clay content. Data from samples taken in 2000 (Lindahl et al., 2008).

In late August 2017, after harvest of an oilseed rape crop, we sampled intact soil cores and loose soil at ca. 3 – 13 cm depth at 35 different locations in the field (Fig. S2). We used stratified sampling from the dataset collected in 2000 to get the best possible coverage of combinations of bulk SOC and clay contents (Fig. 2). The intact soil cores were first used for non-reactive solute transport experiments (Methodological detail in Larsbo et al., 2016) that are not reported here. After these experiments, the soil was dried at ca. 38 °C, crushed and sieved to < 2 mm (referred to as bulk soil). The dried bulk soil was used for soil texture analysis, SOM fractionation and analyses of oxalate-extractable Al (Alox) and Fe (Feox) contents. To assess potential effects of the irrigation experiment, we also measured bulk C and N contents and its ratio as well as Alox and Feox for a subset of the 35 sampling locations in soil samples that had not been irrigated. These properties were similar for irrigated and non-irrigated soil ($R^2 > 0.87$). Based on these measurements of bulk soil chemical properties, we assume that the effects of the irrigation treatment on SOC fractions were also negligible. The loose soil was dried at ca. 38 °C, sieved to < 2 mm and used for soil pH measurement. A digital elevation model for the field was downloaded from Lantmäteriet (resolution: 2 m, https://www.lantmateriet.se/sv/).

2.2. Basic soil properties

Soil texture (sand: 60 – 2000 μm, silt: 2 – 60 μm, clay: < 2 μm) was determined by the pipette method after SOM removal using 10 mL peroxide (35%) and dispersion with a few drops of hydrochloric acid (HCl) and 25 mL chemical dispersant (7 g L^{-1} sodium carbonate, Na_2CO_3 + 33 g L^{-1} Sodium metaphosphate, $(NaO_3P)n$). Soil pH was measured in ultrapure water at a soil:water mass ratio of 1:2.5. Alox and Feox contents were determined in 1 g of soil after extraction with 100 mL of oxalate solution (mixture of 4.8 L ammonium oxalate solution (0.2 mol L^{-1}) and 3.6 L oxalic acid solution (0.2 mol L^{-1}) adjusted to pH 3.0) carried out in the dark. We considered Alox and Feox to represent hydroxides complexed with SOC and SRO mineral phases (Panichini et al., 2012; Wagai et al., 2013; Rasmussen et al., 2018).

2.3. Bulk SOC, bulk N and fractionation

We first measured the inorganic carbon (C) content for five of the 35 samples with varying soil pH (5.9 – 6.3) and clay content (16.5 – 41.7%)

after removing organic carbon by oven-drying at 550 °C. We found that the inorganic C content was$<$0.024 mg g^{-1} which corresponds to$<$0.2% of the total C. Therefore, we assumed that the inorganic C content was negligible, such that organic C equaled total C content for the bulk soil and for all soil fractions. SOM fractionation was conducted according to Zimmermann et al. (2007b) and Poeplau et al. (2013). Briefly, 30 g of soil was placed in a glass beaker and 150 mL of deionized water was added. To disperse soil aggregates, 22 J mL^{-1} energy with a constant power of 20 W was then applied to the soil samples using an ultrasonic probe (Poeplau et al., 2013). The dispersed soils were then wet-sieved (63 μm mesh size) with ca. 2 L deionized water. The fraction$>$63 μm was first dried at ca. 36 °C and density fractionation was then conducted to separate POM from the SOM associated with the sand and aggregate fraction. For this purpose, a sodium polytungstate solution with 1.8 g cm^{-3} density was used. This density fractionation step was carried out twice. After the density fractionation, the sand and aggregate fraction and the POM fraction were gently washed with deionized water. The weight of each fraction was measured after drying at ca. 36 °C. The fraction smaller than 63 μm (silt and clay (SC) fraction) was also dried at ca. 36 °C and ground using a mortar and pestle. This fraction was further used for chemical oxidation experiments to isolate chemically resistant SOM (rSOM) in the SC fraction. For this, 1 g of the SC fraction was placed in a 50 mL centrifuge tube and 50 mL of 7% NaOCl (adjusted to pH 8 by HCl addition) was added. The samples were left for 16 h and then washed with deionized water. This oxidation step was carried out three times and the samples were then dried at ca. 36 °C. The fractionation resulted in five different SOM fractions, namely POM, SOM associated with sand-sized aggregates (sand-OM), SOM associated with silt and clay (SC-OM), oxidation resistant SOM in the SC fraction (rSOM) and non-oxidation resistant SOM in the SC faction (SC-OM–rSOM). Correspondingly, the SOC content in each fraction is expressed as POM-C, Sand-C, SC-C, rSOC and SC-C–rSOC. SOC and N contents in bulk soil and all soil fractions were measured by dry-combustion on a TruMac CN (LECO Corp.). In addition, we report SOC contents in each fraction on a bulk soil basis (mg C g^{-1} bulk) and as the proportion of SOC in each fraction in relation to total SOC (SOCtot) content. The recovery of soil mass, C and N after the fractionation experiment was estimated by calculating ratios of total recovered mass, C and N to initial soil mass, SOCtot and total N contents. We do not show data on total N and N contents in soil fractions since N contents were strongly positively correlated with the SOC content in each fraction. We used the carbon to nitrogen ratio (C:N ratio) as an indicator for the degree of microbial decomposition of SOM (Gregorich et al., 2006).

2.4. Silt-sized soil aggregates

We examined particle and aggregate size distributions in ca. 0.08 g of the SC fraction (particles size $<$ 63 μm) using a laser particle size analyzer (Partica LA-950 V2, Horiba). The Mie Theory was used to obtain volume-based particle and aggregate size distributions. The dried SC fractions were either mechanically dispersed (MD) or dispersed by SOM removal (DSR). For the MD treatment, the samples were placed in ca. 40 mL deionized water and stirred overnight with a magnetic bar (350 rpm). For the DSR samples, 3 mL of hydrogen peroxide (35%) and one drop of HCl were added to the samples with ca. 15 mL of deionized water. The samples were then boiled for at least 6 h to enhance oxidation. Then 1 mL of chemical dispersant (sodium carbonate, Na_2CO_3 7 g L^{-1} + Sodium metaphosphate, $(NaO_3P)n$ 33 g L^{-1}) and distilled water were added, resulting in a final volume of ca. 40 mL. Finally, also the DSR samples were mechanically dispersed overnight (350 rpm). We assumed that the DSR treatment dispersed most of the soil aggregates formed via SOC and clay interactions and at least partly organo-mineral associations (Harada and Inoko, 1977; Poeplau et al., 2019), resulting in disaggregated primary particles (Mikutta et al., 2005; Jensen et al., 2017), while water stable aggregates remained in the MD treatment. We calculated the difference in volumes between the MD and DSR treatments for different size classes (i.e. $<$ 0.5 μm, 0.5 – 1 μm, 1 – 2 μm, 2 – 6 μm, 6 – 20 μm, 20 – 60 μm and 60 – 100 μm size ranges). When MD was smaller than DSR, we interpreted the difference as the volume of primary particles that had been dispersed from silt-sized aggregates upon SOM removal. When MD was larger than DSR, the difference was interpreted as the volume of silt-sized aggregates contained in the MD samples.

2.5. Grain yield data

Grain yields across the Bjertorp field were measured using the yield monitoring system on a Claas combine harvester in 1997, 1999, 2000–2004, 2007, 2010–2013, 2015 and 2016. The grain yield data were filtered to remove extreme values likely caused by machine dynamics such as abrupt velocity changes (Keller et al., 2012). The grain yield data were then converted to relative yield (RY) within each year to account for different crop types (Blackmore et al., 2003; Keller et al., 2012) as:

$$RY_i = \frac{Y_i}{Y_{mean}}$$

where i is the individual location where grain yield was recorded, Y_{mean} is the average grain yield for the respective year. The RY data were then imported to ArcGIS 10.7.1 (ESRI, http://www.esri.com) where interpolation was conducted using the Inverse Distance Weighting (IDW) method implemented in the Geostatistical Analyst extension. We excluded the data from 2003, 2004 and 2011 because yield data were missing for large parts of the field (i.e. $>$ 30% of the area). Details of the interpolation procedure are provided in the supplementary material (page S7). The interpolated relative yield was extracted for soil sampling locations where soil properties were known based on Lindahl et al. (2008) and the present study (Fig. S2). The mean of the relative yields (MRY) for each soil sampling location was then calculated as:

$$MRY_{SSL} = \frac{1}{n}\sum_{1}^{n} RY_{SSL}$$

where SSL is soil sampling location and n is the number of years. The n value differs between soil sampling locations because of missing RY data for some years. The MRY was used in the statistical analysis as described below. We used MRY instead of mean actual yield or mean C input estimated from actual yield (Bolinder et al., 2007), because the actual yields measured by the combine harvester might not be comparable between years due to uncertainties related to the measurement equipment. Yield data within a given year were recorded with the same equipment and settings and should, hence, be reliable.

2.6. Literature search on the relationship between SOC, clay, Alox and Feox in agricultural soils

To set the results from our field-scale study in a wider context, we searched the literature for datasets containing clay, total SOC (or total C), Alox and Feox contents for arable topsoils (0 – 20 cm) under humid continental climates. We focused on these conditions, since positive correlations between SOC and oxalate-extractable Al and Fe are already well known for forest soils (e.g. Mikutta et al., 2006) and some other soil types such as Andisols and Oxisols (e.g. Kramer et al., 2012; Souza et al., 2017b). We found one study from Sweden (Blombäck et al., 2020), one from Norway (Grønsten and Børresen 2009), one from Canada (Beauchemin et al., 2003) and one from Denmark (Paradelo et al., 2016). The dataset from Blombäck et al. (2020) covered agricultural fields mostly located in central and southern Sweden (n = 61) including different types of soils (i.e. texture) and under different management practices. Grønsten and Børresen (2009) sampled soils from different arable fields located in Akershus County in south-east Norway that covered various combinations of clay and SOM contents (n = 21). For this dataset, we

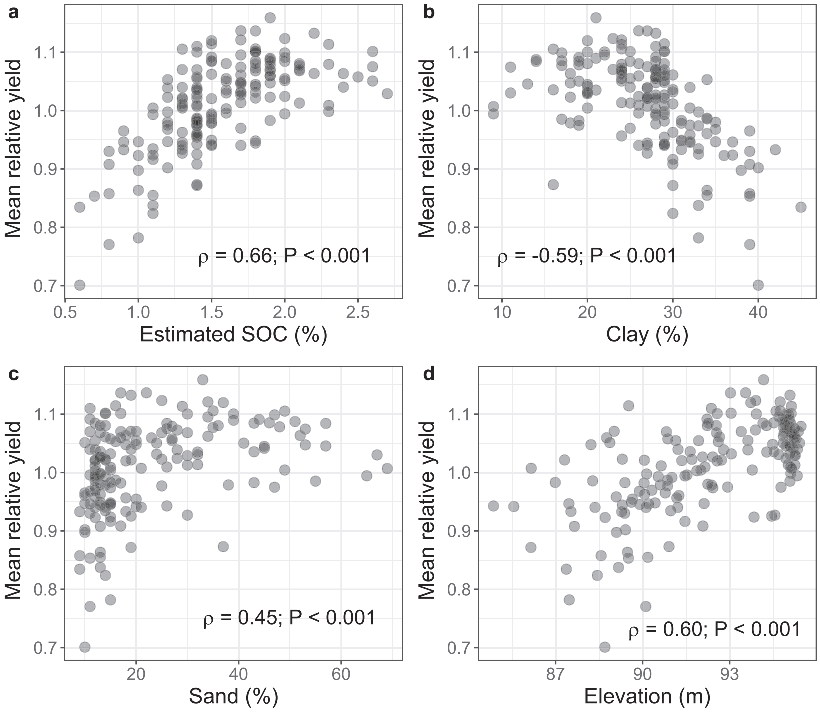

Fig. 3. Relationships between eleven-year mean relative yield and (a) estimated SOC, (b) clay, (c) sand and (d) elevation (n = 162).

Table 1
Mean, standard deviation (S.D.), maximum and minimum values of basic soil properties (n = 35) measured on samples taken in august 2017 and elevation and eleven-year mean relative yield (MRY) at respective soil sampling locations.

	Clay (%)	Silt (%)	Sand (%)	Soil pH	Alox (mg g^{-1})	Feox (mg g^{-1})	Elevation (m)	MRY	SOCtot (mg C g^{-1})
Mean	27.2	47.0	25.8	6.02	1.61	5.64	92.6	1.00	17.0
S.D.	9.1	12.0	20.4	0.25	0.25	1.91	2.7	0.07	4.5
Max.	42.2	61.3	72.0	6.57	2.13	8.81	95.4	1.08	27.2
Min.	8.4	19.5	4.7	5.63	1.08	2.53	87.4	0.82	11.2

converted bulk SOM to bulk C content using a conversion factor of 0.58. Beauchemin et al. (2003) investigated soils sampled from tile-drained, cultivated areas in the Montreal Lowlands, Canada (n = 10). Paradelo et al. (2016) investigated soils taken from one agricultural field (1.26 ha) with a large spatial variation in SOC contents. A statistical summary of these studies is given in Table S2. We combined the data from these studies into one dataset, except for the study by Paradelo et al. (2016), for which raw data were unavailable. From now on, we refer to this as the combined dataset.

2.7. Data analysis and statistics

Some of the soil properties were not normally distributed. Spearman rank correlation coefficients were therefore determined between basic soil properties, SOCtot, SOC in different soil fractions, elevation and MRY for the field scale study and also between SOC and soil properties for the individual and combined datasets from the literature. Spearman correlation coefficients were also calculated for the data obtained in the analysis of silt-sized aggregation. For the Bjertorp field, stepwise and multiple linear regression analyses were conducted to identify potentially important variables for predicting variations in topsoil SOC. Additionally, we used simple linear regression to investigate relationships between physico-chemical properties and SOC for the Bjertorp field as well as for the individual studies from the literature. For all regression analyses, assumptions such as normality and homoscedasticity of the residuals were visually checked. All the statistical analyses were performed in R (R Core Team, 2019). P = 0.05 was used as the significance level.

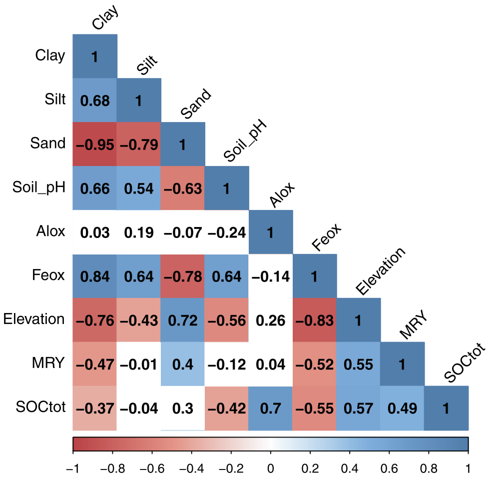

	Clay	Silt	Sand	Soil_pH	Alox	Feox	Elevation	MRY	SOCtot
Clay	1								
Silt	0.68	1							
Sand	−0.95	−0.79	1						
Soil_pH	0.66	0.54	−0.63	1					
Alox	0.03	0.19	−0.07	−0.24	1				
Feox	0.84	0.64	−0.78	0.64	−0.14	1			
Elevation	−0.76	−0.43	0.72	−0.56	0.26	−0.83	1		
MRY	−0.47	−0.01	0.4	−0.12	0.04	−0.52	0.55	1	
SOCtot	−0.37	−0.04	0.3	−0.42	0.7	−0.55	0.57	0.49	1

Fig. 4. Spearman rank correlation coefficients (ρ) for relationships between soil physico-chemical properties, elevation and mean relative yield ($n = 35$). Significant correlations ($P < 0.05$) were highlighted either in red (negative) or in blue (positive). MRY: mean relative yield; SOCtot: total SOC content.

Table 2
Simple and multiple regression analysis between bulk SOC, physico-chemical properties and mean relative yield (MRY). Model 1 is the result of stepwise regression analysis.

	Regression model	Adj. R^2
1	SOCtot = 10.1 Alox − 1.4 Feox + 0.1 Silt + 12.8 MRY – 9.3	77.1%
2	SOCtot = 11.8 Alox – 1.1 Feox + 5.0	69.6%
3	SOCtot = 12.5 Alox + 30 MRY – 33.2	69.6%
4	SOCtot = 12.8 Alox – 3.6	48.4%

3. Results

3.1. Soil properties, elevation and mean relative yield in the entire Bjertorp field

For the sampling locations of Lindahl et al. (2008) which covered the entire field (Fig. S2), mean relative yield (MRY) was positively correlated with SOC (ρ = 0.66, $P < 0.001$; Fig. 3a), sand (ρ = 0.45, $P < 0.001$; Fig. 3c) and elevation (ρ = 0.60, $P < 0.001$; Fig. 3d), whereas it was negatively correlated with clay (ρ = -0.59, $P < 0.001$; Fig. 3b).

3.2. Physio-chemical properties, elevation, MRY and SOCtot for soil sampling locations in 2017

Clay and total SOC (SOCtot) contents of soils sampled in 2017 (Table 1) were very similar to the properties measured in 2000 (clay: 9 – 45%; total SOC: 0.6 – 2.7%). Alox contents (mean 1.61 g kg^{-1}) were much smaller than Feox contents (mean 5.64 g kg^{-1}). The MRY (based on eleven years of data) varied between 0.82 and 1.08 at the field locations sampled in 2017.

The SOCtot content was positively correlated with Alox content (ρ = 0.70, $P < 0.05$), elevation (ρ = 0.57, $P < 0.05$) and MRY (ρ = 0.49, $P < 0.05$), whereas it was negatively correlated with clay (ρ = -0.37, $P < 0.05$), Feox (ρ = -0.65, $P < 0.05$), and soil pH (ρ = -0.55, $P < 0.05$) respectively (Fig. 4). Alox content was not correlated with any variables except SOCtot, while clay, Feox, MRY and elevation were significantly correlated with one another (Fig. 4).

In the stepwise regression analysis (Table 2), Alox, Feox, Silt and MRY were selected as explanatory variables for SOCtot, where the coefficients of Alox and Feox were significantly different from zero ($P < 0.005$) while the coefficients of Silt and MRY were not ($P = 0.08$ and $P = 0.09$ respectively). This best-fit model explained 77% of the variation in SOCtot. Simple linear regression with Alox as an explanatory variable explained 48% of the variation in SOCtot ($P < 0.001$). Also, multiple linear regression analysis with combinations of Alox and either MRY or Feox explained about 70% of the variation in SOCtot and the slopes of these regressions were significantly different from zero ($P < 0.001$; Table 2).

3.3. SOC in different soil fractions

Recoveries of total mass, carbon and nitrogen after the SOM fractionation were on average 98.2% (±0.4 S.D.), 92.3% (±2.2 S.D.) and 90.3% (±2.3 S.D.) respectively. The mass proportion of the sand and aggregate fraction was similar to the sand content determined in the texture analysis for all samples (i.e. all data points fell on the 1:1 line, Fig. S3). This means that most aggregates>63 μm were destroyed by the ultrasonic treatment and wet-sieving procedures. Thus, in the following, we refer to the SOC in the sand-sized aggregate fraction as SOC associated with sand only (Sand-C). Most SOC (ca. 81 ± 4.4%) was contained in the SC fraction (Table 3). The oxidation-resistant SOC (rSOC) in the SC fraction constituted, on average, 14.2 (±3.9) % of SOCtot. POM-C

Table 3
Mean, standard deviation (S.D.), maximum and minimum values of SOM fractions ($n = 35$).

		Bulk	POM	Sand-OM	SC-OM	rSOM in SC	SC-OM–rSOM
SOC content (mg C g^{-1} bulk soil)	Mean	17.0	0.83	0.92	14.0	2.56	11.4
	S.D.	4.5	0.29	0.38	4.2	1.36	2.9
	Max.	27.2	1.77	2.18	23.2	5.78	17.9
	Min.	11.2	0.39	0.46	9.0	1.06	7.4
SOC content (mg C g^{-1} fraction)	Mean	17.0	320	1.64	21.7	4.10	17.6
	S.D.	4.5	16.8	1.63	10.9	3.05	8.0
	Max.	11.2	364	7.76	57.7	15.1	42.6
	Min.	17.0	295	0.56	10.1	1.24	8.37
Proportion of SOC fractions to SOCtot (%)	Mean	100	5.0	5.6	81.7	14.2	67.5
	S.D.	–	1.8	2.3	4.4	3.9	4.5
	Max.	–	10.8	11.8	90.6	23.8	75.2
	Min.	–	2.7	1.9	70.9	8.0	55.7
C:N ratio	Mean	11. 6	19.8	20.7	11.3	49.2	9.7
	S.D.	1.2	1.8	5.0	1.2	18.6	0.60
	Max.	14.2	24.4	34.5	14.0	92.3	10.9
	Min.	10.1	15.4	14.9	10.0	21.8	8.3

POM: particulate organic matter, sand-OM: SOM in the sand fraction, SC-OM: SOM in the silt + clay (SC) fraction, rSOM: oxidation resistant SOM in the SC fraction, SC-OM–rSOM: non-oxidation resistant SOM in the SC fraction, SOCtot: total SOC content.

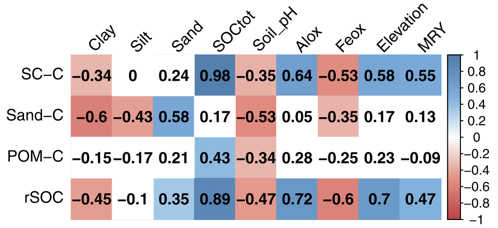

	Clay	Silt	Sand	SOCtot	Soil_pH	Alox	Feox	Elevation	MRY
SC–C	−0.34	0	0.24	0.98	−0.35	0.64	−0.53	0.58	0.55
Sand–C	−0.6	−0.43	0.58	0.17	−0.53	0.05	−0.35	0.17	0.13
POM–C	−0.15	−0.17	0.21	0.43	−0.34	0.28	−0.25	0.23	−0.09
rSOC	−0.45	−0.1	0.35	0.89	−0.47	0.72	−0.6	0.7	0.47

Fig. 5. Spearman rank correlation coefficients (ρ) for relationships between soil physico-chemical properties, elevation, SOCtot and SOC content of each fraction in bulk soil (mg C g^{-1} bulk soil). Significant correlations ($P < 0.05$, $n = 35$) were highlighted either in red (negative) or in blue (positive). SC-C: SOC content in the silt and clay (SC) fraction; Sand-C: SOC content in the sand fraction; POM-C: SOC in the POM fraction; rSOC: oxidation resistant SOC content in the SC fraction.

and Sand-C were minor constituents, with average proportions of 5.0 (±1.8) % and 5.6 (±2.3) % respectively (Table 3). C:N ratios were larger for the more labile fractions (POM and Sand-OM fractions) compared to the SC-OM fraction (Table 3). C:N ratios for the oxidation-resistant SOM (rSOM) in the SC fraction were even larger (Table 3), but this result should be interpreted with care, since N contents in the rSOM of the SC fraction were close to the detection limit.

SC-C and rSOC contents in bulk soil were positively correlated with Alox, SOCtot, elevation and MRY (Fig. 5), whereas SC-C, Sand-C and rSOC contents were negatively correlated with clay, Feox and soil pH (Fig. 5). POM-C content was weakly but negatively correlated with soil pH and positively correlated with SOCtot (Fig. 5). Additionally, we found that the proportion of rSOC to SOCtot was positively correlated with SOCtot and Alox contents (Fig. 6). The C:N ratio for bulk SOM and SOM in the SC fraction was negatively correlated with clay, Feox and soil pH and positively correlated with Alox and SOCtot or SC-C (Table 4). For the labile fractions, the C:N ratio for POM fraction was not correlated with any soil variables, whereas the C:N ratio for the sand-OM fraction was negatively correlated with clay, Feox and soil pH (Table 4).

3.4. Clay aggregation

Fig. 7a shows that the dispersion by SOM removal (DSR) changed the particle and aggregate size distributions relative to mechanical dispersion (MD). There were some clear differences between the two dispersion treatments with a larger volume in the silt-sized (2 – 20 μm) range for the MD treatment relative to the DSR treatment, whereas the volume in the clay-sized (<2 μm) range was larger in the DSR treatment (Fig. 7b). The volume of the released clay-sized particles upon SOM removal (i.e. the volume of DSR–MD in the < 2 μm size range) was positively correlated with the SC-C content (Fig. 7c).

3.5. Literature data

We found positive correlations between Alox and total SOC (or total C) contents for all individual studies, whereas SOCtot was not correlated with clay, pH and Feox (Table 5). In addition, the adjusted coefficients of determination for linear regressions showed that Alox could explain 40.5% of the variation in SOC in Grønsten and Børresen (2009), 74.5% in Beauchemin et al. (2003) and 23.1% in Blombäck et al. (2020). The coefficient of determination for samples in Blombäck et al. (2020) increased to 41.3%, when only samples with clay contents>15% were included. Total SOC was positively correlated with Alox content ($\rho = 0.51$, $P < 0.001$; Fig. 8a) for the combined dataset, whereas it was not correlated with clay, Feox and soil pH (Fig. 8b,c).

4. Discussion

About 80% of SOCtot was contained in the SC fraction and SC-C was

Table 4
Spearman rank correlation coefficients between soil properties and C:N ratios for SOM of bulk soil and each SOM fraction. Significant correlations ($P < 0.05$) were indicated in bold.

	Clay	Silt	Sand	Soil pH	Alox	Feox	SOC*
Bulk SOM	**−0.81**	**−0.52**	**0.78**	**−0.74**	**0.41**	**−0.81**	**0.66**^{1}
POM	−0.28	−0.07	0.27	−0.25	−0.28	−0.01	-0.14^{2}
sand-OM	**−0.58**	**−0.35**	**0.63**	**−0.41**	−0.01	**−0.47**	-0.06^{3}
SC-OM	**−0.75**	**−0.44**	**0.70**	**−0.69**	**0.47**	**−0.82**	**0.69**^{4}
rSOM in SC	**−0.80**	**−0.43**	**0.74**	**−0.57**	0.21	**−0.70**	**0.65**^{5}

*SOC content in bulk soil (SOCtot)^{1} or each SOM fraction (POM-C^{2}, sand-C^{3}, SC-C^{4} or rSOC^{5}). The unit is mg C g^{-1} bulk soil.

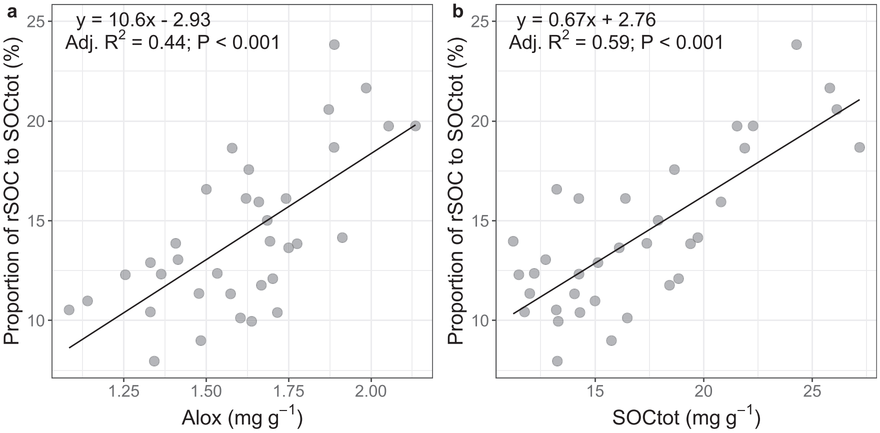

Fig. 6. Relationships between the proportion of rSOC content to SOCtot content and (a) Alox and (b) SOCtot.

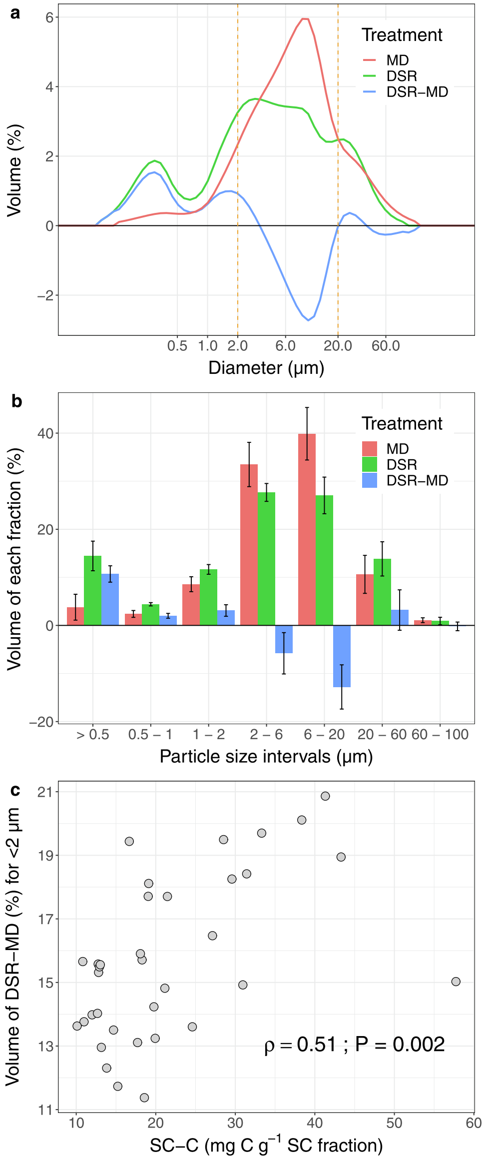

Fig. 7. (a) An example of particle and aggregate size distributions for the silt- and clay-sized (SC) fraction after mechanical dispersion (MD), after dispersion with SOM removal (DSR) and their difference (DSR–MD); (b) Mean of volumes for particle size intervals (>0.5 µm, 0.5 – 1 µm, 1 – 2 µm, 2 – 6 µm, 6 – 20 µm, 20 – 60 µm and 60 – 100 µm) with MD and DSR treatments and their difference (DSR–MD). Error bars indicate standard deviation (n = 35); (c) The relationship between SOC in the SC fraction and the volume of DSR–MD for size classes < 2 µm (i.e. particles < 2 µm released upon SOM removal, n = 35).

Table 5
Correlation coefficients for relationships between total C or SOC and physicochemical properties in different studies on arable topsoils (0 – 20 cm) from four different studies. Significant correlations (P < 0.05) are indicated in bold.

Reference (n: sample size)		clay	Alox	Feox	Soil pH
Grønsten and Børresen (2009) (n = 21)[a]	Total C	0.11	**0.54**	0.06	0.16
Beauchemin et al., (2003) (n = 10)[a]	SOC	0.31	**0.90**	0.61	−0.36
Blombäck et al., (2021) (n = 61)[ac]	Total C	0.02	**0.48**	0.03	−0.19
Blombäck et al., (2021) (n = 45, clay > 15%)[ac]	Total C	**0.43**	**0.69**	0.24	−0.15
Paradelo et al (2016) (n = 45)[b]	SOC	−0.18	**0.97**	−0.15	0.25

[a] Spearman rank correlation coefficients were determined from reported raw data.

[b] Reported Pearson correlation coefficients were extracted from the paper since raw data were not available.

[c] Dataset excluding one sample with total C content > 9%.

strongly positively correlated with SOCtot. These results are consistent with previous studies in Swedish arable soils (Simonsson et al., 2014) and internationally (e.g. Gregorich et al., 2006; Zimmermann et al., 2007a; McNally et al., 2017; Matus, 2021). Even for the samples with sand contents>68%, about 70% of SOCtot was contained in the SC fraction, suggesting that carbon stabilization is mainly restricted to SC sized aggregates and particles. Sand-C was positively correlated with sand content, which is in line with results presented in Li et al. (2013). However, the C:N ratio of sand-OM was similar to that of POM (~20), indicating that sand-OM was also dominated by relatively fresh, untransformed plant-derived OM. The POM-C content was only weakly correlated with soil pH and SOCtot. This may be because the spatial variation in POM-C may have been large compared to the other fractions (Simonsson et al., 2014).

The positive correlation between SOCtot and Alox suggests that Alox may be important for the protection of SOC against microbial decomposition in the Bjertorp field. Here, we discuss possible mechanisms behind this correlation. We also assume that Alox measured in bulk soil was mainly present in the silt + clay fraction (Curtin et al., 2016). Firstly, the oxidation-resistant SOC (rSOC) content was positively correlated with Alox content (Fig. 5). Additionally, the proportion of rSOC to SOCtot increased with Alox contents (Fig. 6a). These results indicate that Alox may have mediated the formation of stable SOC. Indeed, several studies have reported similar relationships between Alox/Feox and rSOC content (Mikutta et al., 2006; Wiaux et al., 2014). Based on ^{14}C analysis, Mikutta et al. (2006) also reported that oxidation-resistant SOC was older than SOCtot. Furthermore, Siregar et al. (2004) and Mikutta and Kaiser (2011) reported that NaOCl-resistant SOC seemed to be protected by associations with Al- and Fe-bearing reactive mineral phases since (1) the NaOCl treatment did not affect Alox and Feox contents and (2) larger amounts of these reactive phases resulted in larger rSOC contents. Secondly, Alox may also be important for physical protection of SOC. In this respect, we acknowledge that rSOC and non-oxidation resistant SOC (SC-C–rSOC) contents do not provide a clear division between physically and chemically protected SOC. For example, some chemically adsorbed SOC may be desorbed and oxidized at the pH value (=8) used in our oxidation experiment (Mikutta et al., 2005). Nevertheless, since about 67% of the SOC was contained in the SC-C–rSOC fraction, our data indicate that a large proportion of SOC may have been physically protected in the SC fraction. Accordingly, we found that when SOM was removed by peroxide, silt-sized aggregates were destroyed and clay-sized particles were released (Fig. 7b). Additionally, the volume of released clay particles upon SOM removal was positively correlated with the SC-C content (Fig. 7c). These results are consistent with the results presented by Jensen et al. (2017), who also reported an increase in the clay-sized fraction upon SOM removal

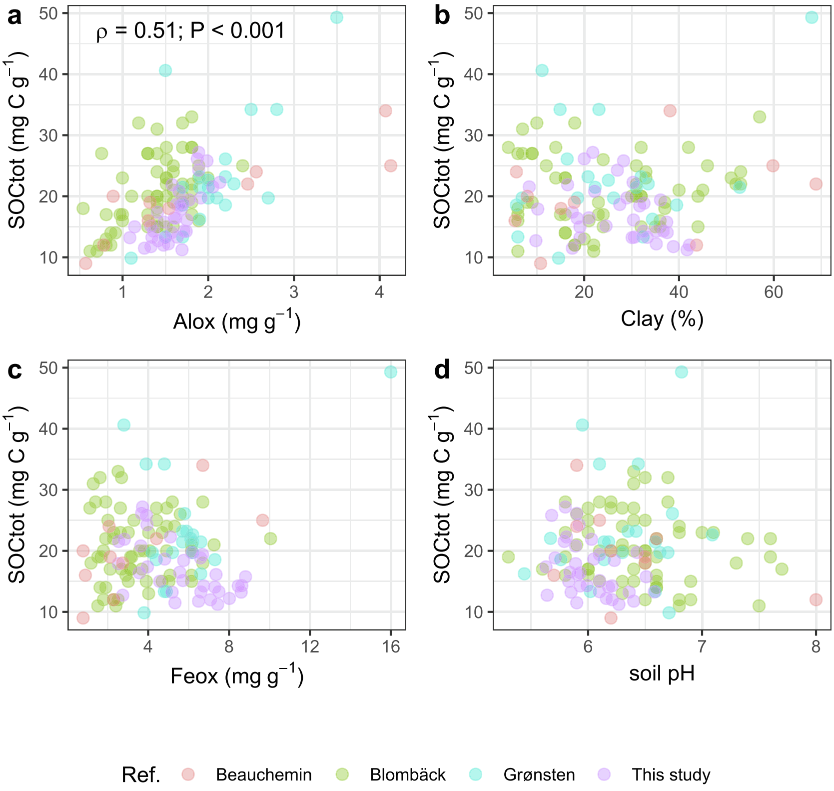

Fig. 8. Relationships between SOCtot (or total C) and (a) Alox, (b) Clay, (c) Feox and (d) soil pH. One sample with total C content > 9% in Blombäck et al. (2021) was not included. Data from Paradelo et al. (2016) were not openly available and hence not included here.

compared to samples without SOM removal. We hypothesize that the observed aggregation may also be important for the physical protection of SOC. In such aggregates, fine POM may be occluded and thereby physically protected from microbial decomposition (Shang and Tiessen, 1998; Virto et al., 2008; Steffens et al., 2017). The C:N ratios of SC-OM were also positively correlated with SC-C content (Table 4), which indicates that clay aggregation may have contributed to the protection of fresh, less decomposed SOM. Additionally, Alox was positively correlated with the C:N ratio of SC-OM (Table 4). Since reactive mineral phases have been suggested as key binding agents for clay aggregation (Shang and Tiessen, 1998; Asano et al., 2018; Totsche et al., 2018), we suggest that Alox content may also have been important for the physical stabilization of SOC in the Bjertorp field. This interpretation is of course only based on correlation analysis; further studies of the mechanisms behind the effects of Al-bearing reactive mineral phases on SOC turnover are needed.

Our field-scale results were supported by the analysis of individual studies in the literature (Table 5) and the combined dataset (Fig. 8a). The coefficients of determination for linear regressions showed that Alox could explain 23.1 – 74.5% of the variation in SOC in these studies. Other factors that may contribute to the unexplained variation in SOC, include (1) unquantified physico-chemical properties such as exchangeable calcium (Rasmussen et al., 2018) and crystalized iron (Hall et al., 2018) and (2) variations in carbon input (Moni et al., 2010; Ogle et al., 2012). The relatively small coefficient of determination (23.1%) for the data from Blombäck et al. (2020) may be due to the fact that this study covered a wide range of soil types and land management across Sweden. The coefficient of determination increased to 41.3% when samples with clay content smaller than 15% were excluded. This may be because clay particles are important as building blocks for silt-sized aggregates (Souza et al., 2017a), as discussed earlier. It should be noted that extractable aluminum concentrations are dependent on the extraction method. For example, Panichini et al. (2012, 2017) reported a strong positive correlation between SOC and pyrophosphate-extractable Al in Andisols. In this study we used Alox as an explanatory variable for SOC since the pH in our soil samples was in the range of 5.5 – 6.5, which indicated that not only organically-complexed SOC but also SRO phases would be important for SOC stabilization (Rasmussen et al., 2018)

It is not clear why Feox content, which was much larger than Alox (Table 1), was not positively correlated with SOCtot (Fig. 4), SC-C and rSOC (Fig. 5) at Bjertorp and for the other arable topsoils listed in Table 5. However, our results are consistent with those of some earlier studies in different climates and soil types, such as Andisols (e.g. Beare et al. 2014) and Oxisols and Ultisols (Barthès et al., 2008; Souza et al., 2017b). In contrast, other studies have suggested that Feox (or pedogenic Fe) may be more important than Alox in SOC stabilization, for example for an agroforestry field in North Carolina (Deiss et al., 2017), Swiss cropland soils (Zimmermann et al., 2007a) and European forest soils (Kaiser and Guggenberger 2000). There are two plausible reasons why Feox may not be effective in SOC protection in the Bjertorp field. First, soil pH in our field was relatively high (5.6 – 6.5) compared to studies on soils under other land uses, such as acidic forest soils. Additionally, there was a positive correlation between Feox content and soil pH in the Bjertorp field (Fig. 4). Lower soil pH may lead to stronger chemical association (e.g. complexation and precipitation) between Fe and SOM (Wagai and Mayer, 2007). Second, the SOC adsorption capacity of Fe-bearing reactive mineral phases is smaller under anoxic conditions, where SRO Fe may be reduced and adsorbed SOC may be released (Hall et al., 2018; Bailey et al., 2019; Huang et al., 2020). We do not know the redox conditions in the topsoil of the Bjertorp field. However, the Feox content was positively correlated with clay content and negatively with elevation, and hence sampling positions in low-lying areas with larger clay contents may have been more prone to anoxic conditions due to higher water contents (Manns et al., 2014; Keiluweit et al., 2018; Inagaki et al., 2020). We did observe signs of temporary anoxic conditions below the plough pan (28 – 43 cm; Fig. 1; Table S1) for one of the soil profiles (i.e. Eutric Stagnosol, Fig. 2). Thus, redox processes may also partly explain the lack of positive correlation between SOC and Feox at Bjertorp.

A weak negative correlation between clay and SOCtot contents suggests that clay content itself did not play a major role in the protection of SOC in the topsoil of the Bjertorp field. However, a number of authors have reported positive correlations between SOC and clay contents in other regions and climates (e.g. Homann et al., 2007; Wiesmeier et al., 2019; Poeplau et al., 2020). One possible explanation for the often observed positive correlations between SOC and clay contents is that clay content may be positively correlated with the contents of Al- and/or Fe-bearing reactive minerals. Several studies show that clay, Alox, Feox and SOC are indeed often positively correlated with each other (e.g. Zinn et al., 2007; Deiss et al., 2017). We suggest that, in addition to clay content, measurements of Alox and Feox may be useful for predicting the spatial variation of SOC in arable topsoils in continental humid climates and hence for modelling C dynamics and estimating the potential for SOC sequestration (Rasmussen et al., 2018; Basile-Doelsch et al., 2020; Wagai et al., 2020).

C:N ratios of bulk SOM and SC-OM were negatively correlated with clay and Feox contents, suggesting that there may be a greater accumulation of microbially-derived SOM with higher clay and Feox contents. This may be because N-rich SOM (such as proteins) is preferentially absorbed on clay surfaces (Kleber et al., 2007; Lutfalla et al., 2019). Keiluweit et al., (2012) also reported that microbial N was preferentially associated with Fe-oxyhydroxides. However, the negative correlation between clay and the C:N ratio of bulk SOM and SC-OM can also be due to increased adsorption/fixation of inorganic nitrogen to clay particles (Jensen et al., 1989; Röing et al., 2006).

We used the eleven-year mean relative yield (MRY) as a proxy for carbon inputs from roots and above-ground residues. The multiple linear regression analyses indicate that C input was also a significant predictor of the spatial variation of SOC in the Bjertorp field. Positive correlations between SOC content and crop (or grain) yield have also been reported globally (Oldfield et al., 2019) and at the field scale (e.g. Kravchenko and Bullock, 2000). It should be noted that the positive correlations between SOC and MRY can be due to the beneficial effects of SOC on crop production (Henryson et al., 2018; Oldfield et al., 2020). Furthermore, the ratio of below-ground biomass to above-ground biomass or grain yield may not be constant. For example, Poeplau and Kätterer (2017) reported lower root biomass and root-to-shoot ratio in soils with larger clay content. The spatial variation of clay content in the field may also result in different soil mechanical properties and availability of water and oxygen (Horn et al., 1994; Gregorich et al., 2011), which would affect root growth and crop production (e.g. Delin and Berglund, 2005; Gregorich et al., 2011; Wood et al., 2016; Börjesson et al., 2018). Correspondingly, we found that the MRY was negatively correlated with clay content and positively with elevation (Fig. 3), which indicates that the low-lying areas of the field with larger clay content may be less suitable for crop production and thereby lead to lower C inputs. This may also explain why SOC was negatively correlated not only with clay but also with Feox, since clay and Feox are highly correlated with each other (Fig. 4).

5. Conclusions

We examined relationships between physico-chemical properties, eleven-year mean relative grain yield (as a proxy for C input) and total SOC and SOC in different soil fractions for a Swedish arable topsoil. We found that total SOC content was positively correlated with oxalate-extractable aluminum (Alox) and that Alox explained ca. 48% of the variability in SOC. The results of SOM fractionation and analysis of clay aggregation further indicated that Alox may be important for physico-chemical stabilization of SOC in silt + clay sized fraction in the Bjertorp field. Our field-scale findings were supported by other studies that showed positive correlations between SOC and Alox contents in agricultural topsoils under climates compatible with our field. Simple linear regression analyses showed that Alox explained 23.1 – 74.5% of the SOC variations for these studies, highlighting the importance of other soil properties and variability in C input for better predictions of SOC variability. On the other hand, both clay (particle size < 2 μm) and oxalate-extractable Fe (Feox) contents seemed to be less important for SOC stabilization in the Bjertorp field. Additionally, a positive relationship between the mean relative yield and total SOC content indicated that C input from crop production could improve the predictions of SOC variability in the Bjertorp field. In future research, larger-scale studies (e.g. national soil inventories) exploring relationships between SOC and Alox and Feox contents may show if these variables are useful for estimating the potential for SOC sequestration and for modelling SOC dynamics in arable topsoils under humid continental climates.

Declaration of Competing Interest

The authors declare that they have no known competing financial interests or personal relationships that could have appeared to influence the work reported in this paper.

Acknowledgements

This study was financed by FORMAS (grant no. 2016-01320). Soil sampling at Bjertorp was possible thanks to the help from Reza Hosseinpour Ashenaabad and Mattias Gustafsson. We thank Ana Maria Mingot Soriano for helping us set up the laser particle size analyzer experiment. We thank Martin Bolinder, Magnus Simonsson, Jon-Petter Gustafsson, Rota Wagai and Claire Chenu for their valuable comments on this work. JF thanks the Heiwa Nakajima Foundation for providing a personal scholarship. We thank Claudia von Brömssen for her advice on the sampling strategy and Rebecca Naomi Ter Borg for her advice on the GIS analysis. We thank Knud Nissen for archiving the grain yield data. We are grateful to Kjell Carlsson, the manager of the Bjertorp farm, for allowing us to take soil samples and to use the grain yield data.

Appendix A. Supplementary data

Supplementary data to this article can be found online at https://doi.org/10.1016/j.geoderma.2021.115345.

References

Arrouays, D., Saby, N., Walter, C., Lemercier, B., Schvartz, C., 2006. Relationships between particle-size distribution and organic carbon in French arable topsoils. Soil Use Manag. 22, 48–51.

Asano, M., Wagai, R., 2014. Evidence of aggregate hierarchy at micro- to submicron scales in an allophanic Andisol. Geoderma 216, 62–74.

Asano, M., Wagai, R., Yamaguchi, N., Takeichi, Y., Maeda, M., Suga, H., Takahashi, Y., 2018. In Search of a Binding Agent: Nano-Scale Evidence of Preferential Carbon Associations with Poorly-Crystalline Mineral Phases in Physically-Stable. Clay-Sized Aggregates. Soil Syst. 2, 32.

Augustin, C., Cihacek, L.J., 2016. Relationships Between Soil Carbon and Soil Texture in the Northern Great Plains. Soil Sci. 181, 386–392.

Bailey, V.L., Pries, C.H., Lajtha, K., 2019. What do we know about soil carbon destabilization? Environmen. Res. Lett. 14, 083004.

Barthès, B.G., Kouakoua, E., Larré-Larrouy, M.-C., Razafimbelo, T.M., de Luca, E.F., Azontonde, A., Neves, C.S.V.J., de Freitas, P.L., Feller, C.L., 2008. Texture and sesquioxide effects on water-stable aggregates and organic matter in some tropical soils. Geoderma 143, 14–25.

Basile-Doelsch, I., Balesdent, J., Pellerin, S., 2020. Reviews and syntheses: The mechanisms underlying carbon storage in soil. Biogeosciences 17, 5223–5242.

Beare, M.H., McNeill, S.J., Curtin, D., Parfitt, R.L., Jones, H.S., Dodd, M.B., Sharp, J., 2014. Estimating the organic carbon stabilisation capacity and saturation deficit of soils: a New Zealand case study. Biogeochemistry 120, 71–87.

Beauchemin, S., Simard, R.R., Bolinder, M.A., Nolin, M.C., Cluis, D., 2003. Prediction of phosphorus concentration in tile-drainage water from the Montreal Lowlands soils. Can. J. Soil Sci. 83, 73–87.

Beck, H.E., Zimmermann, N.E., McVicar, T.R., Vergopolan, N., Berg, A., Wood, E.F., 2018. Present and future Köppen-Geiger climate classification maps at 1-km resolution. Sci. Data 5, 180214.

Blackmore, S., Godwin, R.J., Fountas, S., 2003. The Analysis of Spatial and Temporal Trends in Yield Map Data over Six Years. Biosys. Eng. 84, 455–466.

Blombäck, K., Bolster, C.H., Lindsjö, A., Hesse, K., Linefur, H., Parvage, M.M., 2021. Comparing measures for determination of phosphorus saturation as a method to estimate dissolved P in soil solution. Geoderma 383, 114708.

Bolinder, M.A., Janzen, H.H., Gregorich, E.G., Angers, D.A., VandenBygaart, A.J., 2007. An approach for estimating net primary productivity and annual carbon inputs to soil for common agricultural crops in Canada. Agric. Ecosyst. Environ. 118, 29–42.

Börjesson, G., Bolinder, M.A., Kirchmann, H., Kätterer, T., 2018. Organic carbon stocks in topsoil and subsoil in long-term ley and cereal monoculture rotations. Biol. Fertility Soils 54, 549–558.

Chenu, C., Angers, D.A., Barré, P., Derrien, D., Arrouays, D., Balesdent, J., 2019. Increasing organic stocks in agricultural soils: Knowledge gaps and potential innovations. Soil Tillage Res. 188, 41–52.

Curtin, D., Beare, M.H., Qiu, W., 2016. Texture effects on carbon stabilisation and storage in New Zealand soils containing predominantly 2: 1 clays. Soil Res. 54, 30–37.

Deiss, L., Franzluebbers, A.J., Amoozegar, A., Hesterberg, D., Polizzotto, M., Cubbage, F. W., 2017. Soil Carbon Fractions from an Alluvial Soil Texture Gradient in North Carolina. Soil Sci. Soc. Am. J. 81, 1096–1106.

Delin, S., Berglund, K., 2005. Management Zones Classified With Respect to Drought and Waterlogging. Precis. Agric. 6, 321–340.

Dungait, J.A.J., Hopkins, D.W., Gregory, A.S., Whitmore, A.P., 2012. Soil organic matter turnover is governed by accessibility not recalcitrance. Glob. Chang. Biol. 18, 1781–1796.

Eriksson, A.K., 2016. Phosphorus speciation in Swedish agricultural clay soils Influence of fertilisation and mineralogy. PhD thesis. Swedish University of Agricultural Sciences.

Eriksson, J., Matsson, L., Söderström, M., 2010. Tillståndet i svensk åkermark och gröda, data från 2001–2007. ("Current status of Swedish arable soils and cereal crops. Swedish Environmental Protection Agency, Stockholm, Sweden (In Swedish).

FAO, 2006. Guidelines for soil description, Fourth edition. FOOD AND AGRICULTURE ORGANIZATION OF THE UNITED NATIONS, Rome, p. 2006.

Feng, W., Plante, A.F., Six, J., 2013. Improving estimates of maximal organic carbon stabilization by fine soil particles. Biogeochemistry 112, 81–93.

Gregorich, E.G., Beare, M.H., McKim, U.F., Skjemstad, J.O., 2006. Chemical and Biological Characteristics of Physically Uncomplexed Organic Matter. Soil Sci. Soc. Am. J. 70, 975–985.

Gregorich, E.G., Lapen, D.R., Ma, B.L., McLaughlin, N.B., VandenBygaart, A.J., 2011. Soil and Crop Response to Varying Levels of Compaction, Nitrogen Fertilization, and Clay Content. Soil Sci. Soc. Am. J. 75, 1483–1492.

Greve, M.H., Kheir, R.B., Greve, M.B., Bøcher, P.K., 2012. Using Digital Elevation Models as an Environmental Predictor for Soil Clay Contents. Soil Sci. Soc. Am. J. 76, 2116–2127.

Grønsten, H.A., Børresen, T., 2009. Comparison of two methods for assessment of aggregate stability of agricultural soils in southeast Norway. Acta Agric. Scand. Sect. B: Soil Plant Sci. 59, 567–575.

Hall, S.J., Berhe, A.A., Thompson, A., 2018. Order from disorder: do soil organic matter composition and turnover co-vary with iron phase crystallinity? Biogeochemistry 140, 93–110.

Harada, Y., Inoko, A., 1977. The oxidation products formed from: Soil organic matter by hydrogen peroxide treatment. Soil Sci. Plant Nutr. 23, 513–521.

Hassink, J., 1997. The capacity of soils to preserve organic C and N by their association with clay and silt particles. Plant Soil 191, 77–87.

Henryson, K., Sundberg, C., Kätterer, T., Hansson, P.-A., 2018. Accounting for long-term soil fertility effects when assessing the climate impact of crop cultivation. Agric. Syst. 164, 185–192.

Homann, P.S., Kapchinske, J.S., Boyce, A., 2007. Relations of mineral-soil C and N to climate and texture: regional differences within the conterminous USA. Biogeochemistry 85, 303–316.

Horn, R., Taubner, H., Wuttke, M., Baumgartl, T., 1994. Soil physical properties related to soil structure. Soil Tillage Res. 30, 187–216.

Huang, W., Ye, C., Hockaday, W.C., Hall, S.J., 2020. Trade-offs in soil carbon protection mechanisms under aerobic and anaerobic conditions. Glob. Chang. Biol. 26, 3726–3737.

Inagaki, T.M., Possinger, A.R., Grant, K.E., Schweizer, S.A., Mueller, C.W., Derry, L.A., Lehmann, J., Kögel-Knabner, I., 2020. Subsoil organo-mineral associations under contrasting climate conditions. Geochim. Cosmochim. Acta 270, 244–263.

IUSS Working Group WRB. 2015. World Reference Base for Soil Resources 2014, update 2015 International soil classification system for naming soils and creating legends for soil maps. World Soil Resources Reports No. 106. FAO, Rome.

Jensen, E.S., Christensen, B.T., Sørensen, L.H., 1989. Mineral-fixed ammonium in clay- and silt-size fractions of soils incubated with 15N-ammonium sulphate for five years. Biol. Fertility Soils 8, 298–302.

Jensen, J.L., Schjønning, P., Watts, C.W., Christensen, B.T., Munkholm, L.J., 2017. Soil texture analysis revisited: Removal of organic matter matters more than ever. PLOS ONE 12, e0178039.

Kaiser, K., Guggenberger, G., 2000. The role of DOM sorption to mineral surfaces in the preservation of organic matter in soils. Org. Geochem. 31, 711–725.

Keller, T., Sutter, J.A., Nissen, K., Rydberg, T., 2012. Using field measurement of saturated soil hydraulic conductivity to detect low-yielding zones in three Swedish fields. Soil Tillage Res. 124, 68–77.

Keiluweit, M., Bougoure, J.J., Zeglin, L.H., Myrold, D.D., Weber, P.K., Pett-Ridge, J., Kleber, M., Nico, P.S., 2012. Nano-scale investigation of the association of microbial nitrogen residues with iron (hydr)oxides in a forest soil O-horizon. Geochim. Cosmochim. Acta 95, 213–226.

Keiluweit, M., Gee, K., Denney, A., Fendorf, S., 2018. Anoxic microsites in upland soils dominantly controlled by clay content. Soil Biol. Biochem. 118, 42–50.

Kleber, M., Eusterhues, K., Keiluweit, M., Mikutta, C., Mikutta, R., Nico, P.S., 2015. Chapter One - Mineral-Organic Associations: Formation, Properties, and Relevance in Soil Environments. In: Sparks, D.L. (Ed.), Advances in Agronomy. Academic Press, pp. 1–140.

Kleber, M., Sollins, P., Sutton, R., 2007. A conceptual model of organo-mineral interactions in soils: self-assembly of organic molecular fragments into zonal structures on mineral surfaces. Biogeochemistry 85, 9–24.

Kramer, M.G., Sanderman, J., Chadwick, O.A., Chorover, J., Vitousek, P.M., 2012. Long-term carbon storage through retention of dissolved aromatic acids by reactive particles in soil. Global Change Biol. 18, 2594–2594.

Kravchenko, A.N., Bullock, D.G., 2000. Correlation of Corn and Soybean Grain Yield with Topography and Soil Properties. Agron. J. 92, 75–83.

Lal, R., 2004. Soil Carbon Sequestration Impacts on Global Climate Change and Food Security. Science 304, 1623–1627.

Larsbo, M., Koestel, J., Kätterer, T., Jarvis, N., 2016. Preferential Transport in Macropores is Reduced by Soil Organic Carbon. Vadose Zone J. 15.

Lavallee, J.M., Soong, J.L., Cotrufo, M.F., 2020. Conceptualizing soil organic matter into particulate and mineral-associated forms to address global change in the 21st century. Glob. Chang. Biol. 26, 261–273.

Lehmann, J., Kleber, M., 2015. The contentious nature of soil organic matter. Nature 528, 60–68.

Li, X.G., Chen, Z.M., Li, X.H., Ma, Q., Lin, Y., 2013. Chemical Characteristics of Physically Separated Soil Organic Matter Fractions in Contrasting Arable Soils. Soil Sci. 178, 128–137.

Li, J., Nie, M., Pendall, E., 2020. Soil physico-chemical properties are more important than microbial diversity and enzyme activity in controlling carbon and nitrogen stocks near Sydney. Australia. Geoderma 366, 114201.

Lindahl, A.M.L., Söderström, M., Jarvis, N., 2008. Influence of input uncertainty on prediction of within-field pesticide leaching risks. J. Contam. Hydrol. 98, 106–114.

Lutfalla, S., Barré, P., Bernard, S., Le Guillou, C., Alléon, J., Chenu, C., 2019. Multidecadal persistence of organic matter in soils: multiscale investigations down to the submicron scale. Biogeosciences 16, 1401–1410.

Lützow, M.V., Kögel-Knabner, I., Ekschmitt, K., Matzner, E., Guggenberger, G., Marschner, B., Flessa, H., 2006. Stabilization of organic matter in temperate soils: mechanisms and their relevance under different soil conditions – a review. Eur. J. Soil Sci. 57, 426-445.

Manns, H.R., Berg, A.A., Bullock, P.R., McNairn, H., 2014. Impact of soil surface characteristics on soil water content variability in agricultural fields. Hydrol. Process. 28, 4340–4351.

Matus, F., Amigo, X., Kristiansen, S.M., 2006. Aluminium stabilization controls organic carbon levels in Chilean volcanic soils. Geoderma 132, 158–168.

Matus, F.J., 2021. Fine silt and clay content is the main factor defining maximal C and N accumulations in soils: a meta-analysis. Sci. Rep. 11, 6438.

Mayer, S., Kühnel, A., Burmeister, J., Kögel-Knabner, I., Wiesmeier, M., 2019. Controlling factors of organic carbon stocks in agricultural topsoils and subsoils of Bavaria. Soil Tillage Res. 192, 22–32.

McNally, S.R., Beare, M.H., Curtin, D., Meenken, E.D., Kelliher, F.M., Calvelo Pereira, R., Shen, Q., Baldock, J., 2017. Soil carbon sequestration potential of permanent pasture and continuous cropping soils in New Zealand. Glob. Chang. Biol. 23, 4544–4555.

Mikutta, R., Kaiser, K., 2011. Organic matter bound to mineral surfaces: Resistance to chemical and biological oxidation. Soil Biol. Biochem. 43, 1738–1741.

Mikutta, R., Kleber, M., Kaiser, K., Jahn, R., 2005. Review: Organic Matter Removal from Soils using Hydrogen Peroxide, Sodium Hypochlorite, and Disodium Peroxodisulfate. Soil Sci. Soc. Am. J. 69, 120–135.

Mikutta, R., Kleber, M., Torn, M.S., Jahn, R., 2006. Stabilization of Soil Organic Matter: Association with Minerals or Chemical Recalcitrance? Biogeochemistry 77, 25–56.

Moni, C., Chabbi, A., Nunan, N., Rumpel, C., Chenu, C., 2010. Spatial dependance of organic carbon–metal relationships: A multi-scale statistical analysis, from horizon to field. Geoderma 158, 120–127.

Ogle, S.M., Swan, A., Paustian, K., 2012. No-till management impacts on crop productivity, carbon input and soil carbon sequestration. Agric. Ecosyst. Environ. 149, 37–49.

Oldfield, E.E., Bradford, M.A., Wood, S.A., 2019. Global meta-analysis of the relationship between soil organic matter and crop yields. SOIL 5, 15–32.

Oldfield, E.E., Wood, S.A., Bradford, M.A., 2020. Direct evidence using a controlled greenhouse study for threshold effects of soil organic matter on crop growth. Ecol. Appl. 30, e02073.

Ouédraogo, R.A., Chartin, C., Kambiré, F.C., van Wesemael, B., Delvaux, B., Milogo, H., Bielders, C.L., 2020. Short and long-term impact of urban gardening on soil organic carbon fractions in Lixisols (Burkina Faso). Geoderma 362, 114110.

Panichini, M., Matus, F., Mora, M.L., Godoy, R., Bolan, N.S., Rumpel, C., Borie, F., 2012. Carbon distribution in top- and subsoil horizons of two contrasting Andisols under pasture or forest. Eur. J. Soil Sci. 63, 616–624.

Panichini, M., Neculman, R., Godoy, R., Arancibia-Miranda, N., Matus, F., 2017. Understanding carbon storage in volcanic soils under selectively logged temperate rainforests. Geoderma 302, 76–88.

Paradelo, M., Hermansen, C., Knadel, M., Moldrup, P., Greve, M.H., de Jonge, L.W., 2016. Field-Scale Predictions of Soil Contaminant Sorption Using Visible-Near Infrared Spectroscopy. J. Near Infrared Spectrosc. 24, 281–291.

Percival, H.J., Parfitt, R.L., Scott, N.A., 2000. Factors Controlling Soil Carbon Levels in New Zealand Grasslands Is Clay Content Important? Soil Sci. Soc. Am. J. 64, 1623–1630.

Poeplau, C., Barré, P., Cécillon, L., Baudin, F., Sigurdsson, B.D., 2019. Changes in the Rock-Eval signature of soil organic carbon upon extreme soil warming and chemical oxidation - A comparison. Geoderma 337, 181–190.

Poeplau, C., Don, A., Dondini, M., Leifeld, J., Nemo, R., Schumacher, J., Senapati, N., Wiesmeier, M., 2013. Reproducibility of a soil organic carbon fractionation method to derive RothC carbon pools. Eur. J. Soil Sci. 64, 735–746.

Poeplau, C., Don, A., Six, J., Kaiser, M., Benbi, D., Chenu, C., Cotrufo, M.F., Derrien, D., Gioacchini, P., Grand, S., Gregorich, E., Griepentrog, M., Gunina, A., Haddix, M., Kuzyakov, Y., Kühnel, A., Macdonald, L.M., Soong, J., Trigalet, S., Vermeire, M.-L., Rovira, P., van Wesemael, B., Wiesmeier, M., Yeasmin, S., Yevdokimov, I., Nieder, R., 2018. Isolating organic carbon fractions with varying turnover rates in temperate agricultural soils – A comprehensive method comparison. Soil Biol. Biochem. 125, 10–26.

Poeplau, C., Jacobs, A., Don, A., Vos, C., Schneider, F., Wittnebel, M., Tiemeyer, B., Heidkamp, A., Prietz, R., Flessa, H., 2020. Stocks of organic carbon in German agricultural soils—Key results of the first comprehensive inventory. J. Plant Nutr. Soil Sci. 183, 665–681.

Poeplau, C., Kätterer, T., 2017. Is soil texture a major controlling factor of root:shoot ratio in cereals? Eur. J. Soil Sci. 68, 964–970.

Prout, J.M., Shepherd, K.D., McGrath, S.P., Kirk, G.J.D., Haefele, S.M., What is a good level of soil organic matter? An index based on organic carbon to clay ratio. Eur. J. Soil Sci. n/a.

R Core Team (2019). R: A language and environment for statistical computing. R Foundation for Statistical Computing, Vienna, Austria. URL https://www.R-project.org/. Accessed 4 May 2020.

Rasmussen, C., Heckman, K., Wieder, W.R., Keiluweit, M., Lawrence, C.R., Berhe, A.A., Blankinship, J.C., Crow, S.E., Druhan, J.L., Hicks Pries, C.E., Marin-Spiotta, E., Plante, A.F., Schädel, C., Schimel, J.P., Sierra, C.A., Thompson, A., Wagai, R., 2018. Beyond clay: towards an improved set of variables for predicting soil organic matter content. Biogeochemistry 137, 297–306.

Röing, K., Andrén, O., Mattsson, L., 2006. 'Non-exchangeable' ammonium in soils from Swedish long-term agricultural experiments: Mobilization and effects of fertilizer application. Acta Agric. Scand. Sect. B: Soil Plant Sci. 56, 197–205.

Schmidt, M.W.I., Torn, M.S., Abiven, S., Dittmar, T., Guggenberger, G., Janssens, I.A., Kleber, M., Kögel-Knabner, I., Lehmann, J., Manning, D.A.C., Nannipieri, P., Rasse, D.P., Weiner, S., Trumbore, S.E., 2011. Persistence of soil organic matter as an ecosystem property. Nature 478, 49.

Shang, C., Tiessen, H., 1998. Organic Matter Stabilization in Two Semiarid Tropical Soils: Size, Density, and Magnetic Separations. Soil Sci. Soc. Am. J. 62, 1247–1257.

Simonsson, M., Kirchmann, H., Magid, J., Kätterer, T., 2014. Can Particulate Organic Matter Reveal Emerging Changes in Soil Organic Carbon? Soil Sci. Soc. Am. J. 78, 1279–1290.

Siregar, A., Kleber, M., Mikutta, R., Jahn, R., 2005. Sodium hypochlorite oxidation reduces soil organic matter concentrations without affecting inorganic soil constituents. Eur. J. Soil Sci. 56, 481–490.

Sollins, P., Homann, P., Caldwell, B.A., 1996. Stabilization and destabilization of soil organic matter: mechanisms and controls. Geoderma 74, 65–105.

Souza, I.F., Almeida, L.F.J., Jesus, G.L., Kleber, M., Silva, I.R., 2017a. The mechanisms of organic carbon protection and dynamics of C-saturation in Oxisols vary with particle-size distribution. Eur. J. Soil Sci. 68, 726–739.

Souza, I.F., Archanjo, B.S., Hurtarte, L.C.C., Oliveros, M.E., Gouvea, C.P., Lidizio, L.R., Achete, C.A., Schaefer, C.E.R., Silva, I.R., 2017b. Al-/Fe-(hydr)oxides–organic carbon associations in Oxisols — From ecosystems to submicron scales. Catena 154, 63–72.

Steffens, M., Rogge, D.M., Mueller, C.W., Höschen, C., Lugmeier, J., Kölbl, A., Kögel-Knabner, I., 2017. Identification of Distinct Functional Microstructural Domains Controlling C Storage in Soil. Environ. Sci. Technol. 51, 12182–12189.

Stevens, R.L., Bayard, E., 1994. Clay mineralogy of agricultural soils (Ap horizon) in Västergötland, SW Sweden. GFF 116, 87–91.

Thomsen, I.K., Bruun, S., Jensen, L.S., Christensen, B.T., 2009. Assessing soil carbon lability by near infrared spectroscopy and NaOCl oxidation. Soil Biol. Biochem. 41, 2170–2177.

Totsche, K.U., Amelung, W., Gerzabek, M.H., Guggenberger, G., Klumpp, E., Knief, C., Lehndorff, E., Mikutta, R., Peth, S., Prechtel, A., Ray, N., Kögel-Knabner, I., 2018. Microaggregates in soils. J. Plant Nutr. Soil Sci. 181, 104–136.

Traoré, S., Thiombiano, L., Bationo, B.A., Kögel-Knabner, I., Wiesmeier, M., 2020. Organic carbon fractional distribution and saturation in tropical soils of West African savannas with contrasting mineral composition. Catena 190, 104550.

Van De Vreken, P., Gobin, A., Baken, S., Van Holm, L., Verhasselt, A., Smolders, E., Merckx, R., 2016. Crop residue management and oxalate-extractable iron and aluminium explain long-term soil organic carbon sequestration and dynamics. Eur. J. Soil Sci. 67, 332–340.

Virto, I., Barré, P., Chenu, C., 2008. Microaggregation and organic matter storage at the silt-size scale. Geoderma 146, 326–335.

von Fromm, S.F., Hoyt, A.M., Acquah, G.E., Aynekulu, E., Berhe, A.A., Haefele, S.M., Lange, M., McGrath, S.P., Shepherd, K.D., Sila, A.M., Six, J., Towett, E.K., Trumbore, S.E., Vågen, T.G., Weullow, E., Winowiecki, L.A., Doetterl, S., 2020. Continental-scale controls on soil organic carbon across sub-Saharan Africa. SOIL Discuss. 2020, 1–39.

Wagai, R., Kajiura, M., Asano, M., 2020. Iron and aluminum association with microbially processed organic matter via meso-density aggregate formation across soils: organo-metallic glue hypothesis. SOIL 6, 597–627.

Wagai, R., Mayer, L.M., 2007. Sorptive stabilization of organic matter in soils by hydrous iron oxides. Geochim. Cosmochim. Acta 71, 25–35.

Wagai, R., Mayer, L.M., Kitayama, K., Shirato, Y., 2013. Association of organic matter with iron and aluminum across a range of soils determined via selective dissolution techniques coupled with dissolved nitrogen analysis. Biogeochemistry 112, 95–109.

Wiaux, F., Cornelis, J.T., Cao, W., Vanclooster, M., Van Oost, K., 2014. Combined effect of geomorphic and pedogenic processes on the distribution of soil organic carbon quality along an eroding hillslope on loess soil. Geoderma 216, 36–47.

Wiesmeier, M., Munro, S., Barthold, F., Steffens, M., Schad, P., Kögel-Knabner, I., 2015. Carbon storage capacity of semi-arid grassland soils and sequestration potentials in northern China. Glob. Chang. Biol. 21, 3836–3845.

Wiesmeier, M., Schad, P., von Lützow, M., Poeplau, C., Spörlein, P., Geuß, U., Hangen, E., Reischl, A., Schilling, B., Kögel-Knabner, I., 2014. Quantification of functional soil organic carbon pools for major soil units and land uses in southeast Germany (Bavaria). Agric. Ecosyst. Environ. 185, 208–220.

Wiesmeier, M., Urbanski, L., Hobley, E., Lang, B., von Lützow, M., Marin-Spiotta, E., van Wesemael, B., Rabot, E., Ließ, M., Garcia-Franco, N., Wollschläger, U., Vogel, H.-J., Kögel-Knabner, I., 2019. Soil organic carbon storage as a key function of soils - A review of drivers and indicators at various scales. Geoderma 333, 149–162.

Wood, S.A., Sokol, N., Bell, C.W., Bradford, M.A., Naeem, S., Wallenstein, M.D., Palm, C. A., 2016. Opposing effects of different soil organic matter fractions on crop yields. Ecol. Appl. 26, 2072–2085.

Zimmermann, M., Leifeld, J., Abiven, S., Schmidt, M.W.I., Fuhrer, J., 2007a. Sodium hypochlorite separates an older soil organic matter fraction than acid hydrolysis. Geoderma 139, 171–179.

Zimmermann, M., Leifeld, J., Schmidt, M.W.I., Smith, P., Fuhrer, J., 2007b. Measured soil organic matter fractions can be related to pools in the RothC model. Eur. J. Soil Sci. 58, 658–667.

Zinn, Y.L., Lal, R., Bigham, J.M., Resck, D.V.S., 2007. Edaphic Controls on Soil Organic Carbon Retention in the Brazilian Cerrado: Texture and Mineralogy. Soil Sci. Soc. Am. J. 71, 1204–1214.

Appendix A. Supplementary materials

Oxalate-extractable aluminum alongside carbon inputs may be a major determinant for organic carbon content in agricultural topsoils in humid continental climate

Authors

Jumpei Fukumasu[a*], Christopher Poeplau[b], Elsa Coucheney[a], Nick Jarvis[a], Tobias Klöffel[a], John Koestel[ac], Thomas Kätterer[d], David Nimblad Svensson[a], Johanna Wetterlind[e], Mats Larsbo[a]

Affiliations

a. Department of Soil and Environment, Swedish University of Agricultural Sciences (SLU), Box 7014, 750 07 Uppsala, Sweden

b. Thünen Institute of Climate-Smart Agriculture, Bundesallee 65, 38116 Braunschweig, Germany

c. Soil Quality and Soil Use, Agroscope, Reckenholzstrasse 191, Zürich, CH-8046, Switzerland

d. Department of Ecology, Swedish University of Agricultural Sciences (SLU, Box 7044, 750 07 Uppsala, Sweden

e. Department of Soil and Environment, Swedish University of Agricultural Sciences (SLU), Box 234, 532 23 Skara, Sweden

*Corresponding author: jumpei.fukumasu@slu.se

Tables

Table S1. Summary of soil classification at three locations across the field

Soil type	Depth (cm)	horizon	Matrix color	Mottles (%)	structure	consistency	Gravel (%)	pH	Clay (%)	Silt (%)	Sand (%)	SOM (%)[2]
Stagnic Eutric Cambisol	0 – 30	Ap	10 YR 3/3	1%	blocky subangular	firm	0	7.0	37.4[1]	53.4[1]	9.3[1]	3.5[1]
	30 - 40	B	10 YR 4/2	< 5 %	blocky angular	firm	0	7.1	45.4	49.3	5.3	2.1
	40 - 60	Bw	10 YR 5/4	20 % 7.5 YR 5/8	blocky subangular	fraiable	0	7.3	50.4	47	2.6	1.6
	60 – 100+	Cg	10 YR 4/3	20 % 7.5 YR 5/8 + 20 % bleached iron 10YR 5/1	blocky subangular	fraiable	0	7.6	46.3	50.3	3.4	1.4

Soil type	Depth (cm)	horizon	Matrix color	Mottles (%)	structure	consistency	Gravel (%)	pH	Clay (%)	Silt (%)	Sand (%)	SOM (%)[2]
Eutric Stagnosol	0 - 28	Apg	10 YR 4/3	1% (a few)	blocky subangular	friable	8	6.0	24.6[1]	45.5[1]	30[1]	3.4[1]
	28 - 43	Bg1	10 YR 6 /3	7.5 YR 5/8; 60 %	blocky subangular	friable-firm	1	6.9	34.0	54.8	11.2	2.0
	43 - 60	Bg2	10 YR 4 /3	7.5 YR 5/8; 60 % + 20 % bleached 7.5 YR 6/0	blocky subangular	friable	0	6.9	46.7	49.2	4	2.1
	60 - 100+	Cg	10 YR 5 /4	7.5 YR 5/8; 10 % + 30 - 40 % bleached iron 7.5 YR 6/0	blocky subangular	friable	0	7.1	44.6	52.2	3.2	1.6

Soil type	Depth (cm)	horizon	Matrix color	Mottles (%)	structure	consistency	Gravel (%)	pH	Clay (%)	Silt (%)	Sand (%)	SOM (%)[2]
Haplic Phaeozem[3]	0 - 33	Ahp	10 YR 3 / 2	0	blocky subangular	fraiable	5	6.1	8.4[1]	19.5[1]	72[1]	4.3[1]
	33 - 42	BC	10 YR 4 /6	0	single grain	loose	5	6.3	3.5	6.4	90	1.5
	42 - 48	C	N.D.	N.D.	> 2 massive	-	15	6.3	4.1	4.3	91.7	1.4
	48 - 53	2Cg1	N.D.	N.D.	layered	-	0	6.3	51	42.8	6.3	1.9
	53 - 66	2Cg2	N.D.	N.D.	layered	-	0	6.4	48	43	8.9	2.1
	66 – 73+	3Cg	N.D.	N.D.	layered	-	0	6.5	30.3	54.9	14.9	1.4

[1] soil texture and SOM content for top soils of the three profiles were taken from the data (3 – 13 cm) at locations closest to the three profiles.

[2] SOM content was estimated from loss on ignition (LOI) and a pedotransfer function (SOM = LOI × (1 – 0.5 × clay)) as proposed in Kätterer et al., (2007).

[3] soils deeper than 42 cm was parent material; C: weathered granite stone + Saprolite, 2Cg1: clay layer, 2Cg1: red clay layer, 3Cg: silt layer

Table S2 Statistical summary of studies used for correlation analysis in table 3. References were cited in the main manuscript. One sample with total C content > 9 % in Blombäck et al. (2021) was not included.

Reference	property	Min.	Median	Mean	Max
Blombäck et al., (2020) N = 61	SOC	11	20	21	33
	Clay	4	23	25	57
	pH	5.3	6.4	6.5	7.7
	Alox	0.5	1.4	1.4	2.4
	Feox	1.1	3.1	3.6	10
Grønsten and Børresen (2009) N = 21	SOC	10	21	23	49
	Clay	6	23	25	68
	pH	5.4	6.4	6.3	7.1
	Alox	1.1	2.0	2.1	3.5
	Feox	2.8	5.7	5.9	16
Beauchemin et al., (2003) N = 10	SOC	9	20	20	34
	Clay	5.4	17	27	69
	pH	5.7	6.2	6.4	8.0
	Alox	0.6	1.4	2.0	4.1
	Feox	0.8	2.2	3.2	9.7
Paradelo et al., (2016) N = 45	SOC	18	26	32	84
	Clay	5.5	10.9	10.8	14.0
	pH	6.31	6.69	6.71	7.60
	Alox	0.51	0.78	0.93	2.08
	Feox	0.46	1.12	1.11	1.68

Figures

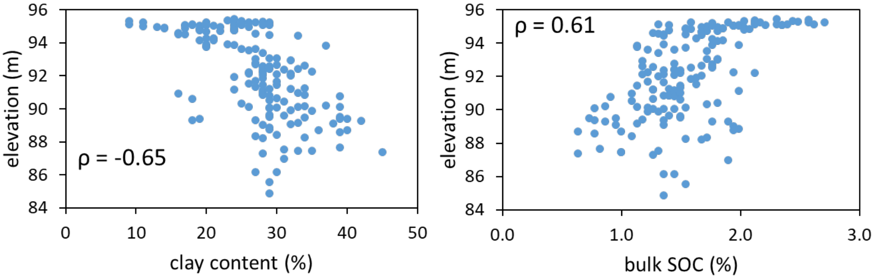

Fig. S1 Relationships between elevation and (a) clay content and (b) estimated SOC content. For these relations, Spearman rank correlation coefficients (ρ) were determined. All three correlations were statistically significant ($p < 0.05$). Data adapted from Lindahl et al. (2008)

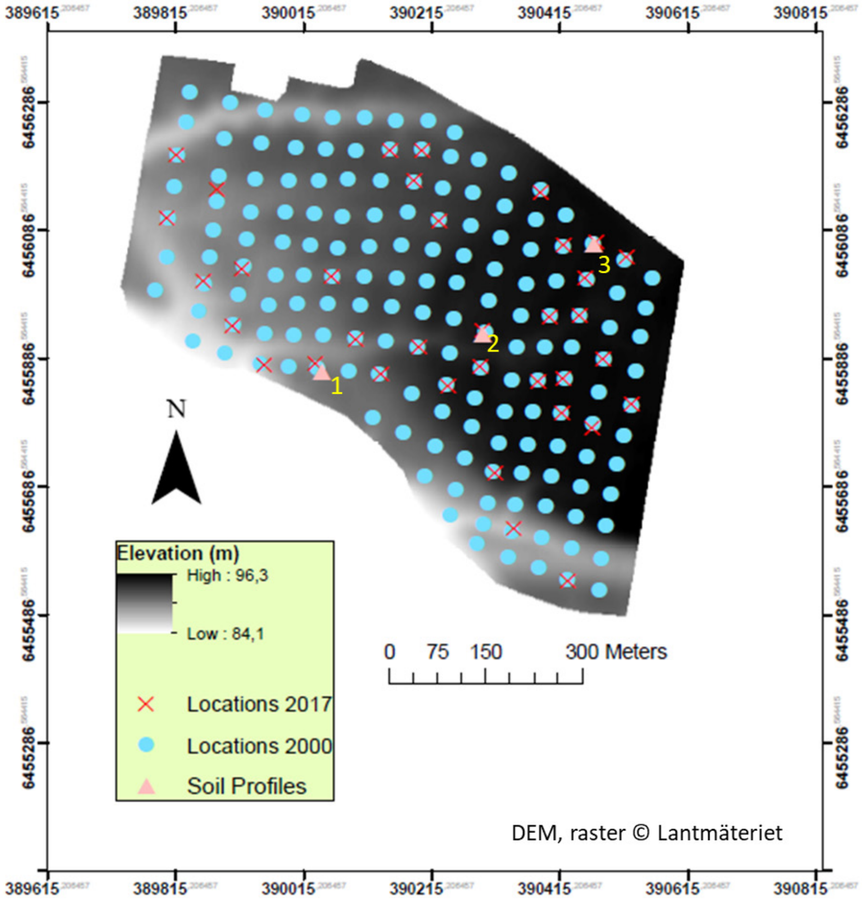

Fig. S2 A digital elevation model (DEM) and soil sampling locations in 2000 (Lindahl et al. 2008; n = 162) and locations in 2017 (This study; n = 35). The locations of three soil profiles are denoted as triangles with 1 (Stagnic Eutric Camnisol), 2 (Eutric Stagnosol) and 3 (Haplic Phaeozem) respectively. These locations are shown in Fig. S1.Coordinate system used here is SWEREF99 TM (unit: meter). The DEM of raster data was downloaded from Lantmäteriet. The map was created using ArcGIS 10.7.1 (ESRI).

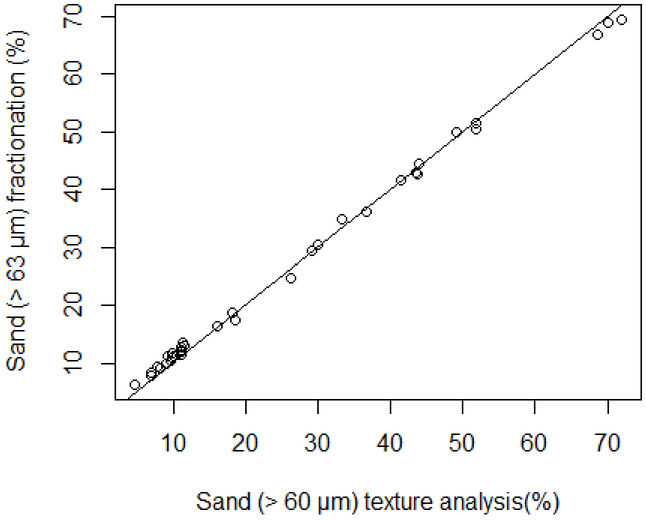

Fig. S3 Relationship between sand content determined by soil texture analysis and sand mass content determined by the fractionation with 1:1 line

Details of the interpolation of the grain yield

The interpolation was conducted using the Inverse Distance Weighting (IDW) method with condition of 20 m search radius, the maximum number of measurements set to 12 and the size of the grid raster set to 2.5 m times 2.5 m. If no grain data existed within the search radius, no interpolated data were assigned. The interpolated RY data were then extracted for soil sampling locations where soil properties were known based on Lindahl et al. (2008) and the present study (Fig. S2). We then further identified the soil sampling locations where at least 6 measurements were available within the search radius thereby excluding locations where the interpolation results depended on only a few grain yield records. For some years, grain yield data were missing in large parts of the field. We, therefore, calculated the proportion of the field where grain yield was available (PGYA, %) as:

$$\mathrm{PGYA} = \frac{Loc_{YA}}{162} \times 100 \qquad (1)$$

where $\mathrm{Loc}_{\mathrm{YA}}$ is number of locations where yield data were available (i.e. >6 grain yield records within the search radius) and 162 is the number of soil sampling locations in Lindahl et al. (2008) whose soil sampling locations covered the entire field (Fig. S2). Years with PGYA below 70% (2003, 2004 and 2011) were excluded from the statistical analysis

References for supplementary materials

Kätterer, T., Andrén, O., Jansson, P.E., 2006. Pedotransfer functions for estimating plant available water and bulk density in Swedish agricultural soils. Acta Agriculturae Scandinavica, Section B — Soil & Plant Science 56, 263-276.

ACTA UNIVERSITATIS AGRICULTURAE SUECIAE

DOCTORAL THESIS NO. 2022:8

This thesis investigated relations between soil organic carbon (SOC), soil structure and physical processes in an agricultural topsoil with large variations in soil mineral constituents. Results indicated that reactive aluminum phases played an important role in SOC stabilization. Although there were associations between SOC and soil pore size distributions, the effects of SOC on preferential solute transport were limited. The findings provide new insights on the effects of SOC sequestration on water and solute dynamics in arable topsoils.

Jumpei Fukumasu received his graduate degree at the Department of Soil and Environment, SLU, Uppsala. He holds an MSc degree in Environmental Pollution from University of Reading, UK and an MSc degree in Social Engineering and Environmental Management from Okayama University, Japan.

ISSN 1652-6880
ISBN (print version) 978-91-7760-891-2
ISBN (electronic version) 978-91-7760-892-9